Copyright Warning & Restrictions

The copyright law of the United States (Title 17, United States Code) governs the making of photocopies or other reproductions of copyrighted material.

Under certain conditions specified in the law, libraries and archives are authorized to furnish a photocopy or other reproduction. One of these specified conditions is that the photocopy or reproduction is not to be "used for any purpose other than private study, scholarship, or research." If a, user makes a request for, or later uses, a photocopy or reproduction for purposes in excess of "fair use" that user may be liable for copyright infringement,

This institution reserves the right to refuse to accept a copying order if, in its judgment, fulfillment of the order would involve violation of copyright law.

Please Note: The author retains the copyright while the New Jersey Institute of Technology reserves the right to distribute this thesis or dissertation

Printing note: If you do not wish to print this page, then select "Pages from: first page # to: last page #" on the print dialog screen

ABSTRACT

VOC REMOVAL FROM NITROGEN BY A MEMBRANE-BASED ABSORPTION-STRIPPING PROCESS

by
Boya Xia

A regenerative membrane-based absorption process has been extensively studied to remove volatile organic compounds (VOCs) from air/N_2 using silicone oil as absorbent. The absorbent liquid is regenerated by applying vacuum in a membrane-based stripper. In this process, there are no flooding, loading and entrainment, which limit the gas/liquid flow rate in the traditional absorption process. In the present study, attention has been focused on the removal of volatile component(s) from binary gas mixtures such as methanol-N_2 and toluene-N_2 and from a model multicomponent mixture of gasoline vapor constituents and nitrogen. The process performance was tested under three conditions: i) absorption with fresh absorbent; ii) both absorption and stripping modules at the same (room) temperature; iii) maintaining different temperatures in the absorption and stripping modules. Henry's law constants and diffusivities of VOCs in silicone oil have been measured at different temperatures for simulation purpose. The experimental results have been compared with theoretical predictions.

VOC REMOVAL FROM NITROGEN BY A MEMBRANE-BASED COMBINED ABSORPTION-STRIPPING PROCESS

by
Boya Xia

A Thesis
Submitted to the Faculty of
New Jersey Institute of Technology
In Partial Fulfillment of the Requirements for the Degree of
Masters of Science in Chemical Engineering

Department of Chemical engineering,
Chemistry and Environmental Science

January 1998

APPROVAL PAGE

VOC REMOVAL FROM NITROGEN BY A MEMBRANE-BASED ABSORPTION-STRIPPING PROCESS

Boya Xia

Dr. Kamalesh K. Sirkar, Thesis Advisor — Date
Professor of Chemical Engineering
New Jersey Institute of Technology

Dr. Robert G. Luo, Committee Member — Date
Assistant Professor of Chemical Engineering
New Jersey Institute of Technology

Dr. Norman W. Loney, Committee Member — Date
Associate Professor of Chemical Engineering
New Jersey Institute of Technology

BIOGRAPHICAL SKETCH

Name: Boya Xia

Degree: Master of Science

Date: January 1998

Undergraduate and Graduate Education:

Master of Science in Chemical Engineering,
New Jersey Institute of Technology, Newark, NJ, 1998

Master of Science in Chemical Engineering,
Beijing University of Chemical Technology, Beijing, China, 1985

Bachelor of Science in Chemical Engineering,
Petroleum University (Huadong), Dongying, Shangdong, China, 1982

Major: Chemical Engineering

ACKNOWLEDGMENT

I would like to express my sincere gratitude to my supervisor, Professor Kamalesh K. Sirkar, for his constant guidance and suggestions throughout this research. Special thanks to Dr. Robert G. Luo and Dr. Norman W. Loney for serving as members of committee and for their valuable suggestions.

I would like to thank Dr. S. Majumdar for constantly supervising and for detailed directions in the experiments. I appreciate the timely help and suggestions from all the members in Membrane Separation and Biotechnology Research Group.

Special thanks to Judy Kapp for her assistance on administration and trivial matters.

I am very grateful to my parents, family, brother and all my friends for their understanding and encouragement.

TABLE OF CONTENTS

TABLE OF CONTENTS
(Continued)

TABLE OF CONTENTS
(Continued)

Chapter **Page**

LIST OF TABLES

LIST OF TABLES
(Continued)

LIST OF TABLES
(Continued)

LIST OF FIGURES

LIST OF FIGURES
(Continued)

Figure **Page**

LIST OF FIGURES
(Continued)

LIST OF FIGURES
(Continued)

Figure **Page**

LIST OF SYMBOLS

A_H	:	Constant in equation 2.9
B_H	:	Constant in equation 2.9
C_{ig}	:	Local concentration of species i in gas phase (gmol/cc)
C_{il}	:	Local concentration of species i in liquid phase (gmol/cc)
D_{ig}	:	Diffusivity of species i in gas phase (cm^2/sec)
D_{igp}	:	Diffusivity of species i in gas phase inside a straight pore (cm^2/sec)
D_{il}	:	Diffusivity of species i in liquid phase (cm^2/sec)
F	:	Volumetric flow rate (cc/min)
H_i	:	Dimensionless Henry's law constant of species i between gas and liquid Phase ($=C_{il}/C_{ig}$)
H_{i1}	:	Dimensionless Henry's law constant of species i between gas phase and immaminery fluid phase
H_{i2}	:	Dimensionless Henry's law constant of species i between liquid phase and immaginery fluid phase
J_i	:	Volumetric flux of specoes i through the membrane (cc/cm^2.s)
j_i	:	Molar flux of species i through the membrane (gmol./(cm^2.s))
L	:	Effective length of the module (cm)
n	:	Number of segments
N_f	:	Number of fibers in the module
N_{GZ}	:	Graetz number ($=<V_t>/(D_{ig}L)$)
p	:	Pressure (psia)
Δp	:	Pressure difference (psia)

LIST OF SYMBOLS
(Continued)

Q_c	:	Permeability of species i through the silicone skin ($cm^3.cm/(cm^2.inHg.s)$)
Q_i	:	Permeability of species i through the membrane ($cm^3.cm/(cm^2.inHg.s)$)
Q_o	:	Overall permeability of species i through composite membrane ($cm^3.cm/(cm^2.inHg.s)$)
q_c	:	Permeability of species i through the silicone skin (cm^2/s)
q_i	:	Permeability of species i through the membrane (cm^2/s)
q_o	:	Overall permeability of species i through composite membrane (cm^2/s)
R	:	Universal gas constant (cc-atm/gmol-°K)
r_i	:	Inside radius of the fiber (cm)
r_c	:	Outside radius of the coated fiber (cm)
r_e	:	Outside radius of hypothetical free surface ($=r_s/N_f^{1/2}$) (cm)
r_o	:	Outside radius of the porous substrate (cm)
r_s	:	Inside radius of the shell (cm)
T	:	Temperature (°K)
t	:	Temperature (°C)
$<V_s>$	:	Volumetric flow rate of liquid in the shell side per fiber (ml/sec)
$<V_t>$	:	Volumetric flow rate of gas inside the tube per fiber (cc/sec)
x	:	Mole fraction in feed stream
y	:	Mole fraction in permeate stream

LIST OF SYMBOLS
(Continued)

Greek Symbols

α_{ij}	:	Separation factor of species i to j
α^{*}_{ij}	:	Ideal separation factor of species i to j (=q_i/q_j or Q_i/Q_j)
γ	:	Ratio of permeate-side pressure to feed-side pressure
Δ_{ig}	:	Ratio of VOC diffusivity in N_2 at any pressure to that at atmospheric pressure
δ	:	Thickness of the membrane (cm)
δ_c	:	Thickness of the silicone skin (cm)
δ_o	:	Overall thickness of the composite membrane (cm)
Φ	:	Ratio of gas phase VOC concentration at the module exit to that at the module entrance
ϕ_i	:	Dimensionless concentration of species i
$<\phi_i>$	:	Average dimensionless concentration of species i
λ	:	Ratio of volumetric gas flow rate at any axial location inside the fiber to that at atmospheric pressure.
ξ	:	Dimensionless radius (=r/r_i)
ρ	:	Absorbent liquid density (gm/ml)

Subscripts

c	:	Nonporous silicone skin
F	:	Feed side
g	:	Gas

LIST OF SYMBOLS
(Continued)

Greek Symbols

α_{ij}	:	Separation factor of species i to j
α^{*}_{ij}	:	Ideal separation factor of species i to j (=q_i/q_j or Q_i/Q_j)
γ	:	Ratio of permeate-side pressure to feed-side pressure
Δ_{ig}	:	Ratio of VOC diffusivity in N_2 at any pressure to that at atmospheric pressure
δ	:	Thickness of the membrane (cm)
δ_c	:	Thickness of the silicone skin (cm)
δ_o	:	Overall thickness of the composite membrane (cm)
Φ	:	Ratio of gas phase VOC concentration at the module exit to that at the module entrance
ϕ_i	:	Dimensionless concentration of species i
$<\phi_i>$	:	Average dimensionless concentration of species i
λ	:	Ratio of volumetric gas flow rate at any axial location inside the fiber to that at atmospheric pressure.
ξ	:	Dimensionless radius (=r/r_i)
ρ	:	Absorbent liquid density (gm/ml)

Subscripts

c	:	Nonporous silicone skin
F	:	Feed side
g	:	Gas

CHAPTER 1

INTRODUCTION

VOCs are carbon compounds that photochemically react with nitrogen oxides or other airborne chemicals to form smog. Each year, it is estimated that approximately 500 million pounds of VOCs are discharged from process exhaust streams. It is well known that VOCs can produce harmful effects on human health. For example, low to moderate levels of long term exposure to toluene can cause tiredness, confusion, weakness, drunken-type action, memory loss etc. Repeated exposure to high levels can cause permanent brain and speech damage, vision and hearing problems or even unconsciousness and death. Hexane can cause convulsions and death at 40,000 ppm and narcosis at 30,000 ppm (U.S. Department of Health, Education, and Welfare, 1970). At a concentration of 5,000 ppm, it can result in dizziness/giddiness in 10 minutes. From an environmental viewpoint, discharging of VOC to atmosphere is unacceptable. In addition, as solvents have become expensive, discharging them into atmosphere as spent gases is not economically sensible. Under the Clean Air Act Amendments of 1990 and various regulations promulgated by the U.S. Environmental Protection Agency (EPA), VOC emissions from all types of vents, processing streams or leaks will have to be reduced.

Ruddy and Carroll (1993) summarized various methods currently used in VOC abatements, such as thermal oxidation, catalytic oxidation, condensation, absorption, and activated carbon adsorption. The evaluation and selection of an appropriate VOC

abatement technology depends upon many factors such as the environmental, economic, and energy impacts of installing, operating, and maintaining the equipment. No single method meets every need.

Oxidizers are destruction devices, where VOCs are combusted, or destroyed without being recovered. It is difficult to have 100% of the impurities oxidized. First, the temperature must be significantly high for oxidation to take place at all or to occur fast enough. Second, sufficient contacting between the impurities and oxygen must be ensured for a sufficiently long time to achieve complete oxidation. Thermal oxidizers usually operate at 1300~1800 ^{o}F and can destroy 95% to 99% of VOCs. It is good for VOC concentration ranges from 100~2,000 ppm. Catalytic systems operate at a lower temperature---usually about 700~900 ^{o}F, which requires less combustion energy. The catalytic oxidizer is well suited to low concentrations and is often used for vent controls where flow rate and VOC content are variable. It can achieve more than 90 % of destruction efficiency (Ruddy and Carroll, 1993).

Condensation can be a very simple and low-cost process. It is most efficient for VOCs with boiling points above 100 ^{o}F at concentrations above 5,000 ppm. Low condenser temperature provides better VOC recovery but increases the cost significantly.

Absorption is probably one of the most important gas purification techniques. It involves the transfer of a substance from the gaseous to the liquid phase through the phase boundary. Desorption (or stripping) represents a special case of the same operation in which the material moves from the liquid to the gaseous phase. Most absorbers are either packed, or plate, or spray towers. Occasionally, ventruri scrubbers or other special

scrubbers are also used. This system can handle VOC-contaminated gas streams in the concentration range of 500 to 5,000 ppm. The efficiency for VOC removal is about 95% to 98%.

Adsorption is of increasing importance in gas purification and forms the basis for commercial processes that remove water vapor, organic solvents, odors, and other vapor-phase impurities from gas streams. In adsorption, the VOCs are removed from gas streams by concentration on the surface of a solid material. The solids best suited to adsorption are very porous, with very large effective surface area, which are obtained with materials such as carbon, alumina, or silica gel. Carbon is very effective in adsorbing nonpolar organic molecules, particularly, near their normal boiling points. It is used for the recovery of hydrocarbon solvents, the removal of odors and other trace impurities from gas streams. Usually, it is not economical to throw away the adsorbent after it has been once saturated with the adsorbate; therefore, it is customary to regenerate the absorbent beds. Bed regeneration is done by heat or vacuum and the solvents are recovered as a condensate. Variable flow rates and VOC concentrations are not disruptive to carbon adsorbers. But carbon bed performance is sensitive to the moisture content of the gas stream being treated. The performance of the carbon decreases when the relative humidity is more than 50%. And it is not recommended for VOC streams containing ketones because of exothermic polymerization on the carbon surface.

Gas separations based on membranes have only recently become commercially available for VOC control. More than 60 membrane vapor separation systems have been installed worldwide in chemical processing plants and petroleum facilities to recover hydrocarbon vapors, chlorofluorocarbons (CFCs), hydrochlorofluorocarbons (HCFCs), vinyl chloride,

and other high-value materials (Baker et al., 1996). It is most cost competitive when the VOC concentration is greater than 1,000 ppmv (Baker et al. (1996) and Cha et al. (1997)). A typical membrane process for gas separation, called vapor permeation, is illustrated in Figure 1.1. The driving force for separation can be established either by applying a high pressure on the feed side and/or maintaining a low pressure on the permeate side. When VOC-contaminated air stream flows past the surface of the VOC-selective membrane, VOC permeates through the membrane preferentially. The VOC on the permeate side of the membrane is then compressed, cooled, and/or condensed for recovery of the organic solvents. The degree to which the components are separated is governed by the characteristics of the membrane (selectivity and permeability) and the relative driving force (for example, partial pressure difference of the component between the two sides of the membrane).

Bagavandoss (1996) has studied the permeation behavior of three hydrocarbons: butane, pentane and hexane. The gas mixture he employed was ~12% butane, ~4% pentane, ~1% hexane and ~83% nitrogen; this is a common concentration profile of off-gas from gasoline storage tanks. Removal of hydrocarbons as high as 99% was observed at lower feed flow rates (~5cc/min) in his experiments. A mathematical model was developed to simulate the separation results of binary mixtures based on the solution-diffusion model. More work needs to be done with the simulation of the multicomponent mixtures.

For contacting-based gas purification processes using membranes, Sirkar (1992) has provided a review of earlier developments. Recently, a regenerative absorption-based membrane separation process has been proposed (Poddar et al., 1996a, 1996b) to remove VOCs from air/N_2 using silicone or Paratherm oils as the absorbent. Figures 1.2 and 1.3

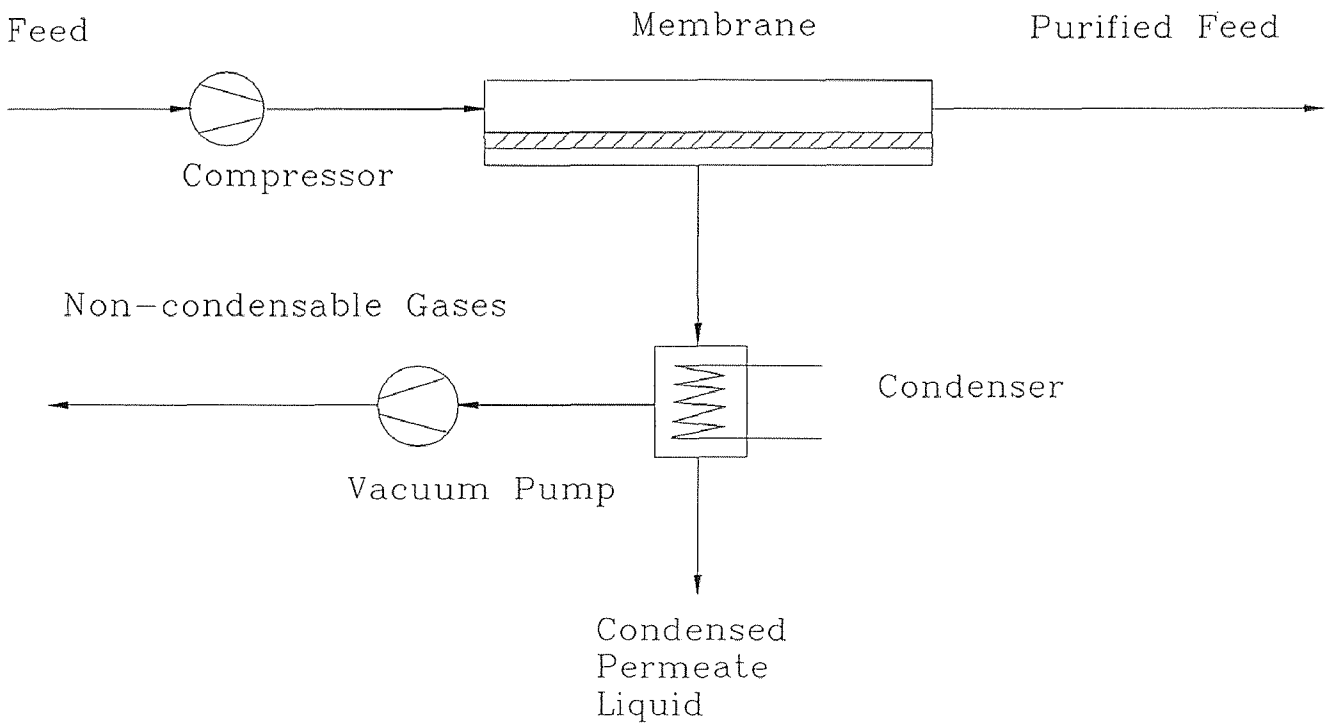

Figure 1.1 Vapor Permeation Process

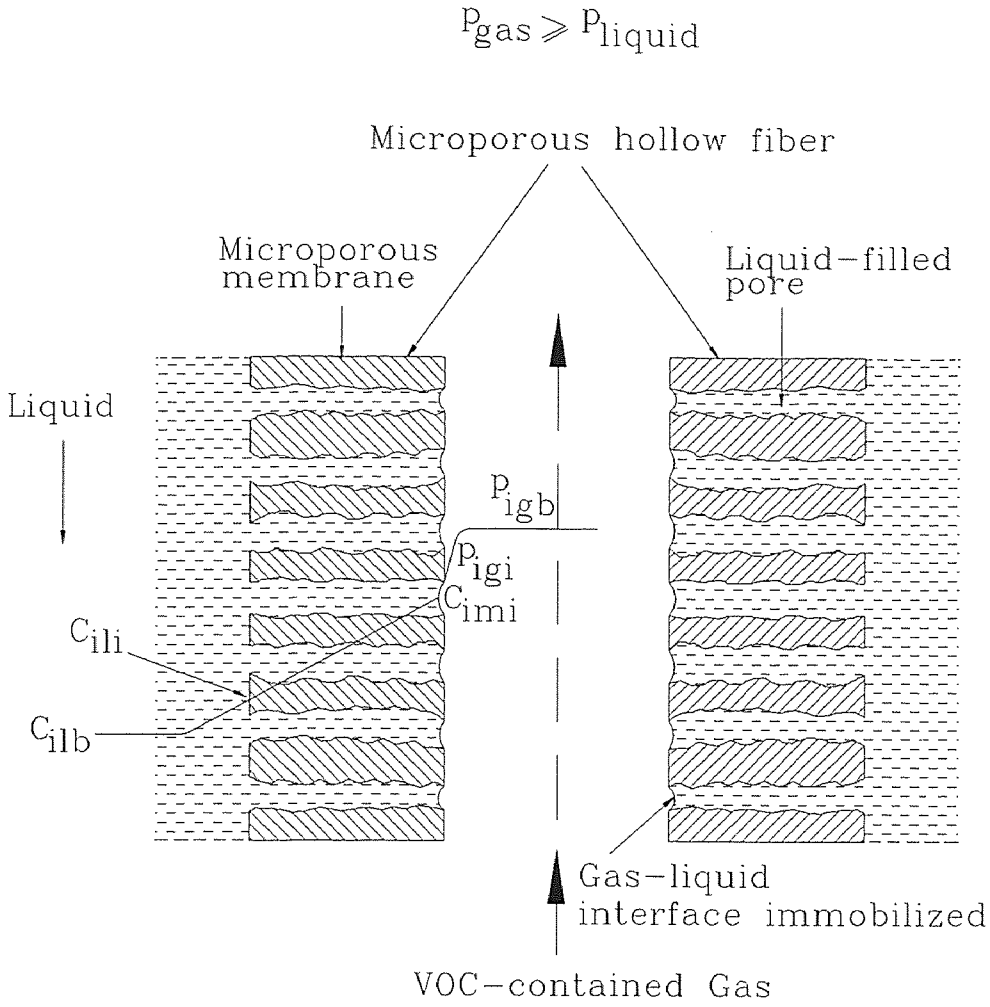

Figure 1.2 Local Partial Pressure and Concentration Profiles of VOC in Absorption Module with Microporous/Porous Hollow Fibers

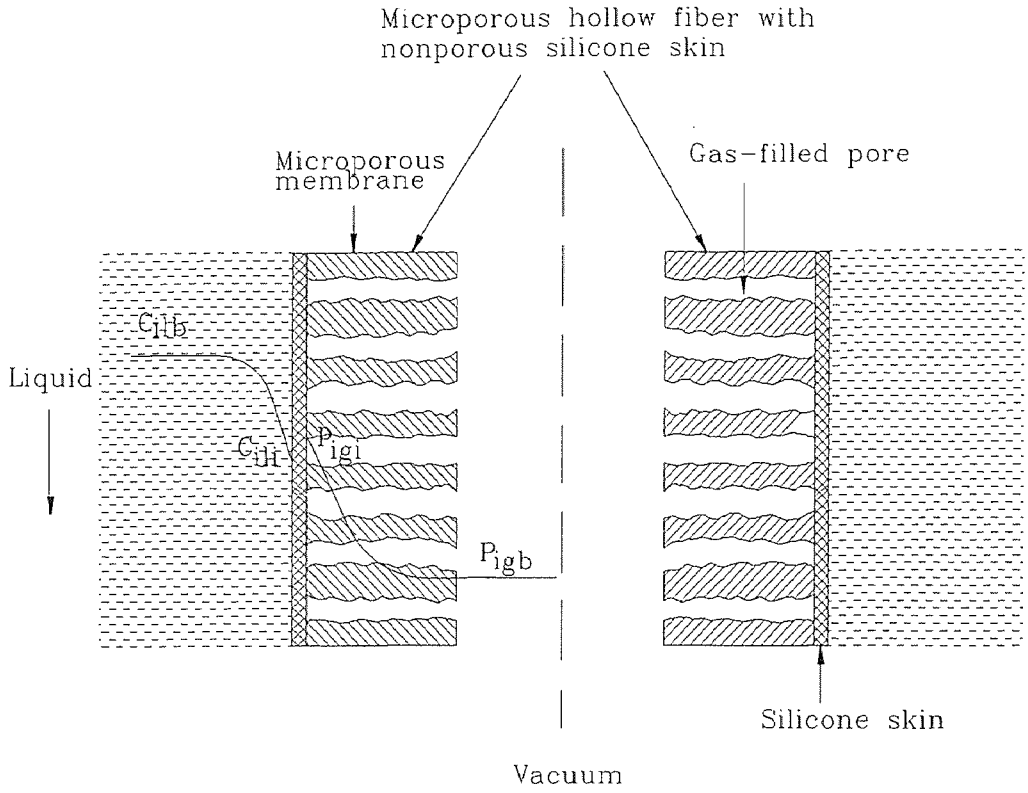

Figure 1.3 Local Partial Pressure and Concentration Profiles of VOC in Stripping Module with Microporous/Porous Hollow Fibers Having a Nonporous Silicone Skin on the Outer Surface

illustrate the basic concept for this process. Microporous hollow fibers were used in the absorption part of the process as shown in Figure 1.2. The position of the gas-liquid interface is determined by the pore size, the pressure difference across the membrane and the interaction between the membrane material and the absorbent liquid. The pressure differential (Δp) at which the liquid breaks through the pores not wetted by the liquid or the gas breaks through a pore wetted by a liquid is described by the Laplace equation (Poddar, 1995):

$$\Delta p = 2(\gamma / r)\cos\theta \tag{1.1}$$

Where γ is surface tension, r is the pore radius and θ is the contact angle.

For hydrophobic substrates and an organic nonpolar oil, the pores will be spontaneously wetted. The pores will remain filled with the absorbent if the gas phase is at an appropriate pressure (in Poddar (1995), 3 psi higher than the liquid). The VOCs in the feed side (inner side of the fiber) were absorbed in the absorbent, diffuse through the absorbent in the pores and the bulk layer in the shell side and were carried out of the absorption module to the stripping module.

The fibers in the stripping module (Figure 1.3) are microporous fibers having a non-porous silicone skin on the outer surface. Vacuum was applied to the tube side of the module to regenerate the absorbent. The VOCs being absorbed in the absorbent were stripped under vacuum, permeated through the membrane to the tube side, and then were condensed in a condenser to recover the solvent.

This process has several merits over traditional gas-liquid contactors (Poddar, 1995), such as:

- High surface area per unit volume of the contactor;
- High volumetric mass transfer coefficient;

- No flooding, loading or entraintment encountered in the traditional absorption processes;
- Small and compact;
- Easy to scale up.

Poddar et al. have studied on the separation of VOCs by membrane-based absorption (Poddar et al., 1996a) and membrane-based absorption-stripping processes (Poddar et al., 1996b). They have conducted experiments using either toluene, or methanol, or acetone, or methylene chloride present in nitrogen; they operated the absorption and stripping modules at room temperature. It was observed that the feed gas containing 999 ppmv of methylene chloride was brought down to around 20 ppmv when the feed gas flow rate was low. A mathematical model was developed to simulate this process. Experimental data were in good agreement with the predictions from the theoretical model. However, the overall performance was controlled by the stripping process due to the lower stripping temperature and lower membrane area of the stripping module.

The vapor permeation process is highly efficient for concentrated gas stream purification; the membrane-based absorption-stripping process can satisfy the low concentration requirement for high purification of N_2 or air. From an overall viewpoint, if the separation has to be done from a high concentration (above 10%) to a very low concentration (10-20 ppmv), these two processes have to be combined together. The feed gas with high concentration of VOCs is first treated in the vapor permeation process, and then the exiting gas stream from the first step is fed to the membrane-based absorption-stripping process as the second step.

A few experiments of this hybrid process were conducted using 6000 ppmv of methylene chloride and nitrogen mixture (Poddar et al., 1997). At a gas flow rate of 60 cc/min, the methylene chloride concentration was reduced to 2 ppmv.

In the current study, attention is focused on the membrane-based absorption-stripping process. The objective is to operate the absorption module at room temperature and the stripping module at a high temperature (above 50 ^{o}C) to improve the overall performance of the regenerative absorption-stripping process proposed by Poddar et al. (1996b). The results were compared with those obtained from the simple membrane-based absorption process using fresh absorbent. Furthermore, a modified absorption-stripping model was used to predict the separation results. The gas mixtures concerned in this work are binary gas mixtures, such as methanol-N_2 and toluene-N_2, and a multicomponent mixture of gasoline vapor constituents (butane, pentane and hexane) and nitrogen. In addition, the temperature dependence of Henry's law constants and diffusivities of VOCs in silicone oil were measured for the simulation purpose. This study prepares the ground for an advanced hybrid process of vapor permeation and regenerative absorption-stripping processes.

CHAPTER 2

THEORY

This chapter is concerned with the theoretical aspects of the process simulation and the principles of measurements of some physical parameters and module characteristics.

2.1 Models for Membrane-Based Absorption and Stripping Process

The principle of membrane-based absorption-stripping process has been introduced in Chapter 1. The mathematical models proposed by Poddar et al. (1996a, 1996b) were modified to accommodate different operating temperatures in the absorption and stripping modules and were used to simulate the separation results obtained with methanol-nitrogen and gasoline-nitrogen systems.

In the models by Poddar et al. (1996a, 1996b), the absorption and stripping processes were considered separately. First, generalized models were developed for absorption and stripping process respectively in hollow fiber modules, and then these two models were coupled together to get the overall results of the combined absorption-stripping process. The models are briefly introduced here.

2.1.1 A General Model for VOC Absorption

In the modules being studied, two different types of fibers are used: porous fiber with no coating and with a nonporous coating on the outer surface. There are two possibilities for the fluid in the pores. It may be either gas or absorbent liquid, depending upon which

type of fibers is used and the operating conditions (pressure difference between gas and liquid phases). In order to apply the model to both fibers, an imaginary fluid was considered to fill the pores of the fibers. The dimensionless Henry's law constant of species i between the gas phase and the imaginary fluid phase is H_{i1} and the one between the imaginary fluid phase and the absorbent phase is H_{i2}.

Countercurrent operating mode is employed. The whole length of the module is divided into n segments with equal length of ΔZ (=L/n). A small segment from the feed exiting end of the module was first considered. The VOC concentrations at the absorbent inlet and feed gas outlet ($C_{ig,out}$) were either known or assumed to have some value. The average entering gas concentration and average exiting absorbent concentration of the segment were obtained by simultaneously solving species mass balance equations for the gas phase and liquid phase and species diffusion equation (if the fibers are coated, a permeation equation must be included) along with appropriate boundary conditions:

$$\langle \phi_{ig} \rangle = \frac{-2\pi\Delta_{ig}P}{n\lambda}(\phi_{im}|_{\xi_o} - H_{i1}\phi_{ig}|_{\xi=1})\left(\frac{D_{ig}L}{\langle V_t \rangle}\right)_{ref} + \phi_{ig,out} \tag{2.1}$$

$$\langle \phi_{il} \rangle = \frac{-2\pi L D_{il} Qe'}{n\langle V_s \rangle[(A\xi_e / \xi_c) - B]}(\phi_{im}|_{\xi_o} - H_{il}\phi_{ig}|_{\xi=1}) + \phi_{il,in} \tag{2.2}$$

Where ϕ_{ig} (= $C_{ig}/C_{ig,in}$), ϕ_{il} (= $C_{il}/C_{ig,in}$), ϕ_{im} (=$C_{im}/C_{ig,in}$) and ξ (=r/r_i) are dimensionless concentrations and dimensionless radius. The dimensionless gas-phase concentration ϕ_{ig} at ξ=1 and membrane-phase concentration ϕ_{im} at $\xi=\xi_o$ are expressed as:

$$\phi_{ig}|_{\xi=1} = \frac{\phi_{ig,out}(QY + H_{i2} + H_{i2}P/a) + 4PX\phi_{il,in}}{QY + H_{i2}(1 + P/a + 4PXH_{il})} \tag{2.3}$$

$$\phi_{im}|_{\xi_o} = \frac{\phi_{ig,out}[H_{i1}QY + (H_{i1}H_{i2}P/a)] + \phi_{il,in}(1 + 4PXH_{i1})}{QY + H_{i2}(1 + P/a + 4PXH_{i1})} \tag{2.4}$$

In the above equations, a, A, B, e', P, Q, X and Y are parameters related to diffusivities of gas and liquid, VOC permeance through the membrane, tortuosity, porosity and geometrical properties of the membrane; they have been defined by Poddar et al. (1996a). $<\phi_{ig}>$ and $<\phi_{il}>$ calculated from the above equations are used as known data for the next segment. The same procedure was repeated up to the last segment. The entering gas concentration for the last segment obtained from the calculation is then compared with the real feed gas concentration. If the difference is within the range of the allowable error, the original assumption of $C_{ig,out}$ is correct. Otherwise another value of $C_{ig,out}$ has to be tried until the error condition is satisfied.

One item to be considered now is what kind of an imaginary fluid is in the pores. Two cases were specified by Poddar et al. (1996a):

Case 1. Absorption in porous fibers

In this case, there is no coating outside the fibers. Under suitable operating conditions, pores of the fibers are filled with the absorbent liquid. So, the imaginary fluid is the absorbent. Thus, $H_{i2}=1$, $H_{i1}= H_i$ $(= C_{il}/C_{ig})$, $D_{if}= D_{il}$ and $\xi_o=\xi_c$.

Case 2. Absorption in skinned fibers

The absorbent could not enter the pores since a nonporous coating exists. The pores must be filled with gas. So, $H_{i1}=1$, $H_{i2}= H_i$ and $D_{if}= D_{igp}$. Here, D_{igp} is the diffusivity of gas species i in the pore.

2.1.2 A General Model for VOC Stripping

The porous fibers with a particular kind of coating were used in the stripping modules. The VOC-containing absorbent liquid obtained at the outlet of the absorption module was allowed to flow through the shell side while vacuum was applied to the tube side. It is

reasonable to suppose that the average VOC concentration in the tube side is a constant along the length of the module because it must be extremely low due to the high vacuum. The dimensionless concentrations were redefined as:

$$\phi_{ig}^{s} = \frac{C_{ig}^{s}}{C_{il,in}^{s}} \quad \text{and} \quad \phi_{il}^{s} = \frac{C_{il}^{s}}{C_{il,in}^{s}} \tag{2.5}$$

A small segment of length ΔZ was first taken from the absorbent inlet end of the module. An analytical solution (equation 2.6) for the average liquid outlet concentration of species i from the segment was obtained by solving the governing equations (Poddar et al., 1996b):

$$\left\langle \phi_{il}^{s} \right\rangle = \phi_{il,in}^{s} - \frac{2\pi (r_o)_{\ln} L_s q_o}{n\delta_o \left\langle V_s \right\rangle} \left[\frac{\phi_{il,in}^{s} - H_i \left\langle \phi_{ig}^{s} \right\rangle}{H_i + a_s Y} \right] \tag{2.6}$$

$$\left\langle \phi_{ig}^{s} \right\rangle = \frac{p_i^{s}}{RTC_{il,in}^{s}} \tag{2.7}$$

Where p_i^s is the partial pressure of species i in the tube side. $\phi^s_{il,in}$ is known for the first segment (=1). The calculated $<\phi^s_{il}>$ is then the $\phi^s_{il,in}$ for the next segment, and so on. The average liquid concentration of species i exiting from the other end of the module is equal to $<\phi^s_{il}>$ for the last segment multiplying the $C^s_{il,in}$ for the first segment.

2.1.3 Calculation Method for Absorption-Stripping at Different Temperatures

The models mentioned above were coupled together to simulate the membrane-based combined absorption-stripping separation process (Poddar, 1995; Poddar et al., 1996b). In the above-metioned program, the temperatures of absorption and stripping were the same. The diffusivities of VOCs in the absorbent as well as Henry's law constants were the same values for the absorption and stripping processes.

This program was modified to accept different absorption and stripping temperatures. First, the correlation of temperature dependence of Henry's Law constant was obtained in the temperature range of about 25-75 °C and different absorption and stripping temperatures were put in the data file. Second, correlations of temperature dependence of VOC diffusivities were measured using the method described in section 2.2.2. These correlations were added to the program for simulation, instead of using the same diffusivity values for absorption and stripping in the data file.

2.2 Principles of Measurements of Physical Parameters

As discussed in section 2.1, the Henry's law constant and diffusivity of VOCs in absorbent are needed as input data for simulation. These parameters were previously measured at room temperature for a few VOCs (Poddar et al., 1996a; Poddar and Sirkar, 1996; Poddar, 1995). But in the present study, the stripping module is operated at temperatures up to 75 °C. Data from Poddar et al. are no longer sufficient.

Generally, the diffusivity of a small species is directly proportional to the temperature and inversely to the liquid viscosity. The widely used correlation for diffusivity is the Wilke-Chang equation (Reid et al., 1977):

$$D_{il} = 7.4 * 10^{-8} \frac{(\phi M_l)^{1/2} T}{\mu_l V_i^{0.6}} \tag{2.8}$$

Here, ϕ: association factor of the absorbent;

M_l: molecular weight of the absorbent;

T: absolute temperature;

μ_l: viscosity of the absorbent;

V_i: molar volume of species i at its normal boiling temperature.

It is well known that Henry's law constant H_i varies with temperature. The dependence may be expressed as:

$$H_i = \exp\left(\frac{B_{Hi}}{T} - A_{Hi}\right) \tag{2.9}$$

where T is the temperature in ^{o}K, A_{Hi} and B_{Hi} are constants. Although A_{Hi} and B_{Hi} values were given by Poddar (1995), it is necessary to verify them experimentally because they were obtained in the temperature range of 25.65-45.9 ^{o}C for toluene, methanol, methylene chloride and acetone.

In order to find out the dependency of these parameters with temperature, the methods used by Poddar and Sirkar (1996) and Poddar (1995) were employed to obtain the experimental values at different temperatures.

2.2.1 Measurement of Henry's Law Constant

Mackay and Shiu (1981) have reviewed three methods of determination of Henry's law constant. The first one concerns vapor pressure and solubility data; it is difficult to obtain the solubility data for the system used in this study. The second one requires direct measurement of the concentrations in gas and liquid phases under equilibrium conditions. This method has a shortcoming in terms of accuracy at low concentrations. The third one uses a batch air stripping technique. It is hard to achieve equilibrium in such a technique. Robbins (1993) presented a new method, called Static Headspace Method. It was adopted in the experiments by Poddar (1995). The principle of measurement of dimensionless Henry's law constant, H_i, was described in this article and is concisely reviewed here.

In this method, chemical and thermal equilibrium must be established within the enclosed sampling vessel when solutes are present at low concentrations.

Applying Henry's law to the equilibrium system, one has

$$C_{il} = H_i C_{ig} \tag{2.10}$$

where H_i is a dimensionless Henry's law constant.

In order to obtain H_i value, a material balance for the system is expressed as

$$V_o C_{io} = V_l C_{il} + V_g C_{ig} \tag{2.11}$$

where V_o, V_g and V_l are the total volume of the sample, and the volumes of headspace and the liquid. C_{io}, C_{ig} and C_{il} are the concentrations corresponding to V_o, V_g and V_l respectively.

Because the vapor pressure of silicone oil and the concentration of VOC in liquid phase are very low so that the evaporation of both VOC and liquid matrix does not affect the liquid volume very much, the assumption of equal values of V_o and V_l is tenable. Substitution of equation 2.10 into 2.11 yields

$$\frac{1}{C_{ig}} = \frac{H_i}{C_{io}} + \frac{1}{C_{io}}\left(\frac{V_g}{V_l}\right) \tag{2.12}$$

A linear relationship exists between vapor concentration, C_{ig}, and the gas chromatograph (GC) area count, A_p:

$$C_{ig} = R_f A_p \tag{2.13}$$

where R_f is the response factor. Combination of equations 2.12 and 2.13 gives:

$$\frac{1}{A_p} = \frac{H_i R_f}{C_{io}} + \frac{R_f}{C_{io}}\left(\frac{V_g}{V_l}\right) \tag{2.14}$$

A plot of $1/A_p$ versus V_g/V_l will be a straight line. H_i can be obtained from the result of dividing the y-intercept by the slope.

2.2.2 Measurement of the Diffusivity of VOC through Silicone Oil

The diffusivity of VOC through the absorbent liquid is a basic design parameter in a membrane-based absorption-stripping process. Various sources for calculating the diffusivity of a particular species in a liquid were summarized in a paper (Poddar et al., 1996a). In this study, the diffusivities of VOCs in silicone oil and paratherm oil were indirectly measured by means of experiments of vapor permeation in a microporous hollow fiber module at room temperature. The absorbent was first immobilized in the pores of the microporous hollow fibers. The VOC gas mixture was introduced to the tube side of the module while a sweeping gas (nitrogen) was conducted to the shell side to facilitate the VOC permeation. The mathematical model for prediction of the diffusivity is based on a special case of the VOC absorption model, i.e. case 1, in which the imaginary fluid is the absorbent and the liquid in the shell side is modified to the sweeping gas. Therefore, $H_{i1}=H_{i2}=H_i$. The interfacial concentrations become:

$$\phi_{isp}\Big|_{\xi_o} = \frac{\phi_{ig,out} H_i QY + \phi_{isp,in}(1+4PXH_i)}{QYH_i + H_i^2(1+4PXH_i)} \tag{2.15}$$

and

$$\phi_{ig}\Big|_{\xi=1} = \frac{\phi_{ig,out}(H_i + QY) + 4PX\phi_{isp,in}}{QY + H_i(1+4PXH_i)} \tag{2.16}$$

where ϕ_{isp} is the sweeping gas concentration. The analytical solutions were obtained for a small segment of length ΔZ and used stepwise from the feed gas outlet to the feed gas inlet. A value of D_{il} value was first assumed and then verified by comparing the real feed gas concentration with the calculated feed gas concentration.

2.3 Measurement of the Module Characteristics

There are two parameters that determine the performance efficiency of a given membrane: selectivity (or separation factor) and flux (or permeability).

The permeability, Q_i, or q_i, is a very characteristic membrane parameter for a given species i; it is often described as an intrinsic parameter. It is defined in terms of the steady-state volumetric or molar flux of species i, J_i, or j_i, and the pressure or concentration driving force, Δp_i or ΔC_i, normalized by the membrane thickness , δ,

$$Q_i=J_i/(\Delta p_i/\delta) \quad \text{or} \quad q_i=j_i/(\Delta C_i/\delta) \tag{2.17}$$

The units of Q_i and q_i are cm^3(S.T.P.).cm/(cm^2.in Hg.s) and cm^2/s respectively. The quantity actually measured from experiments is often the permeance, Q_i/δ or q_i/δ, which is the ratio of the species permeability to the membrane thickness in the unit of cm^3(S.T.P.)/(cm^2.in Hg.s) or cm/s.

Membrane selectivity towards gas mixtures (or separation factor) is usually expressed in terms of a separation factor α_{ij}:

$$\alpha_{ij}=(y_i/y_j)/(x_i/x_j) \tag{2.18}$$

where y_i, x_i, y_j, x_j refer to the mole fraction of components i and j in the product and feed streams, respectively.

The ideal separation factor is given by the ratio of the permeabilities:

$$\alpha_{ij}^{*} = Q_i / Q_j \tag{2.19}$$

For a successful separation, the separation factor must be much greater than unity. If $\alpha_{ij}=1$, no separation is achieved.

The permeance and separation factor of membranes can be measured through vapor permeation experiments described in Chapter 3. The permeance can be calculated simply from experimental data by equation 2.17. For the separation factor measurement, the

configuration shown in Figure 2.1 is employed. In the above gas permeation mode of operation, one end of the permeate side was closed. The corresponding concentrations of the streams are identified in Figure 2.1. Three gas stream concentrations were known or analyzed; the permeate concentration at the closed end, $y_{i,in}$, can be expressed as follows by the cross flow criterion:

$$\frac{y_{i,in}}{1-y_{i,in}} = \frac{\alpha_{ij}^{*}(x_{i,out} - \gamma y_{i,in})}{(1-x_{i,out}) - \gamma(1-y_{i,in})} \tag{2.20}$$

where

$$\gamma = \frac{p_p}{p_F} \tag{2.21}$$

$$\alpha_{ij}^{*} = \frac{(Q_i/\delta)}{(Q_j/\delta)} \tag{2.22}$$

The logarithmic mean pressure-driving force is given by:

$$\Delta p_{\ln,i} = \frac{(p_F x_{i,in} - p_p y_{i,out}) - (p_F x_{i,out} - p_p y_{i,in})}{\ln \dfrac{(p_F x_{i,in} - p_p y_{i,out})}{(p_F x_{i,out} - p_p y_{i,in})}} \tag{2.23}$$

The overall separation factor can be calculated from the following equation:

$$\alpha_{CO_2/N_2} = \frac{(F_p y_{CO_2,out} / \Delta p_{\ln,CO_2})}{(F_p y_{N_2,out} / \Delta p_{\ln,N_2})} \tag{2.24}$$

where F_p is the volumetric gas flow rate from the permeate side (cc/min).

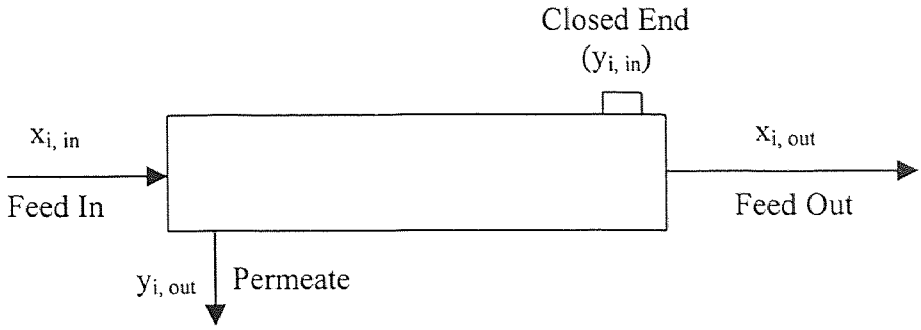

Figure 2.1 Schematic for Measurement of Separation Factor

CHAPTER 3

EXPERIMENTAL

3.1 Chemicals

Silicone oil (200 fluid, Dow Corning, Midland, MI) was used as an absorbent liquid. Paratherm heat transfer fluid (NF™, Paratherm Corporation, Conshohocken, PA) was used as bath fluid for the cooling bath.

The properties of these two chemicals are listed in Table 3.1

Table 3.1 Properties of Silicone and Paratherm Oil

Properties	Silicone Oil	Paratherm Oil
Chemical name	Polydimethylsiloxane	-
Molecular weight	300 (avg)	350 (avg)
Density	0.98 @ 77°C	0.87 @ 77°C
Viscosity	50 cs @ 77°C	35 cp @ 77°C
Vapor pressure	< 5mm Hg @ 77°C	0.001 mm Hg @ 100°C 0.026 mm Hg @ 200°C
Surface Tension	-	28 dynes/cm @ 77°C
Flash point	605 °F	-
pour point	-94 °F	-45 °F
Melt point	-42	-
Refractive index	1.402	1.4768
Appearance	Colorless, clear liquid	Colorless, clear liquid
Other properties	Nontoxic, nonbioactive, nonstinging to skin, high oxidation resistance	Nontoxic, FDA/USDA approved for use in food and pharmaceuticals

The following chemicals were used for determination of Henry's law constant:

1. Methanol, HPLC grade (Fisher Scientific, Springfield, NJ);
2. Toluene, certified A. C. S. (Fisher Scientific, Springfield, NJ);
3. Pentane, HPLC grade (Sigma-Aldrich, St. Louis, MO);
4. Hexane, HPLC grade (Fisher Scientific, Springfield, NJ).

3.2 Gases

Separation experiments were carried out with the following gas mixtures:

1. Toluene: 940 ppmv, balance nitrogen (Matheson, Rutherford, NJ);
2. Methanol: 1100 ppmv, balance nitrogen (Matheson, Rutherford, NJ);
3. Butane: 9840 ppmv; pentane: 2740 ppmv; hexane: 314 ppmv; balance nitrogen (Matheson, Rutherford, NJ).

The following gases were used to characterize the membrane modules:

1. Nitrogen zero (Matheson, Rutherford, NJ);
2. Carbon dioxide, bone dry (Matheson, Rutherford, NJ);
3. Carbon dioxide-Nitrogen mixture with 5.04 % CO_2 (Matheson, Rutherford, NJ).

3.3 Modules

A total of seven modules were utilized in various experiments. Geometric characteristics of the modules are provided in Table 3.2. Module EPA/AS-1, which has no coating, was always used for absorption. Other modules were used for stripping or permeance measurement.

Table 3.2 Geometrical Characteristics of Different Hollow Fiber Modules Used in the Experiments

Module No.	Type of Fiber	Type of Coating	Fiber ID/OD (μm)	Effective Length (cm)	Shell ID (cm)	No.of Fibers	Void Fraction (%)	Mass Transfer Area (cm^2)	Mass Transfer Area/Volume (cm^2/cm^3)
EPA/AS-1	Celgard X-10	None	100/150	31.0	0.37	102	83.23	149.00	44.70
EPA/AS-2	Celgard X-10	Silicone	240/300	20.5	0.80	300	57.81	579.62	56.25
EPA/AS-3	KPF-205	Silicone Fluoro-polymer	210/266	30	0.37	106	45.21	265.60	82.38
EPA/AS-4	KPF-205	Silicone Fluoro-polymer	210/266	30.48	0.635	300	47.35	764.13	79.16
EPA/AS-5	KPF-205	Silicone	210/266	30.48	0.635	300	47.35	764.13	79.16
EPA/AS-6	KPF-205	Silicone	210/266	20.0	0.635	300	47.35	501.40	79.16
EPA/AS-7	Celgard X-10	Silicone	210/266	20.0	0.636	300	47.35	501.4	79.16

3.4 Experimental Setup and Procedure for Absorption Experiment and Spent-Oil Regeneration

3.4.1 Experimental Setup and Procedure for Absorption Experiment

Figure 3.1 shows the schematic diagram of the setup for absorption. Before passing the absorbent through the dried module (porous hollow fiber with no skin), it was wetted by dropping some absorbent into the shell side. A specific gas mixture was passed through the tube side of the absorption module countercurrent to the absorbent flow. The gas flow rate was controlled by a mass flow transducer (Model 8102-1451, Matheson, E. Rutherford, NJ) and a flow controller (Model 8209, Matheson, E. Rutherford, NJ). The actual value was measured by a bubble flow meter. Fresh absorbent was pumped from an absorbent container to the shell side of the absorption module and then to a spent-absorbent collector by a metering pump (10313M, LMI, Milton Roy, Acton, MA). The absorbent flow rate was adjusted via the pump pulse and stroke. A bypass pipe filled with air was located at the liquid inlet line of the absorption module to reduce the pressure pulsing. Gas pressure in the absorption module was maintained about 3 psi higher than the absorbent pressure by adjusting a back pressure regulator (Model 10BP, Fairchild, Rochelle Park, NJ) to keep the gas-liquid interface at the pore mouth of the inner tube wall of the fiber. To protect the GC column from accidental oil leakage, an oil-trap was placed downstream of the gas after the module. The purified gas was introduced to the GC (HP5890 Series II, Hewlett Packard, Wilmington, DE) to analyze the composition. All experiments were run at room temperature.

The GC operating parameters and analytical parameters are listed in Tables 3.3 and 3.4 respectively. VOC-nitrogen mixture was injected into the GC column through an autosampling valve that was controlled by nitrogen zero gas at 80 psig. Flame ionization

AC: ABSORBENT CONTAINER
BFM: BUBBLE FLOW METER
BPR: BACK PRESSURE REGULATOR
FC: FLOW CONTROLLER
GC: GAS CHROMATOGRAPH
GMC: GAS MIXTURE CYLINDER
HFAM: HOLLOW FIBER ABSORPTION MODULE
MP: METERING PUMP
OT: OIL TRAP
PG: PRESSURE GAUGE
SP: SAMPLING PORT
T: THERMOMETER
TWV: THREE WAY VALVE

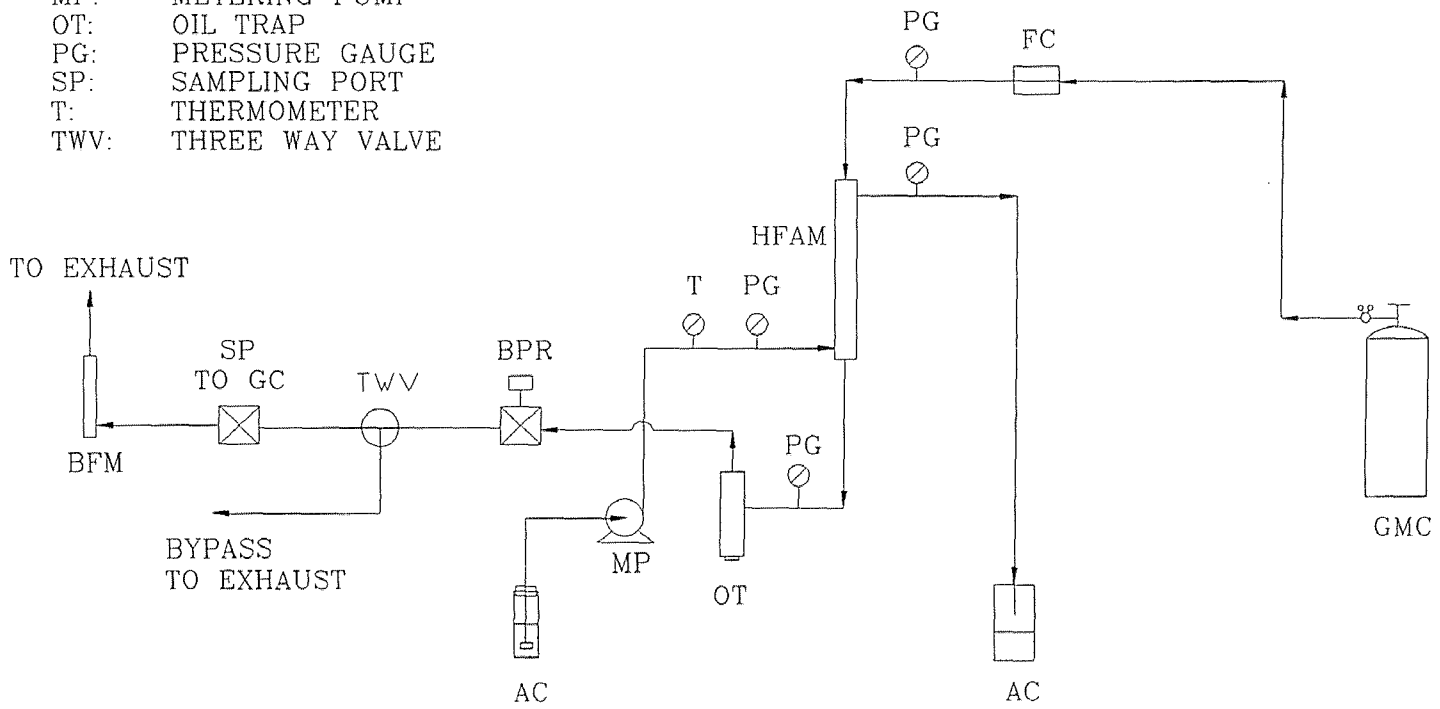

Figure 3.1 Schematic Diagram of Absorption

detector along with an 8'x1/8" packed column (Carbograph, 60/80 mesh) was used to analyze the volatile organic components. The calibration curves for VOCs were generated in the following manner. A VOC-nitrogen mixture at a high concentration level from a gas cylinder was mixed with nitrogen zero gas to get different VOC mixtures of low concentration level (Figure 3.2). The resulting gas mixture was then sent to the GC and the response was recorded by an integrator (HP 3396 Series II, Hewlett Packard, Wilmington, DE). Calibration results are plotted in Figures 3.3-3.10.

Table 3.3 Operating Parameters of GC (HP5890 Series II) for Detecting Various VOCs

VOC	Column Temperature (°C)	Injector Temperature (°C)	Detector temperature (°C)
Butane, Pentane, Hexane, Methanol	150	200	200
Toluene	200	200	200

Table 3.4 Operating Parameters for Analytical Gases Used in GC (HP5890 Series II)

	Gas	Flow rate, cc/min
Gas 1 for FID	Air Zero	300
Gas 2 for FID	Hydrogen Zero	30
Carrier Gas	Helium Zero	30

3.4.2 Spent-Oil Regeneration for Oil Reuse

In this series of experiments, a large amount of fresh oil was consumed. From the viewpoint of saving oil, the spent-oil must be regenerated in a certain manner.

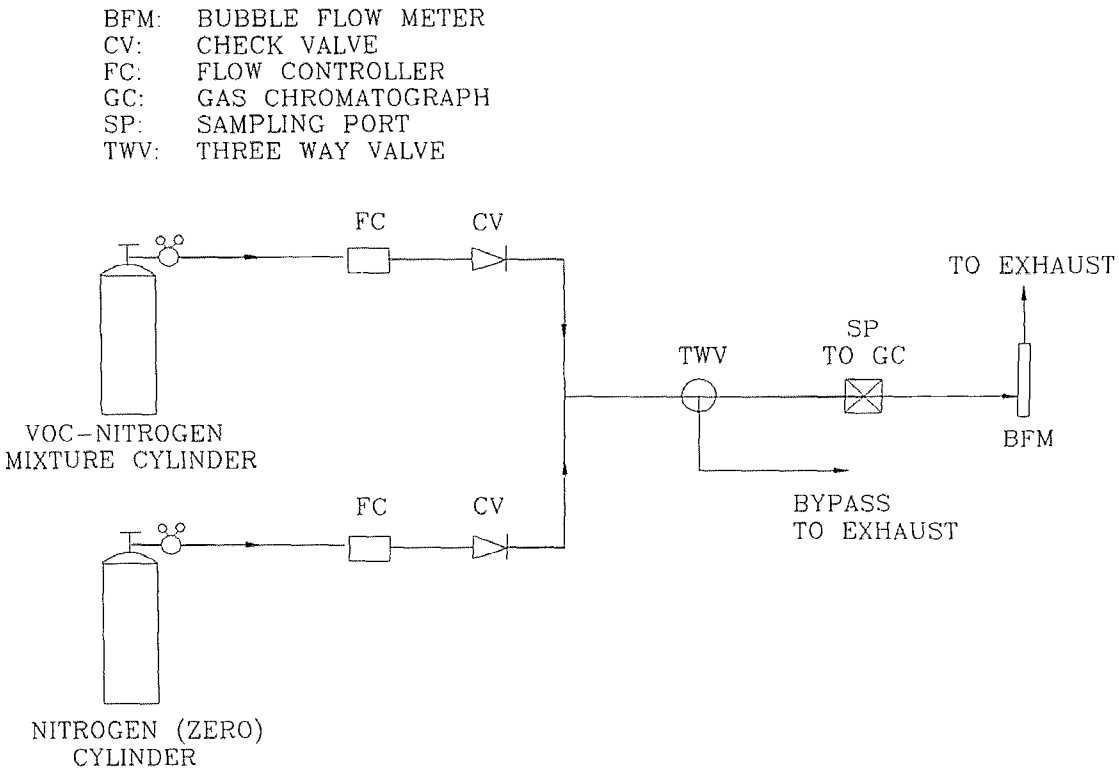

Figure 3.2 Schematic Diagram for Calibration Setup

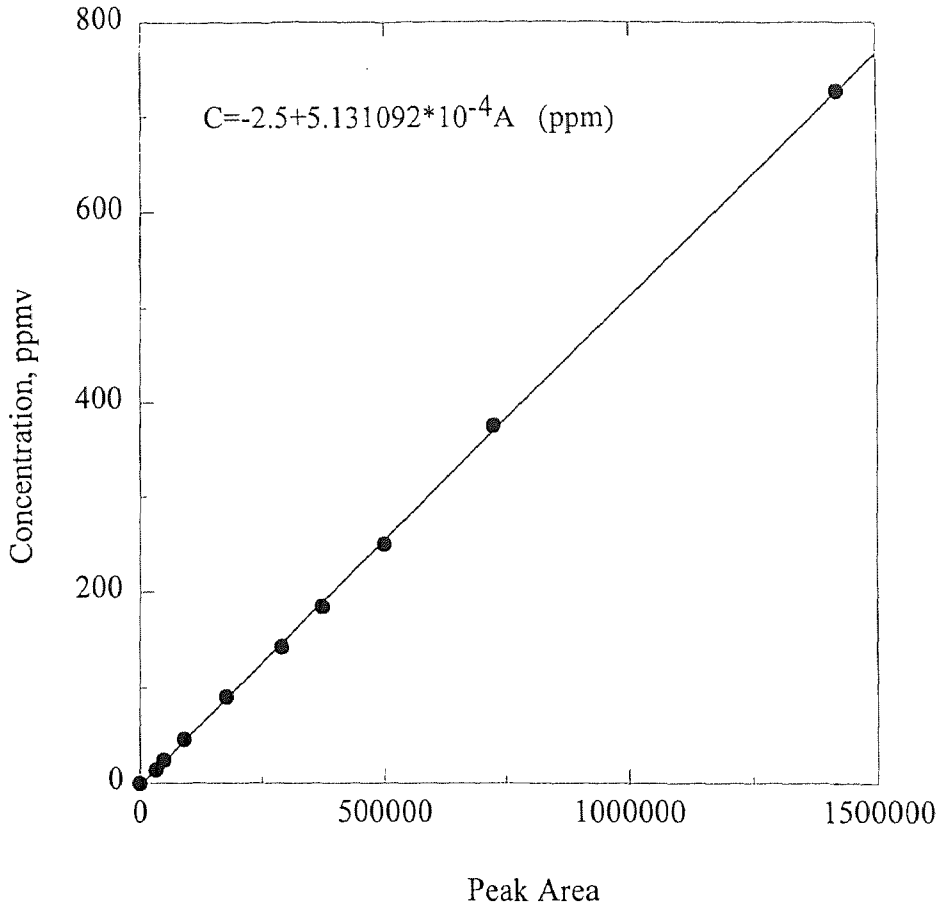

Figure 3.3 Calibration Curve for Butane at Low Concentrations

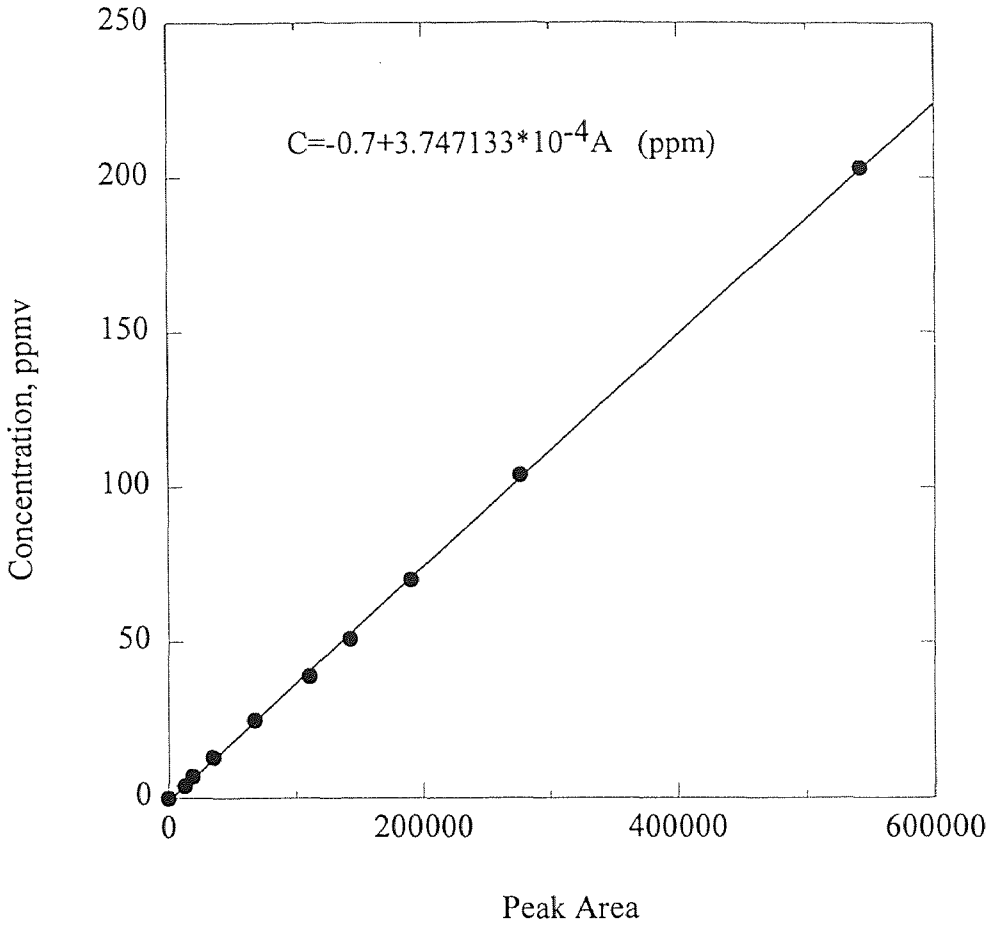

Figure 3.4 Calibration Curve for Pentane at Low Concentrations

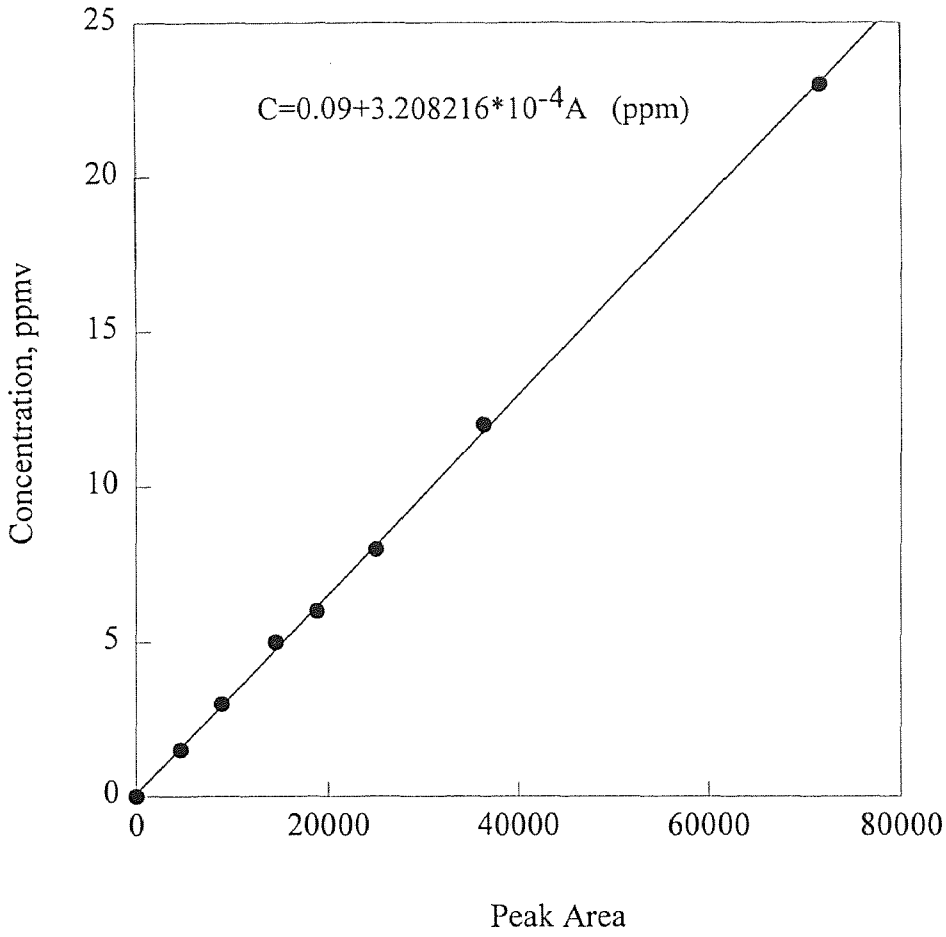

Figure 3.5 Calibration Curve for Hexane at Low Concentrations

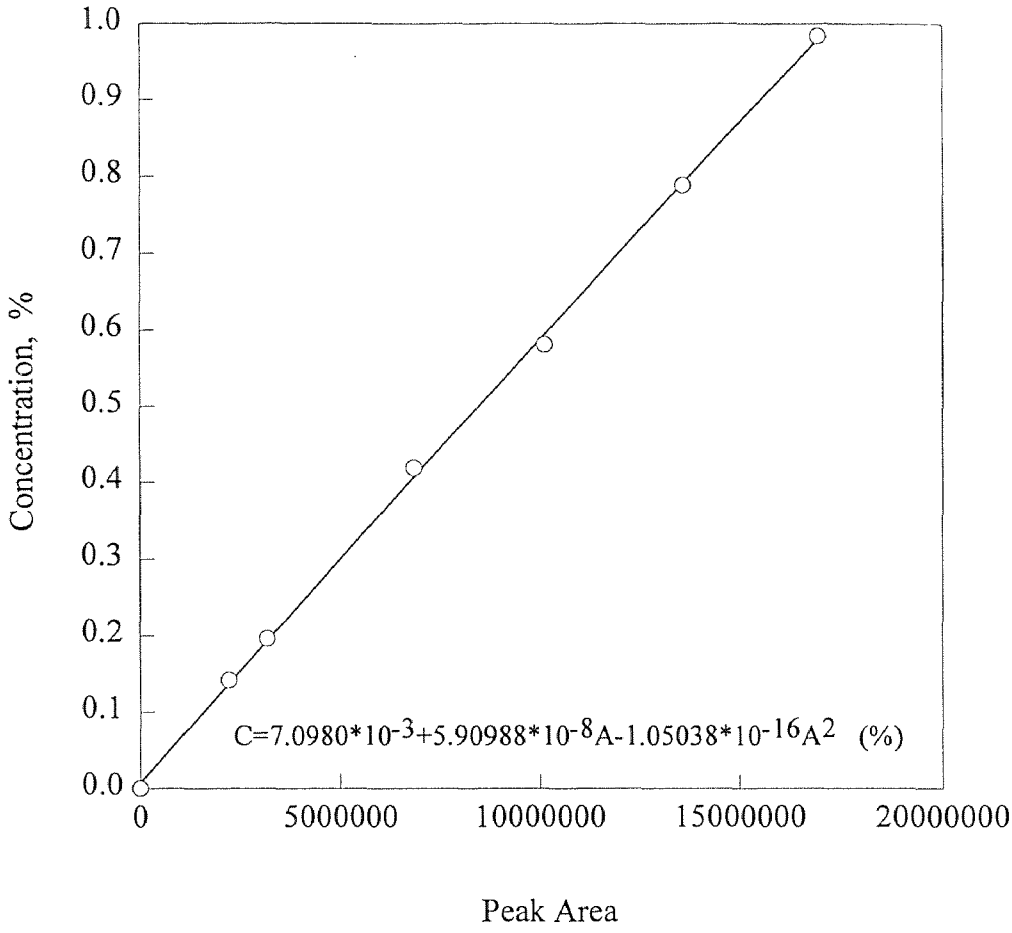

Figure 3.6 Calibration Curve for Butane at High Concentrations

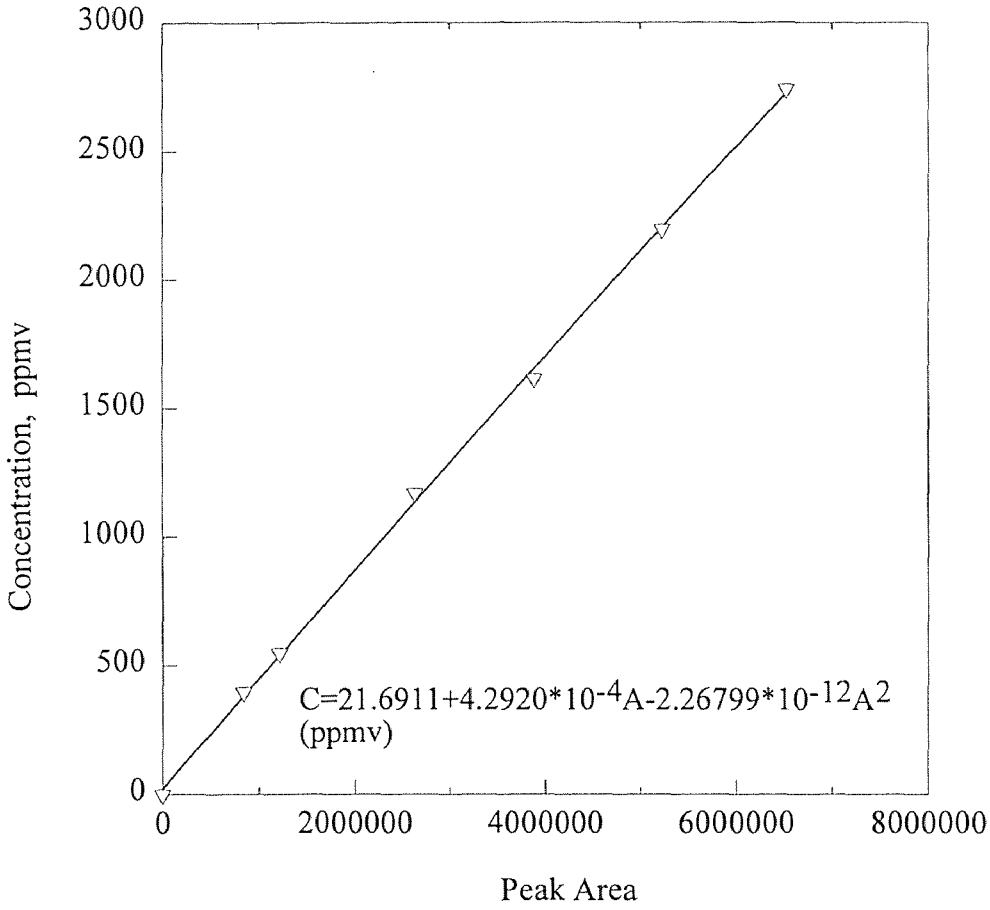

Figure 3.7 Calibration Curve for Pentane at High Concentrations

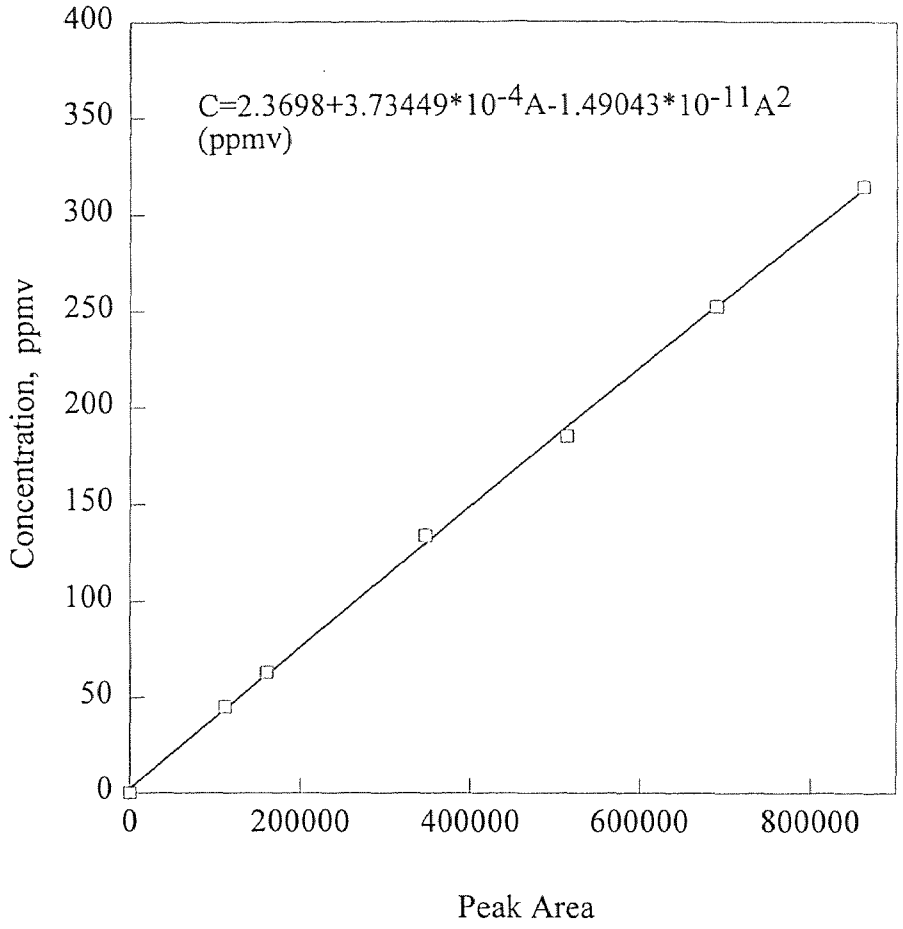

Figure 3.8 Calibration Curve for Hexane at High Concentrations

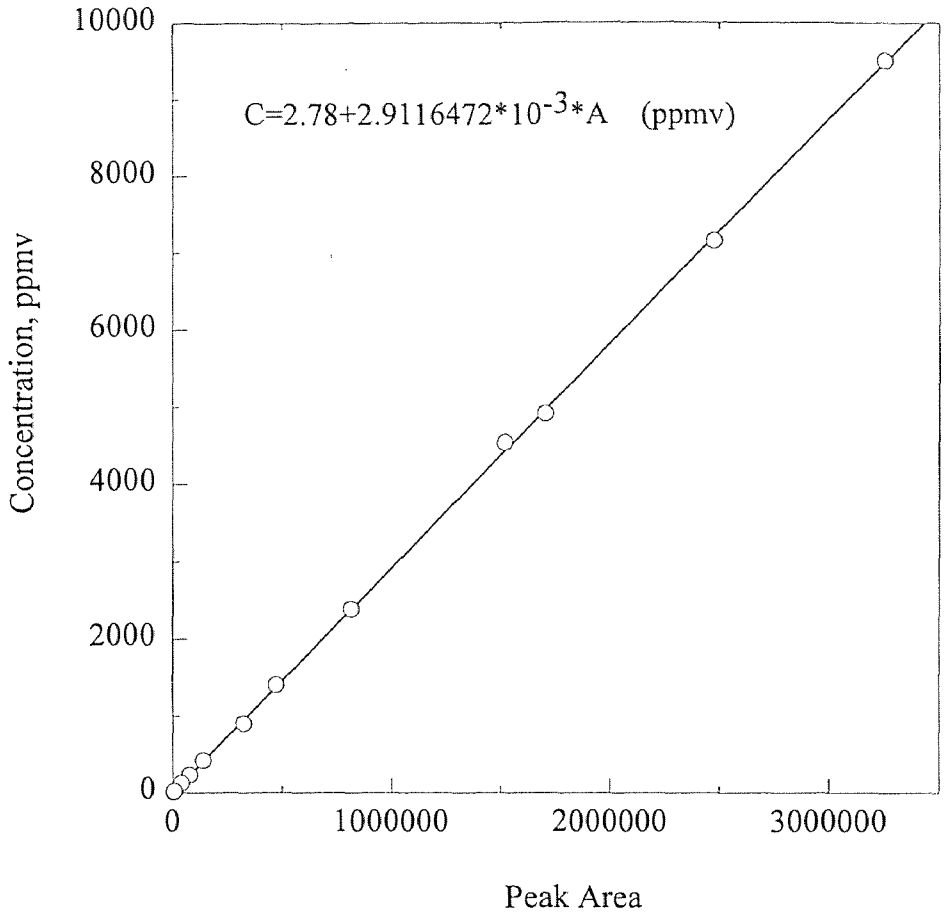

Figure 3.9 Calibration Curve for Methanol

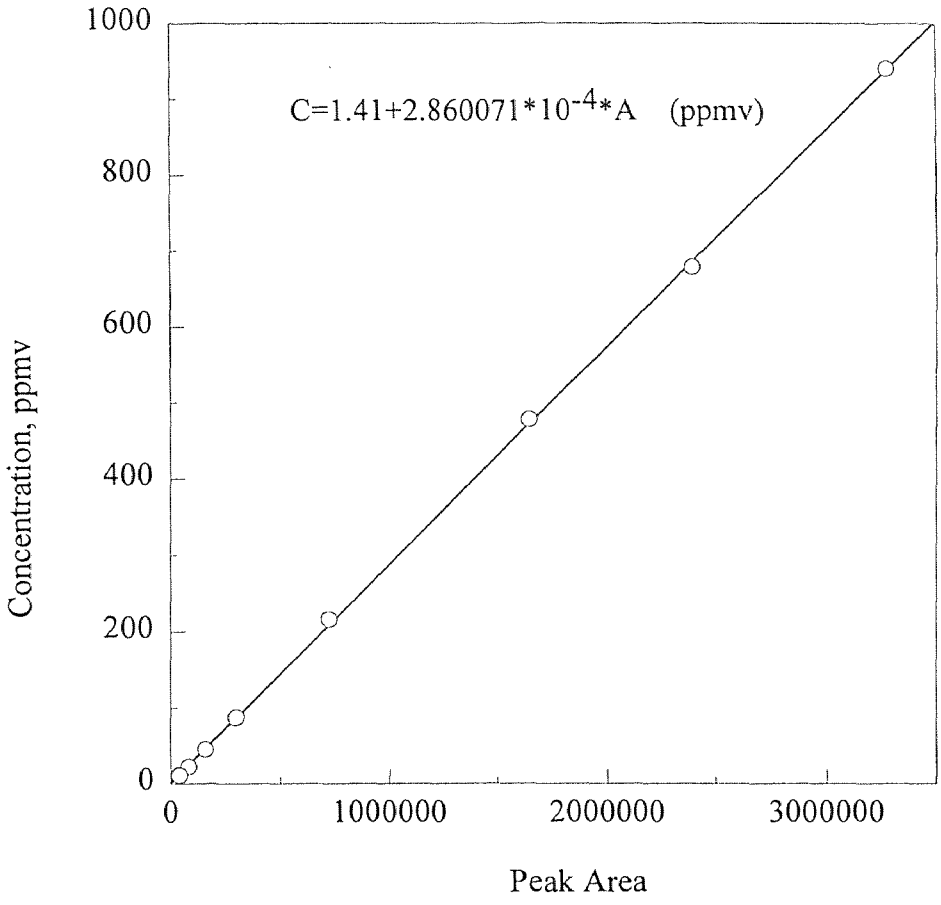

Figure 3.10 Calibration Curve for Toluene

To regenerate the absorbent, the silicone oil was placed in a pressure vessel; a vacuum was applied and small amount of air was allowed to bubble through the oil for about two days. Then pure nitrogen gas was introduced through the pressure vessel and the exit gas was injected to the GC to see if any contaminant can be detected (Figure 3.11). If not, the absorbent was ready for reuse.

3.5 Experimental Setup and Procedure for Combined Absorption-Stripping

The schematic diagram of the setup for combined absorption-stripping runs at room temperature is illustrated in Figures 3.12 and 3.13. It is similar to that of the absorption setup. The difference is that one or two modules are needed in series as the stripper. The absorbent was pumped from an absorbent container to the shell side of the absorption module and stripping module(s) sequentially and returned to the absorbent container for recirculation. To regenerate the absorbent, vacuum was applied to the tube side(s) of the stripping module(s).

3.6 Experimental Setup and Procedure for Combined Absorption-Stripping with Heating-Cooling System

As shown in Figure 3.14, a heater and a cooler were added to the combined absorption-stripping setup. The heating tape was wrapped outside the copper tubing through which the absorbent was flowing. An immersion chiller (Cole-Parmer, Niles, Illinois) with flexible corrugated probe was used to cool down the absorbent. A coiled copper tubing from the outlet of the stripping module was placed into the cooling bath. The bath fluid used in this study was Paratherm oil. The inlet temperatures of the absorption module and the stripping module were measured by thermometers.

CE: CLOSED END
HF: HOLLOW FIBER
HFM: HOLLOW FIBER MODULE
PG: PRESSURE GAUGE
PP PRESSURE POT
PR PRESSURE REGULATOR
TLP: THREE LAYER PORTING
V: VALVE

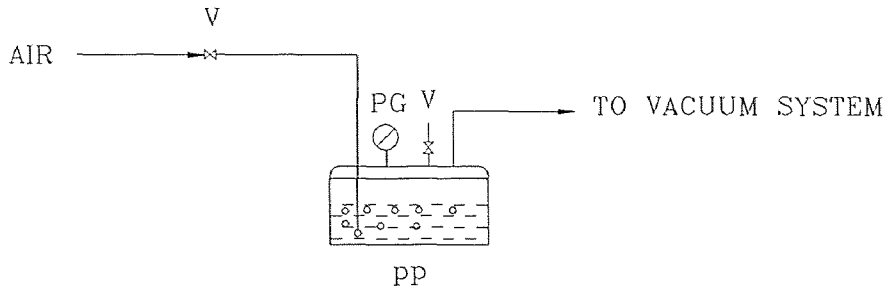

A. ABSORBENT REGENERATION

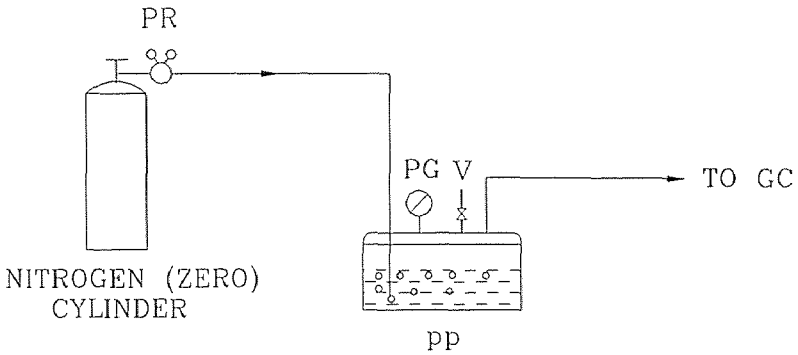

B. TEST FOR CONTAIMINENTS IN ABSORBENT

Figure 3.11 Schematic Diagram for Absorbent Regeneration

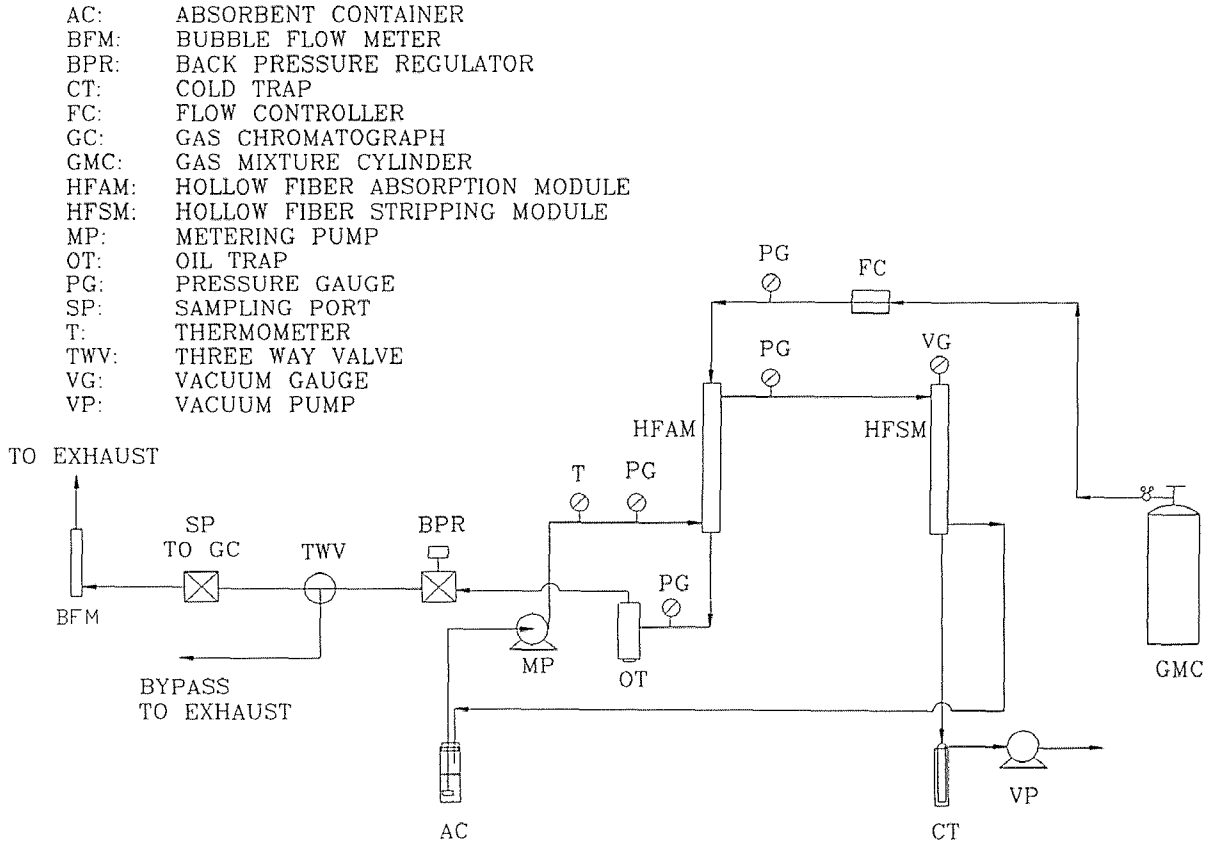

Figure 3.12 Schematic Diagram of Combined Absorption-Stripping

AC: ABSORBENT CONTAINER
BFM: BUBBLE FLOW METER
BPR: BACK PRESSURE REGULATOR
CT: COLD TRAP
FC: FLOW CONTROLLER
GC: GAS CHROMATOGRAPH
GMC: GAS MIXTURE CYLINDER
HFAM: HOLLOW FIBER ABSORPTION MODULE
HFSM: HOLLOW FIBER STRIPPING MODULE
MP: METERING PUMP
OT: OIL TRAP
PG: PRESSURE GAUGE
SP: SAMPLING PORT
T: THERMOMETER
TWV: THREE WAY VALVE
VG: VACUUM GAUGE
VP: VACUUM PUMP

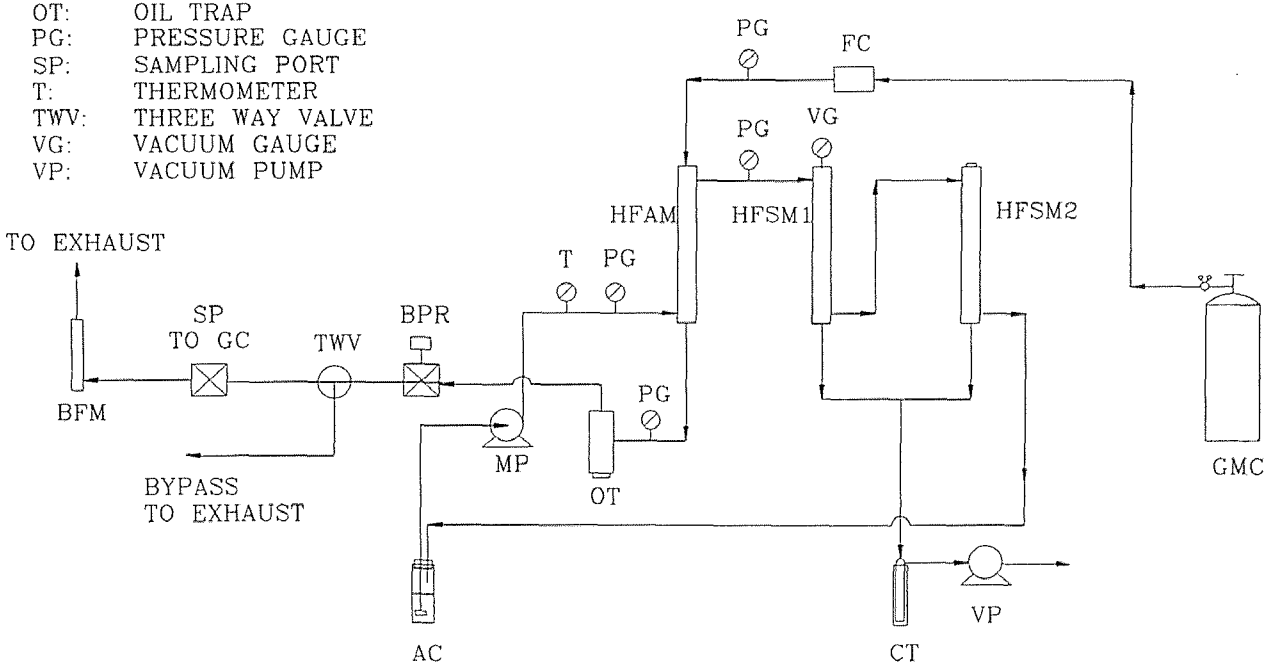

Figure 3.13 Schematic Diagram of Combined Absorption-Stripping (Two Stripping Modules in Series)

AC: ABSORBENT CONTAINER
BFM: BUBBLE FLOW METER
BPR: BACK PRESSURE REGULATOR
CT: COLD TRAP
FC: FLOW CONTROLLER
GC: GAS CHROMATOGRAPH
GMC: GAS MIXTURE CYLINDER
HFAM: HOLLOW FIBER ABSORPTION MODULE
HFSM: HOLLOW FIBER STRIPPING MODULE
MP: METERING PUMP
OT: OIL TRAP
PG: PRESSURE GAUGE
SP: SAMPLING PORT
T: THERMOMETER
TWV: THREE WAY VALVE
VG: VACUUM GAUGE
VP: VACUUM PUMP

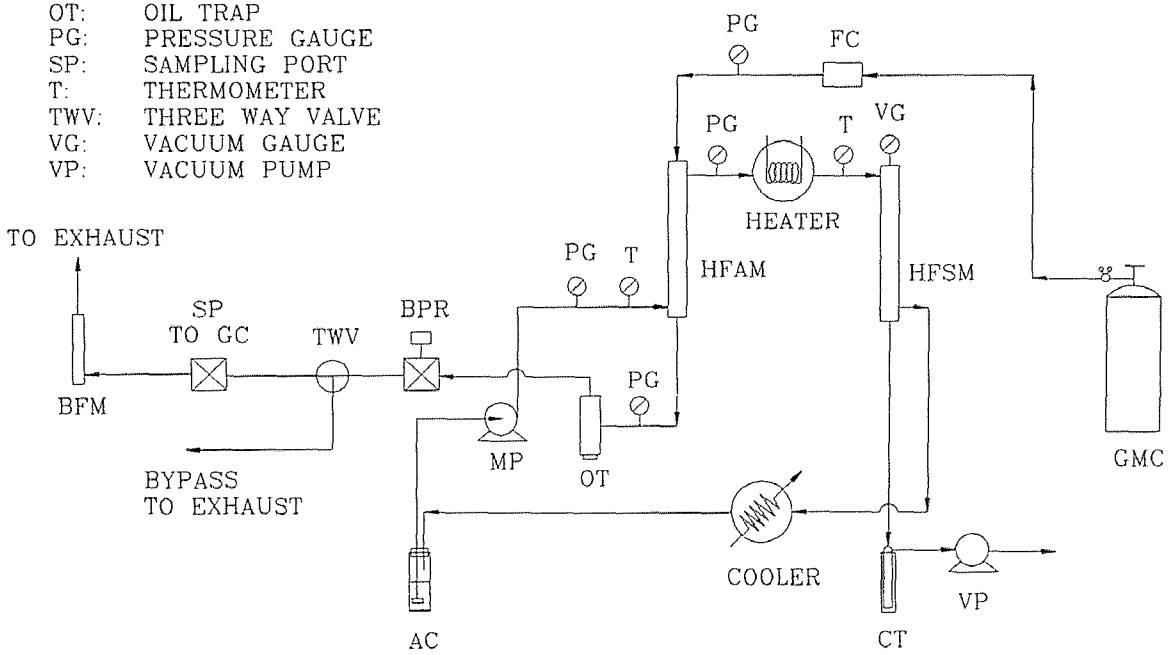

Figure 3.14 Schematic Diagram of Combined Absorption-Stripping with Heating-Cooling System

3.7 Measurement of Henry's Law Constant

As mentioned before, Henry's law constant is required for theoretical prediction of the extent of VOC removal by membrane-based absorption-stripping processes.

In the experiment, silicone oil and a specific VOC liquid were first chilled in a refrigerator. Then both were taken out and put in an ice bath for preparation of the stock solution. The stock solution was made by mixing a certain amount of the VOC liquid and the silicone oil. The concentrations of the solution were about 150 ppmv for toluene, 1000 ppmv for methanol, pentane and hexane respectively, depending upon the magnitude of the GC response. Different volumes of stock solution were taken and added into different sample vials, and immediately sealed. The exact volume of the solution added to the vial, V_l, is calculated from the weight of the solution divided by the density of it which is given in Poddar and Sirkar (1996):

$$\rho_l = 0.980 - 8.356 * 10^{-4} t \tag{3.1}$$

where t is the temperature in $^{\circ}C$.

The headspace volume, V_g, is equal to the difference between the volume of empty vial, V_t (22 ml), and the volume of the solution, V_l.

The sample vials thus prepared were put into the headspace autosampler. GC (Varian Star 3400, Sugarland, TX) having a 6'x1/8" column (0.3% carbowax 20 M) was connected to the Headspace device (Tekmar 7000, Cincinnati, OH) to analyze the concentration (to get the response area count). The operating parameters of the GC and the headspace sampler for all VOCs studied are listed in Tables 3.5, 3.6 and 3.7.

One of the important parameters for the headspace sampler is the equilibration time. During this time the solvent in the liquid phase is evaporated into the gas phase. Initially, as the equilibration time increases, the GC area count increases. After some time, the GC

Table 3.5 Operating Parameters of GC (Varian Star 3400) for Detecting Various VOCs

VOC	Column Temperature (°C)	Injector Temperature (°C)	Detector temperature (°C)
Pentane, Hexane, Methanol, Toluene	150	220	250

Table 3.6 Operating Parameters for Analytical Gases Used in GC (Varian Star 3400)

	Gas	Flow rate
Gas 1 for FID	Air Zero	300
Gas 2 for FID	Hydrogen Zero	30
Carrier Gas	Nitrogen Zero	30

Table 3.7 Operating Parameters of Headspace Autosampler

Platten Equilibration Time	0.5 min.
Sample Equilibration Time	25~40 min.
Mixing Time	0.1 min.
Mixing Power	1
Stabilization Time	0.5 min.
Sample Vial Pressure	3.5 psig
pressurization Time	0.15 min.
pressure Equilibrium Time	0.15 min.
Loop Fill Time	0.12 min.
Loop Equilibration Time	0.15 min.
Injection Time	3.00 min.

area count reaches a constant value. So, sufficient time must be provided to allow the sample to reach the equilibrium state. From Figure 3.15, one could see that the area count is almost constant after 20 minutes. So, the optimum equilibration time is set to be 25 minutes for both pentane and hexane. The equilibration time for toluene and methanol was determined by Poddar and Sirkar (1996) to be 40 minutes.

3.8 Experimental Setup and Procedure for Measurement of VOC Diffusivity in Silicone Oil

Like Henry's law constant, the diffusivity of the VOC in silicone oil is a necessary physical parameter in the simulation of the separation process under consideration. Experiments were carried out in order to get diffusivities of VOCs in silicone oil at high temperatures.

Module EPA/AS-1 was taken off from the previous experimental setup and filled with fresh silicone oil in the shell side. The oil was then drained. The module thus prepared was then put in the setup shown in Figure 3.16. The whole module was immersed in a heating bath for maintaining the temperature at a high value. The bath fluid (water) was heated up to a certain temperature by an electrical heater (HAAKE E52). A specific VOC-containing gas mixture at a fixed flow rate and a pressure of 5 psig (regulated by a back pressure regulator) was passed through the tube side of the module while nitrogen zero gas was conducted through the shell side of the module countercurrently with the VOC mixture flow. The flow rates of the VOC-N_2 mixture and the sweeping gas were measured by bubble flow meters. A sample of the spent feed stream was injected to the GC (HP 5890 Series II) to analyze the VOC concentration. The diffusivity was calculated using a computer program available in Poddar (1995).

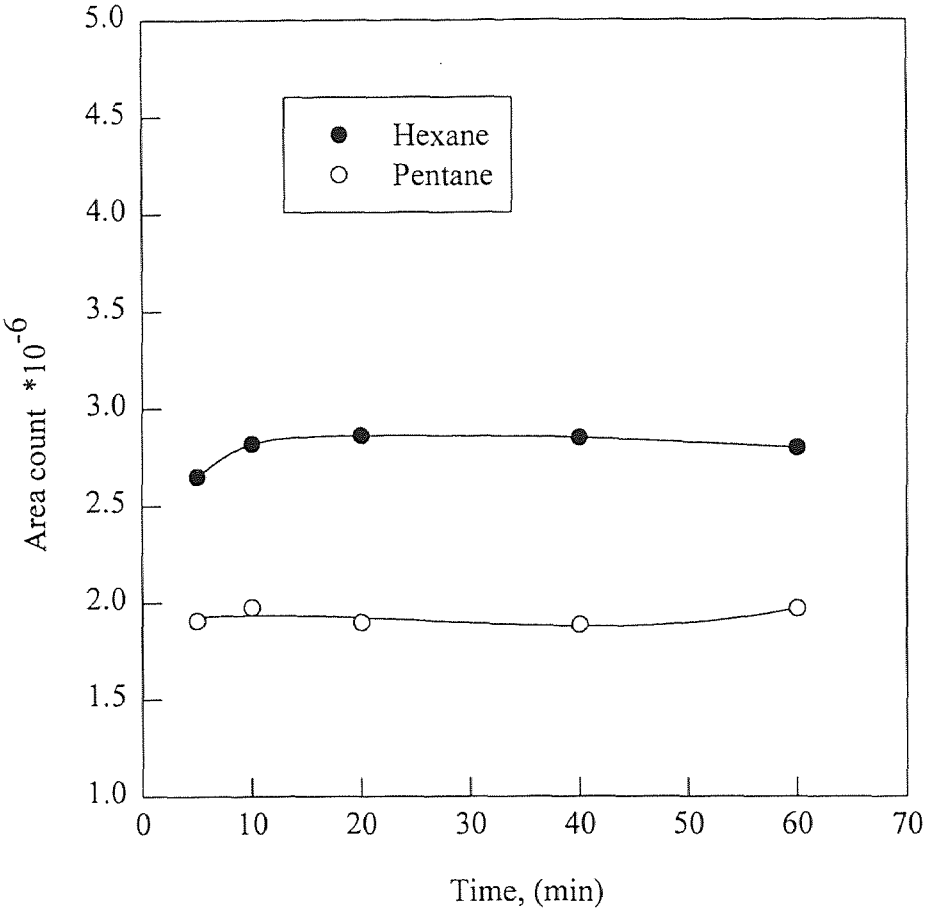

Figure 3.15 Time vs. Headspace VOC Concentration (in Terms of Area Count)

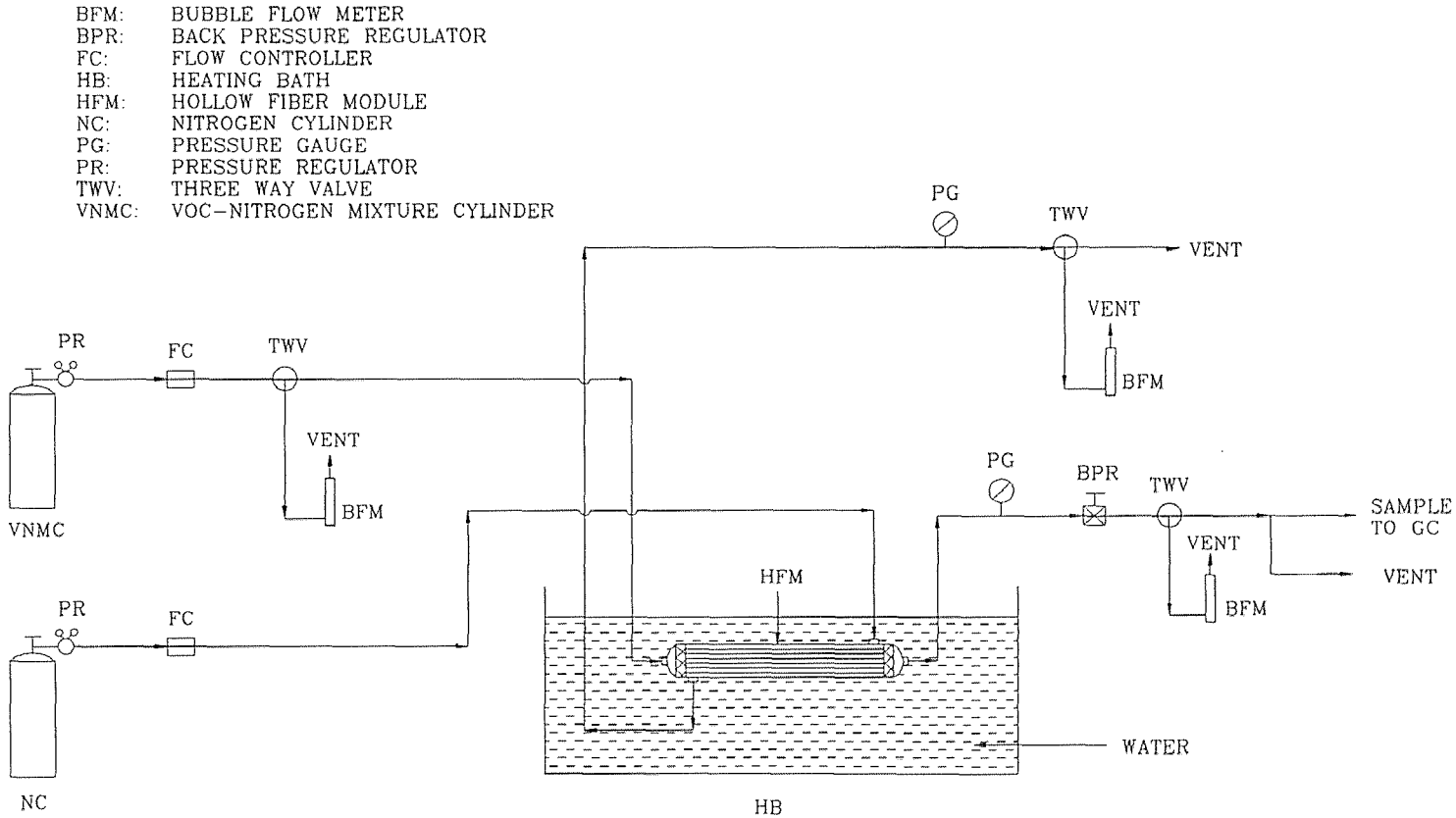

Figure 3.16 Schematic Diagram for Determination of VOC Diffusivity through Silicone Oil

3.9 Measurement of Module Characteristics

The permeability (or permeance) and separation factor of membranes can be measured through vapor permeation experiments as indicated below.

3.9.1 Measurements of Nitrogen or Carbon Dioxide Permeance

Figure 3.17 provides the experimental scheme for nitrogen or carbon dioxide permeation. The N_2 or CO_2 gas at a fixed pressure (10, 15, or 20 psig) was passed through the tube (or shell) side of the module. The flow rate on the permeate side was measured by a bubble flow meter. The permeance was calculated by equation 2.17.

For the measurement of the VOC permeance, VOC-N_2 mixtures were used. The setup is similar to that for the measurement of separation factors as shown in the following section. The calculation procedure is more complicated. A computer program is available in Poddar (1995).

3.9.2 Measurement of the Separation Factor

The setup for the measurement of the separation factor is shown in Figure 3.18. A specific CO_2/N_2 gas mixture was connected to the tube side of the module. A fixed gas pressure (15 psig) at the feed side was maintained by adjusting the back pressure regulator. The feed gas flow rate was set to an appropriate value. The flow rates of the feed, retentate, and permeate gas streams were measured by bubble flow meters. The retentate and permeate streams were sent to GC to analyze the CO_2 and N_2 concentrations.

BFM: BUBBLE FLOW METER
CE: CLOSED END
GC: GAS CYLINDER
HFM: HOLLOW FIBER MODULE
PG: PRESSURE GAUGE
PR: PRESSURE REGULATOR

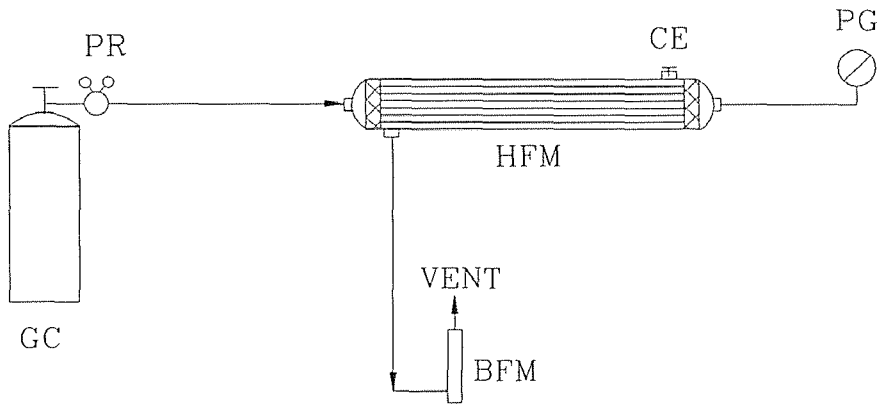

Figure 3.17 Schematic Diagram of Nitrogen or Carbon Dioxide Permeation

BFM: BUBBLE FLOW METER
BPR: BACK PRESSURE REGULATOR
CE: CLOSED END
FC: FLOW CONTROLLER
GMC: GAS MIXTURE CYLINDER
HFM: HOLLOW FIBER MODULE
PG: PRESSURE GAUGE
PR: PRESSURE REGULATOR
TWV: THREE WAY VALVE

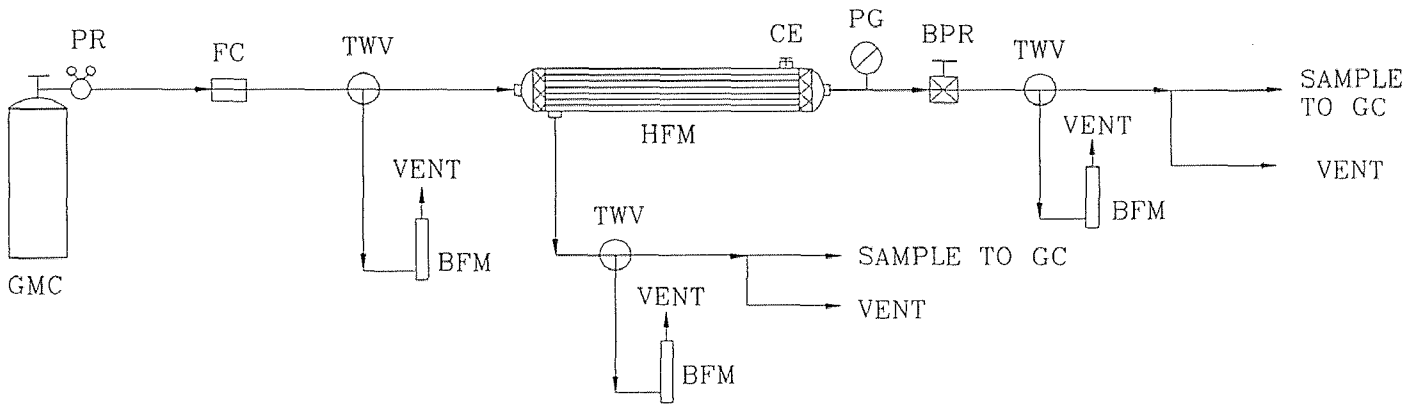

Figure 3.18 Schematic Diagram of Vapor Permeation

The separation factor was calculated as discussed in section 2.3.

A program to calculate the permeance, Q_i/δ, and the separation factor written in Mathematica is provided in Appendix C.

A gas chromatograph (Varian 3700, Sugarland, TX) equipped with a TCD was used for monitoring the CO_2/N_2 composition. Helium was used as the carrier gas. A CTR I column (outer column: 6'x1/4", packed with activated molecular sieve, inner column 6'x1/8" packed with porous polymer mixture, ALLTECH, Deerfield, IL) was connected to the GC. The GC operating parameters are included in Table 3.8. The GC response was recorded by an integrator (HP 3390A, Hewlett Packard).

Table 3.8 Operating Parameters of GC (Varian 3700) for Detecting N_2/CO_2

Column Temperature (°C)	Injector Temperature (°C)	Detector temperature (°C)
40	121	121

Figures 3.19 and 3.20 provide the calibration curves for CO_2 and N_2 respectively. Three standard CO_2-N_2 mixture cylinders (Matheson, Rutherford, NJ) of different concentrations were used for the calibration.

3.10 Leak Test

Modules EPA/AS-4, 5, 6 and 7 were purchased from AMT Inc. (Minnetonka, MN). They were tested for leakage prior to use.

Leak test checks whether there is any leakage from the fibers and the potting at the two ends of the module. For newly-made modules, leak test is absolutely needed. One has to check the leakage with used modules also if operational difficulties or poor performance are encountered.

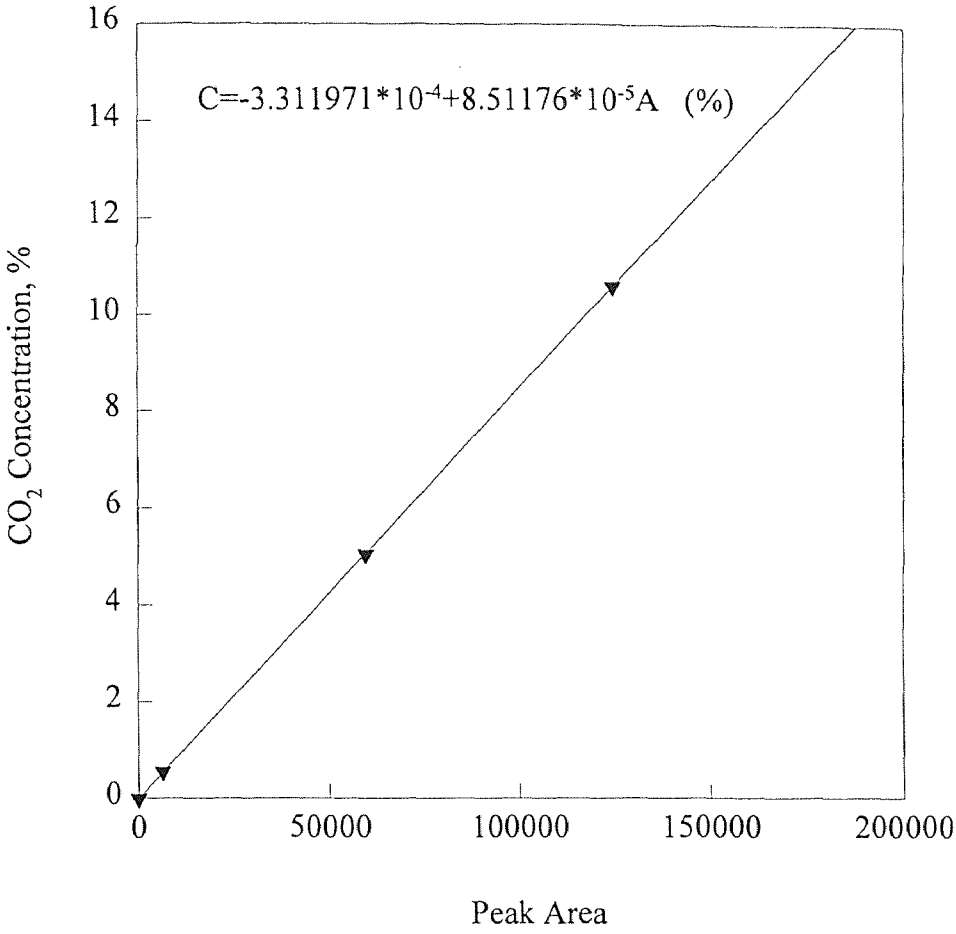

Figure 3.19 Calibration Curve for CO_2

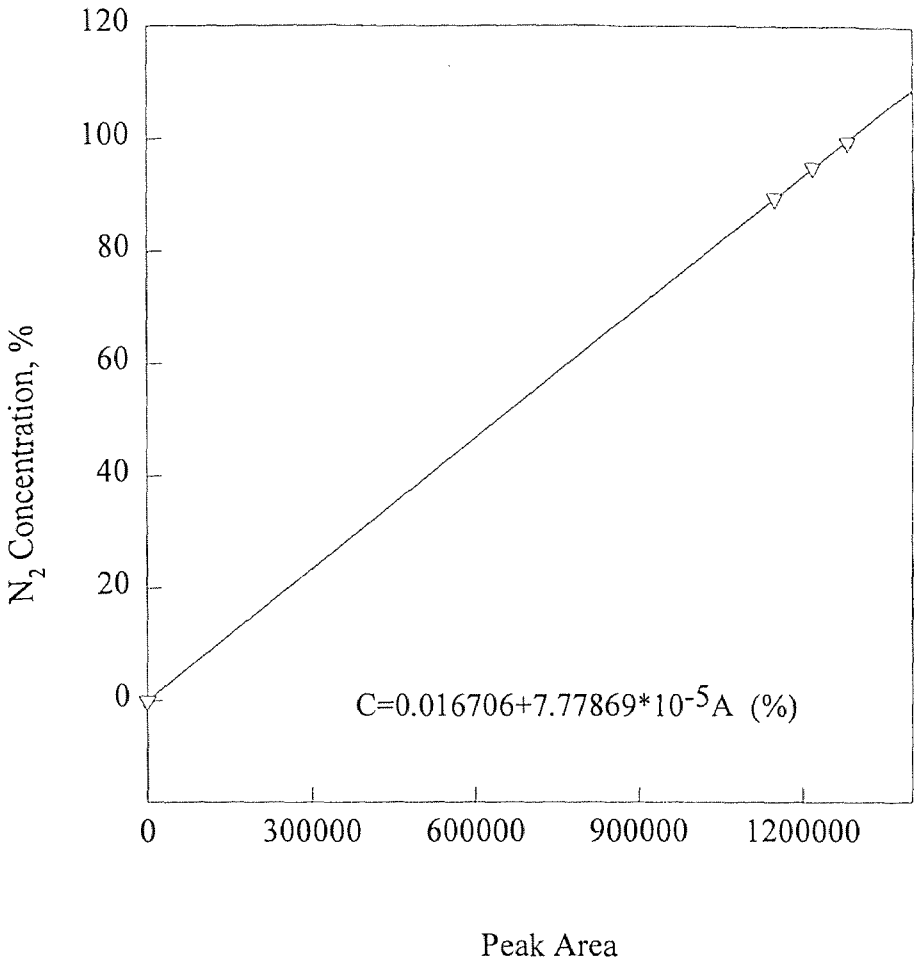

Figure 3.20 Calibration Curve for N_2

A schematic diagram for leak test is shown in Figure 3.21. Two fittings on two ends of the module were taken off so that the ends of the fibers could be seen. And one plug on the shell side was slightly tightened. Water in a pressure vessel was pressurized to a certain pressure (such as 10, 15 and 20 psig) by nitrogen gas so that water was forced to go through the tubing to the shell side of the module. When water started flowing out of the slightly closed end of the shell side, the latter was immediately tightened until no water leaked out. Two hours were allowed to pass. If no water came out from the two ends of the fibers and the potting parts, the module was assumed to be leak-frre. Otherwise, the module had to be fixed or can not be used any more.

CE: CLOSED END
HF: HOLLOW FIBER
HFM: HOLLOW FIBER MODULE
PG: PRESSURE GAUGE
PR: PRESSURE REGULATOR
PV: PESSURE VESSEL
TLP: THREE LAYER PORTING

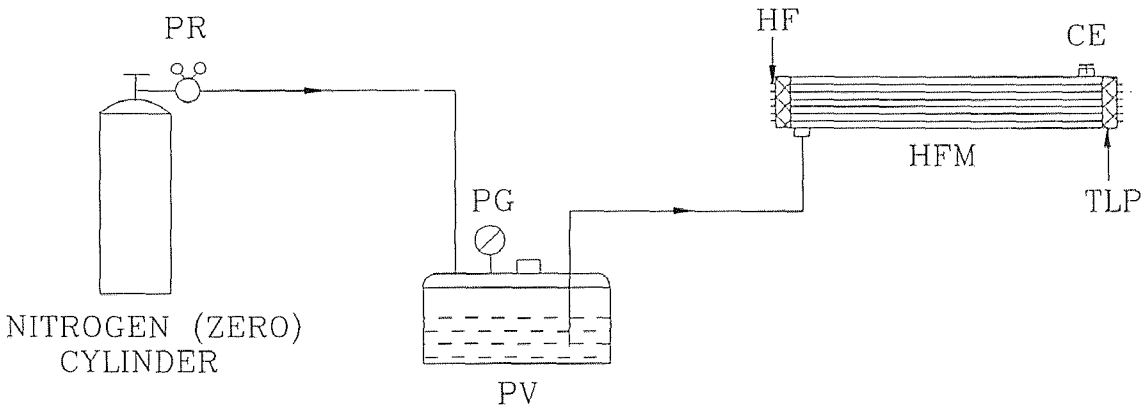

Figure 3.21 Schematic Diagram for Leak Test

CHAPTER 4

RESULTS AND DISCUSSION

In this chapter, the experimental results are provided for three cases: absorption only; combined absorption-stripping using the same temperature for absorption and stripping; combined absorption-stripping at different temperatures for absorption and stripping. The results are provided in graphical form and are also tabulated in Appendix A. Results of Henry's law constants and diffusivities of toluene, methanol, pentane and hexane in silicone oil are also provided here. The permeances of CO_2, N_2 and the VOCs through some of membranes are given here. Further, the separation results of methanol-nitrogen and pentane/hexane-nitrogen systems for absorption and stripping at different temperatures are compared with the numerical results obtained from a modified absorption-stripping model.

4.1 Results of Measurement of Physical Parameters

Individual results of measurements of physical parameters, such as the Henry's law constant, diffusivity, permeance and separation factor of the membrane, are presented separately in this section. Experimental methods for the parameters have been described in sections 3.7-3.9.

4.1.1 Henry's Law Constant

Experimental results of Henry's law constants of four VOCs in silicone oil determined by the Static Headspace Method are plotted in Figures 4.1 to 4.4. Experimental data for methanol at 64.85 °C show somewhat larger scatter than usual (Figure 4.2), resulting in lower accuracy. It is apparent from equation 2.14 that Henry's law constant is equal to the intercept ($H_i R_f / C_{io}$) divided by the slope (R_f / C_{io}) of each curve in Figures 4.1 to 4.4. Calculated results are listed in Tables A2 to A5. A sample calculation can be found in Appendix B. In order to find out the temperature dependence of Henry's law constant, natural logarithms of Henry's law constants at different temperatures are plotted against the reciprocals of the temperatures in Figure 4.5. It is clear that the magnitude of Henry's law constants of VOCs follow the order of those of toluene, hexane, pentane and methanol. Some experimental data from Poddar (1995) are also shown in this figure. Results from linear regression of $\ln(H_i)$ vs. 1/T are shown in Table 4.1. A_H and B_H for methanol and toluene are obtained from the data of present work and Poddar (1995) to extend the applicable temperature range.

Table 4.1 Parameters of Temperature Dependent Henry's Law Constant in Silicone Oil

VOC	A_H	B_H
methanol	4.0156	2034.0894
toluene	1.7505	2269.0401
hexane	2.8916	2344.2817
pentane	1.5480	1731.8710

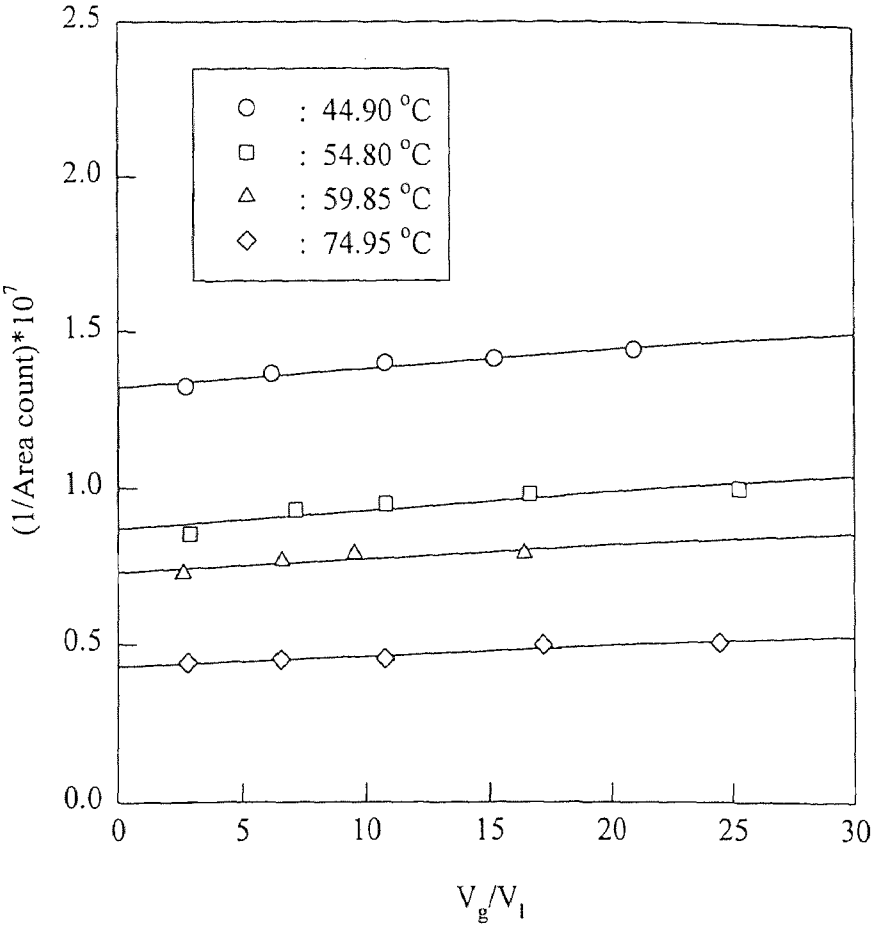

Figure 4.1 Plots of Reciprocal of Peak Area vs. Ratio of Headspace Volume to Liquid Sample Volume for Determination of Henry's Law Constant of Toluene in Silicone Oil at Different Temperatures

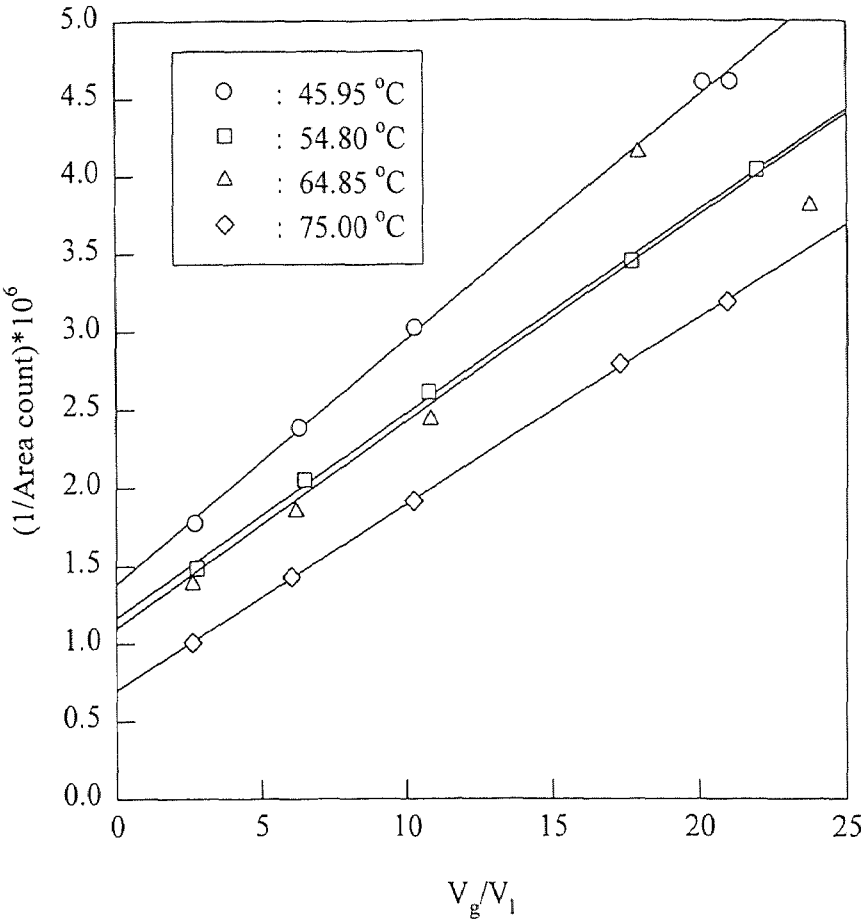

Figure 4.2 Plots of Reciprocal of Peak Area vs. Ratio of Headspace Volume to Liquid Sample Volume for Determination of Henry's Law Constant of Methanol in Silicone Oil at Different Temperatures

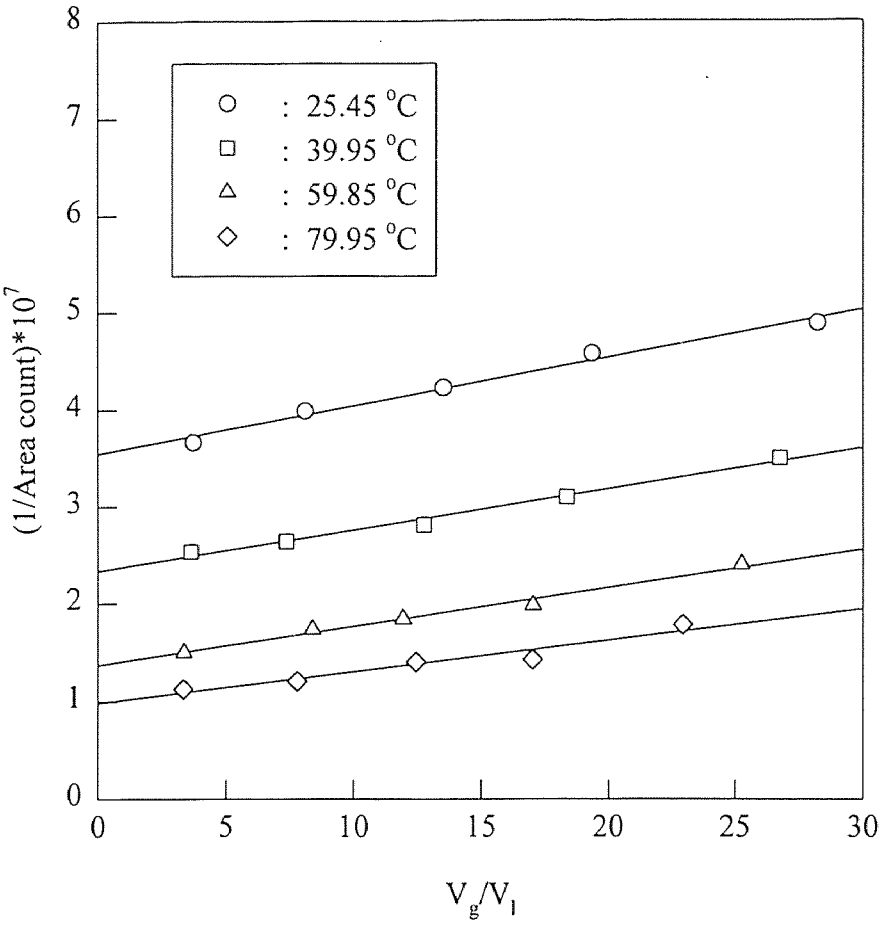

Figure 4.3 Plots of Reciprocal of Peak Area vs. Ratio of Headspace Volume to Liquid Sample Volume for Determination of Henry's Law Constant of Pentane in Silicone Oil at Different Temperatures

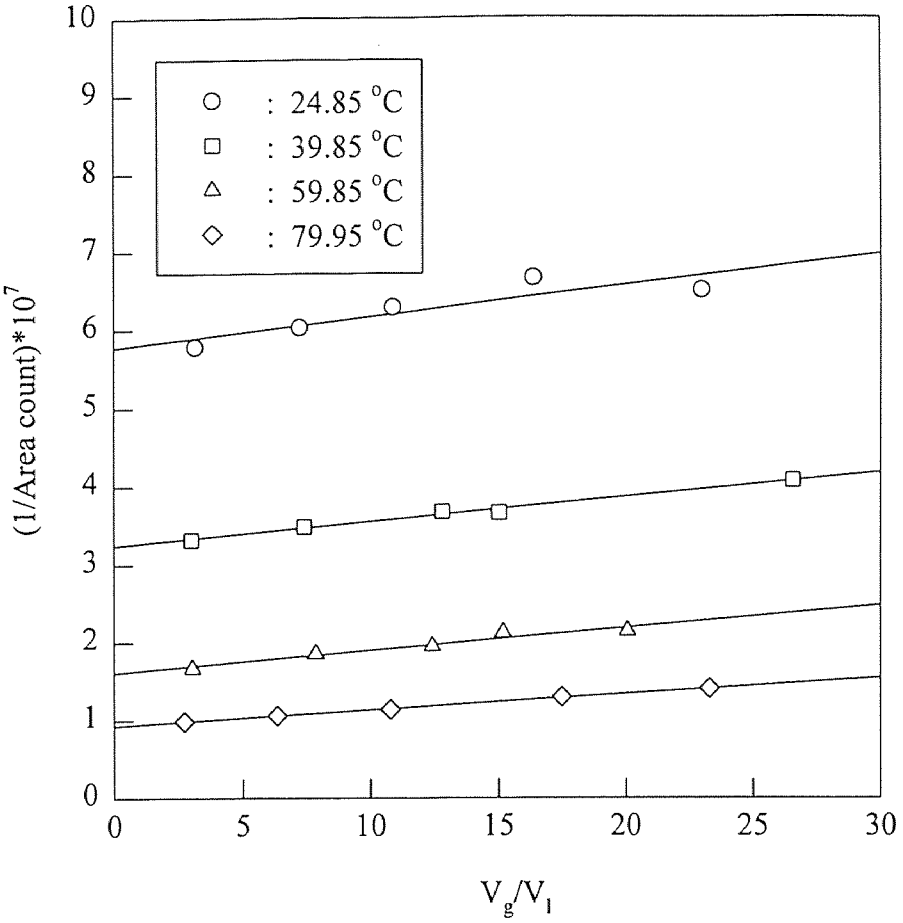

Figure 4.4 Plots of Reciprocal of Peak Area vs. Ratio of Headspace Volume to Liquid Sample Volume for Determination of Henry's Law Constant of Hexane in Silicone Oil at Different Temperatures

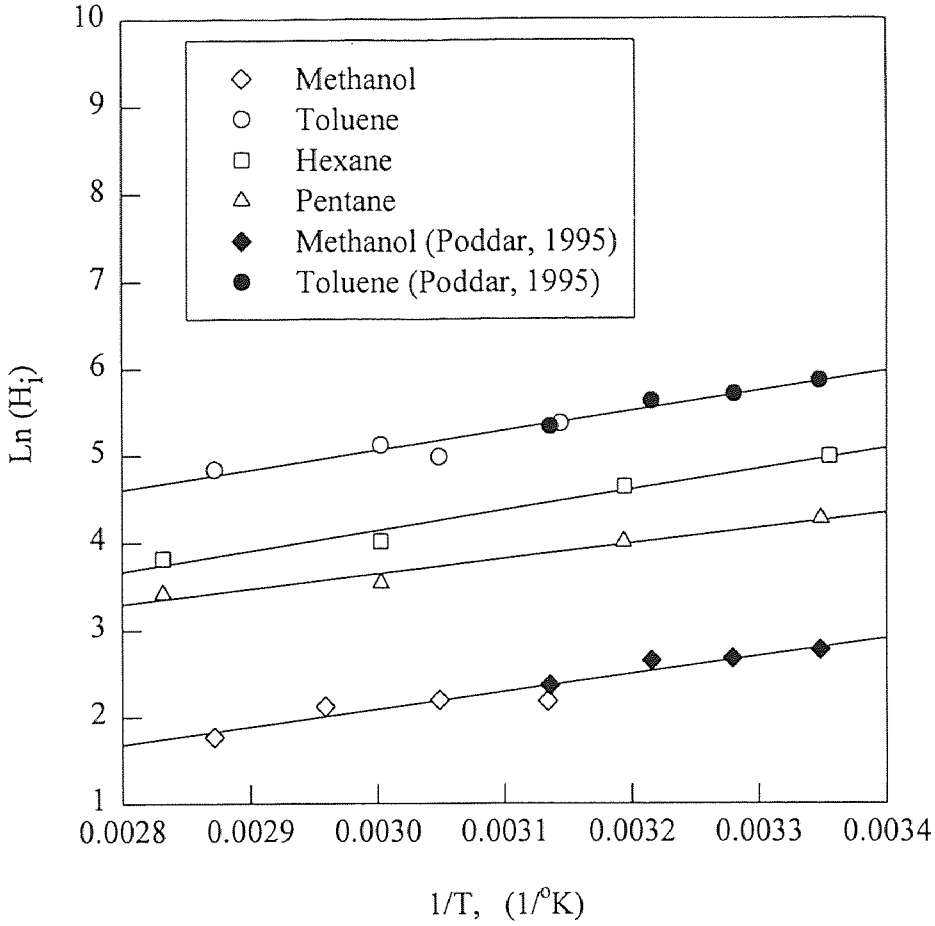

Figure 4.5 Variation of Natural Logarithm of Henry's Law Constant with the Reciprocal of Absolute Temperature for Various VOCs in Silicone Oil

Table 4.2 Calculated Henry's Law Constants for Methanol and Toluene in Silicone Oil from This Study and Poddar (1995)

VOC	Temperature, °C	Calculated H_i (This Study)	Calculated H_i (Poddar's Study)
Methanol	45	10.7821	11.3448
	55	8.8734	9.5460
	65	7.3872	8.1149
	75	6.2150	6.9630
Toluene	45	217.3442	218.1206
	55	174.8875	173.7398
	65	142.5451	140.2638
	75	117.5567	114.6388

Table 4.2 presents comparisons of calculated Henry's law constants using A_H and B_H obtained in this investigation with those in Poddar (1995) extrapolated to the present temperature range. Data of this study are in good agreement with Poddar (1995). Comparisons are possible only for methanol and toluene.

The Henry's law constant for butane was not measured. There were difficulties in preparing the stock solution used in the Static Headspace method since butane is a gas at room temperature. It may be measured by adopting the batch gas absorption technique (Lee and Foster, 1990).

4.1.2 Diffusivity

The diffusivities of the VOCs in silicone oil were evaluated using the indirect vapor permeation method detailed in section 3.8. Results are summarized in Table 4.3. Diffusivities of toluene in silicone oil are of the same order of magnitude as in Poddar

Table 4.3 Diffusivities of VOCs in Silicone Oil

VOC	Temperature, °C	Diffusivity*10^6, cm^2/s,
Methanol	23	10.6282
	48	21.8260
	60	25.4806
Toluene	20	2.6073
	49	3.7977
	66	4.8767
Pentane	20	1.1812
	47	2.2631
	66	2.7383
Hexane	20	1.7840
	47	2.4877
	66	3.1474

et al. (1996a) but somewhat lower. However, the measured values of methanol diffusivity in silicone oil are an order of magnitude higher than those of Poddar et al. (1996a). As predicted by the Wilke-Chang equation (equation 2.8), the diffusivity increases withincreasing temperature. The temperature dependences of VOC diffusivities in silicone oil are illustrated in Figures 4.6 and 4.7. The following correlations are obtained from a second order linear regression of the data:

For methanol-silicone oil system:

$$D_{il} = -4.9053 * 10^{-4} + 2.8397 * 10^{-6} T - 3.8746 * 10^{-9} T^2 \quad (4.1)$$

For toluene-silicone oil system:

$$D_{il} = 3.6607 * 10^{-5} - 2.5887 * 10^{-7} T + 4.8744 * 10^{-10} T^2 \quad (4.2)$$

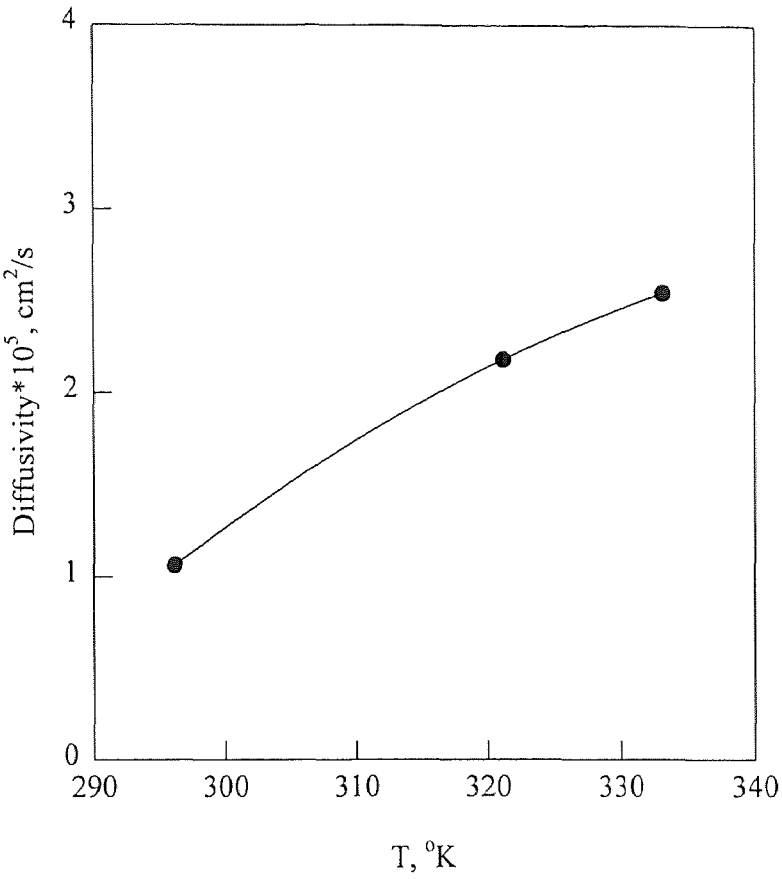

Figure4.6 Temperature Dependence of Methanol Diffusivity in Silicone Oil

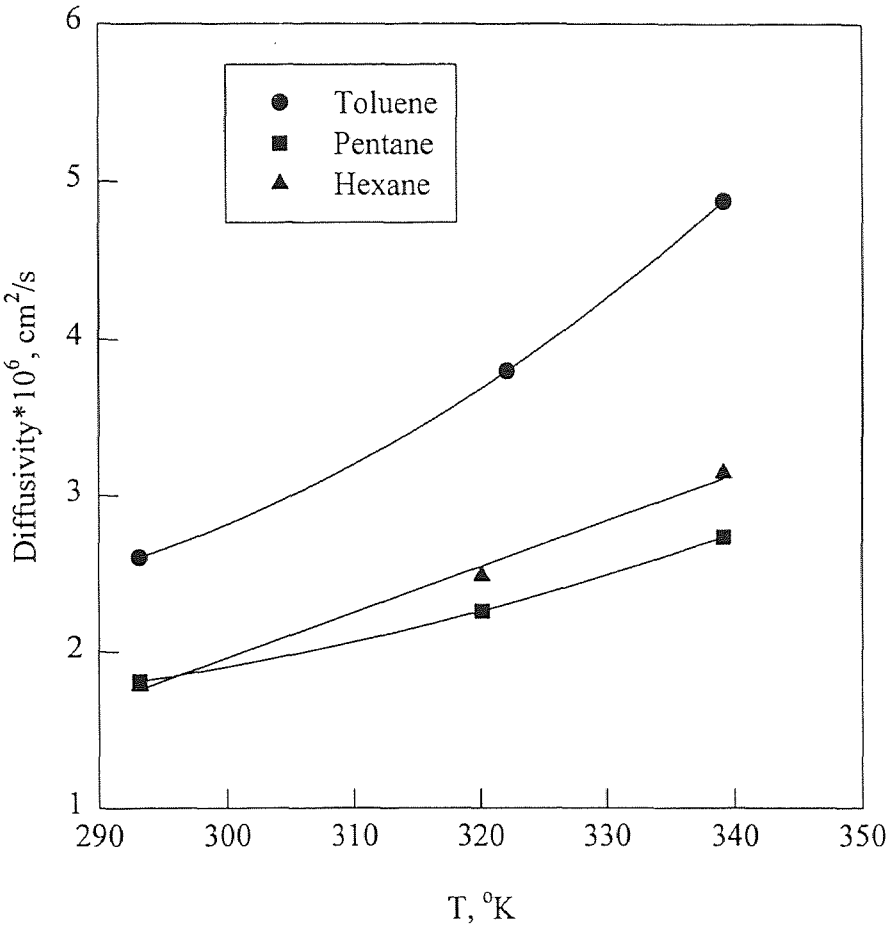

Figure 4.7 Temperature Dependence of Diffusivities of Toluene, Pentane and Hexane in Silicone Oil

For pentane-silicone oil system:

$$D_{il} = 1.3811 * 10^{-5} - 9.3729 * 10^{-8} T + 1.8010 * 10^{-10} T^2 \quad (4.3)$$

For hexane-silicone oil system:

$$D_{il} = 1.1808 * 10^{-5} - 8.9372 * 10^{-8} T + 1.8822 * 10^{-10} T^2 \quad (4.4)$$

where T is the temperature in ^{o}C and D_{il} is the diffusivity in cm^2/s.

4.1.3 Permeance and Separation Factor

The permeances and separation factors were measured for newly-procured modules. Modules # EPA/AS-4, 5 and 6 were first tested for leakage. Results are provided in Table 4.4. The values of permeance have been determined from pure gas permeation experiments. Separation factors have been determined from CO_2-N_2 mixture separation. VOC permeance through modules EPA/AS-6 and 7 was also obtained from experiments using methanol-nitrogen (1100 ppmv methanol) and toluene-nitrogen (940 ppmv toluene) and gasoline-nitrogen (9840 ppmv butane, 2740 ppmv pentane and 314 ppmv hexane) mixtures (see Table 4.5).

Table 4.4 Characterization of New Stripping Modules via Permanent Gas Permeation/ Separation

Module	N_2 Permeance Scc/cm^2.s.cmHg $*10^5$	CO_2 Permeance Scc/cm^2.s.cmHg $*10^4$	Separation Factor $\alpha_{CO2\text{-}N2}$
EPA/AS-4	2.08	3.45	8.7
EPA/AS-5	2.47	2.54	8.1
EPA/AS-6	1.39	1.73	10.5

Table 4.5 Permeance of VOCs through Different Membranes

Module	VOC	Permeance*10^3, cm/s	
		Composite membrane q_o/δ_o	Silicone Skin q_c/δ_c
EPA/AS-6	Methanol	5.4420	5.5128
	Toluene	3.2133	3.2552
EPA/AS-7	Butane	2.6515	2.6810
	Pentane	3.0468	3.0838
	Hexane	3.5339	3.5812

4.2 Results of Absorption-Only Experiments

Experiments were carried out at room temperature in two different ways: variation of feed gas flow rate at a fixed absorbent flow rate and variation of absorbent flow rate at a fixed feed gas flow rate. The hydrocarbon concentrations in the purified gas stream are plotted in the figures against the feed gas flow rate and against the silicone oil flow rate respectively. At the absorbent flow rate of 3.8-3.9 ml/min (Figure 4.8), the butane outlet concentration varied with increasing gas flow rate from 3 ppmv to 1395 ppmv whereas pentane concentration was increased to only 16 ppmv. At a gas flow rate of less than 4.7 cc/min, pentane was not detected in the purified gas stream. When the feed gas flow rate was maintained at 7.7-8.9 cc/min and the absorbent flow rate was changed from 0.7-7.0 ml/min (Figure 4.9), 260-1236 ppmv of butane and less than 5 ppmv of pentane were present in the treated gas. If the silicone oil flow rate was increased to 4.4 ml/min or more, pentane was no longer detected in the feed outlet stream. Note that, no hexane was detected at the outlet gas stream in the range of variables studied for both of the above-mentioned cases. In all absorption-only experiments studied, 86.2%+ of butane, 99.4%+ of pentane and 100% of hexane were removed from the feed gas.

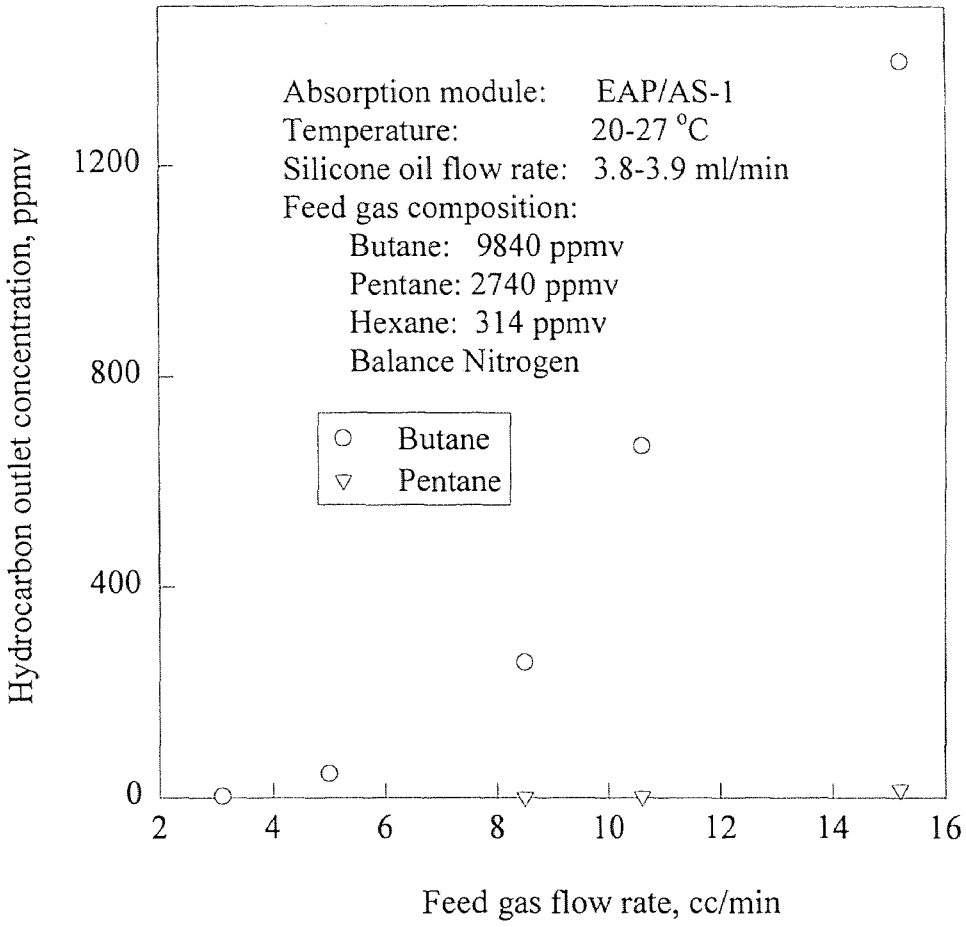

Figure 4.8 Variation of Hydrocarbon Outlet Concentration with Feed Gas Flow Rate (Absorption Only)

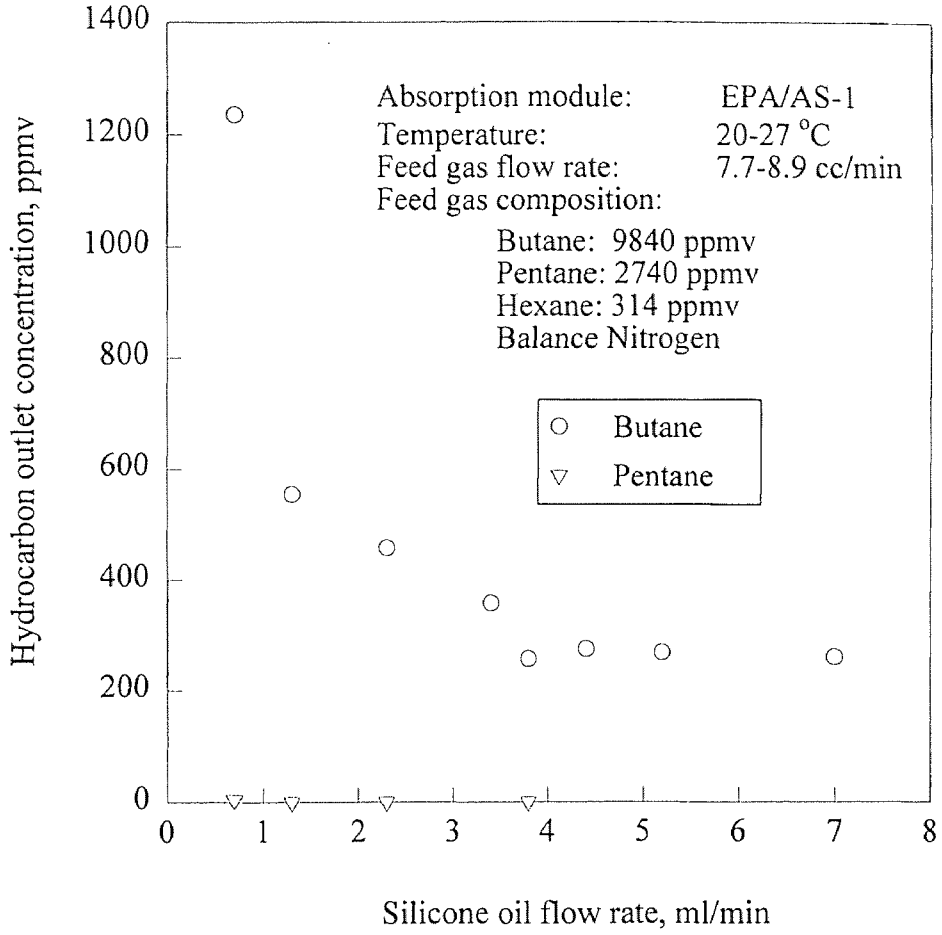

Figure 4.9 Variation of Hydrocarbon Outlet Concentration with Silicone Oil Flow Rate at High Gas Flow Rate (Absorption Only)

To get the best VOC removal performance, the feed gas flow rate should be kept at a low value and the silicone oil flow rate should be high enough. Figure 4.10 presents such a result. No pentane and hexane were detected in the gas outlet stream; less than 6 ppmv of butane in the purified gas stream was achieved under the conditions that the feed gas flow rate is in the range of 3.1-3.7 cc/min and silicone oil flow rate is larger than 2.7 ml/min. Under these conditions, removal of 99.9 % of butane, and essentially 100% of pentane and hexane from nitrogen were successfully obtained.

4.3 Results of Combined Absorption-Stripping at Room Temperature

The results of simple absorption using fresh absorbent were quite encouraging. However, a large amount of absorbent was consumed. To decrease the cost of the operation, the absorbent must be regenerated and reused. Therefore, the results from a combined absorption-stripping process are examined now.

The experimental procedure has been presented in section 3.5. Results for gasoline vapor (butane, pentane, and hexane) are illustrated in Figures 4.11 and 4.12. The hydrocarbon outlet concentration decreased with decreasing feed gas flow rate or with increasing absorbent flow rate; this is similar to that in simple absorption. Examination of Figures 4.9 and 4.12 indicates that, at approximately the same feed gas flow rate, the hydrocarbon outlet concentrations (butane: 1596-2478 ppmv, pentane: 312-512 ppmv, and hexane: 28-52 ppmv) obtained by combined absorption and stripping at room temperature are significantly higher than those obtained by simple absorption, although the silicone oil flow rate is increased to 10.9 ml/min. All three hydrocarbon components appear in the outlet gas stream. The reason could be insufficient stripping of the VOC-containing

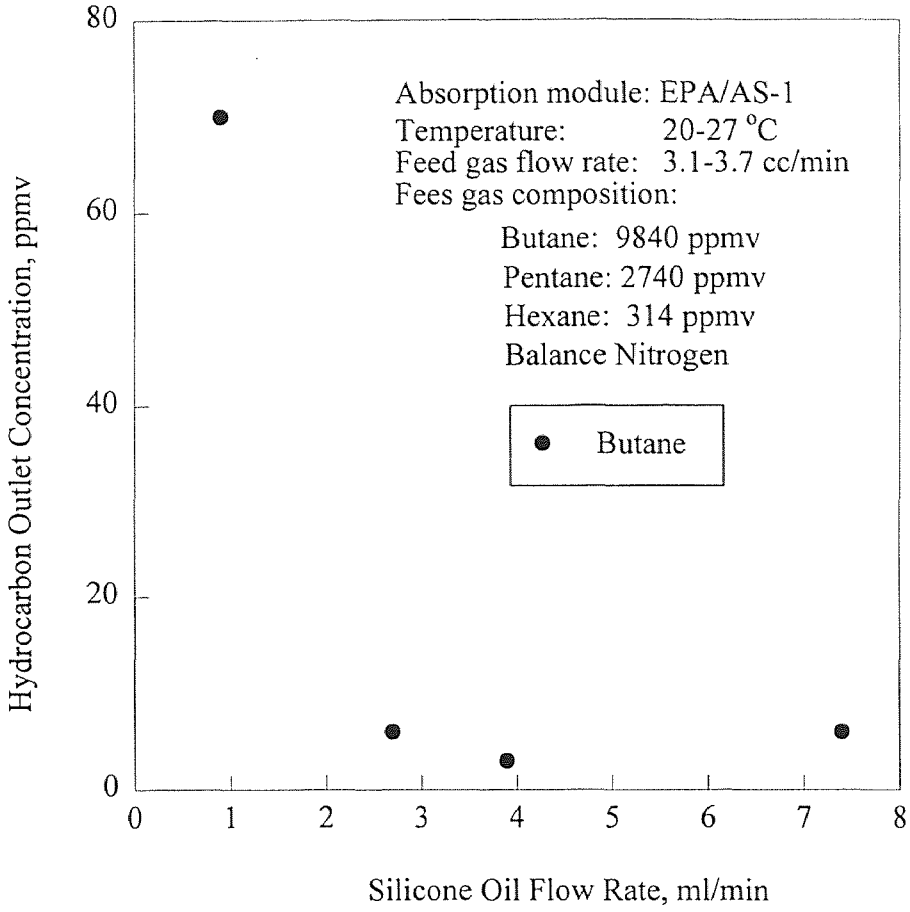

Figure 4.10 Variation of Hydrocarbon Outlet Concentration with Silicone Oil Flow Rate at Very Low Gas Flow Rate (Absorption Only)

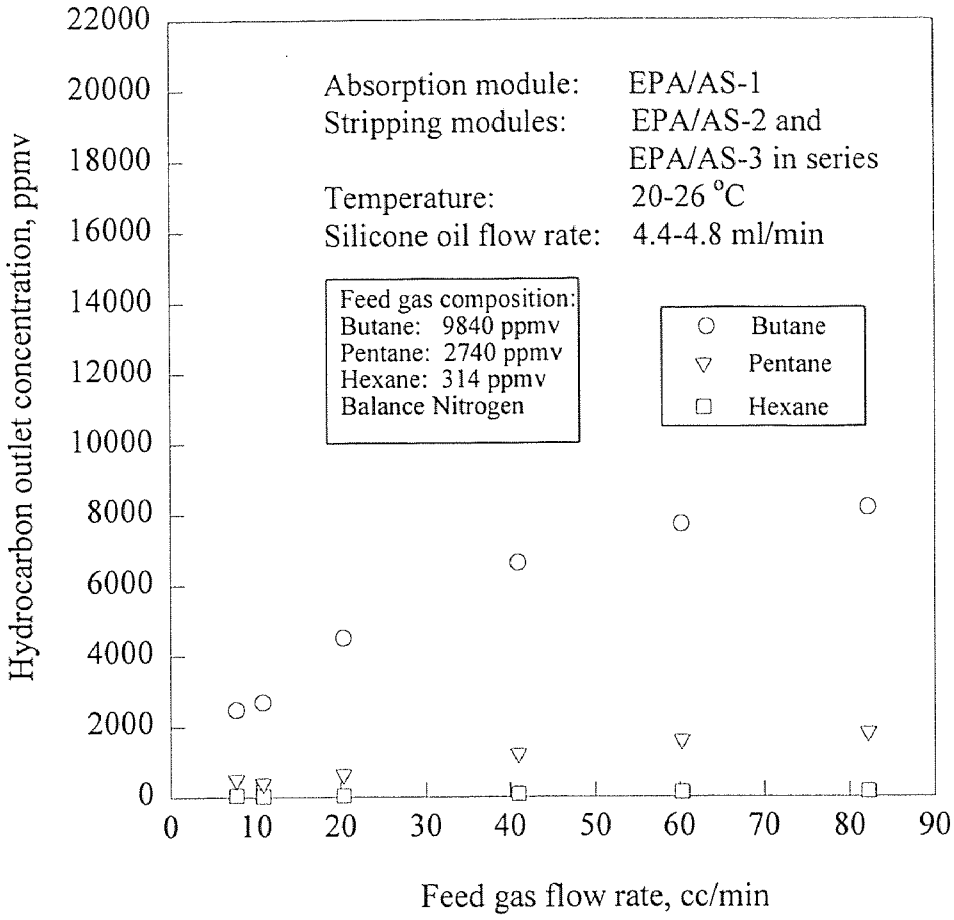

Figure 4.11 Variation of Hydrocarbon Outlet Concentration with Feed Gas Flow Rate (Combined Absorption-Stripping)

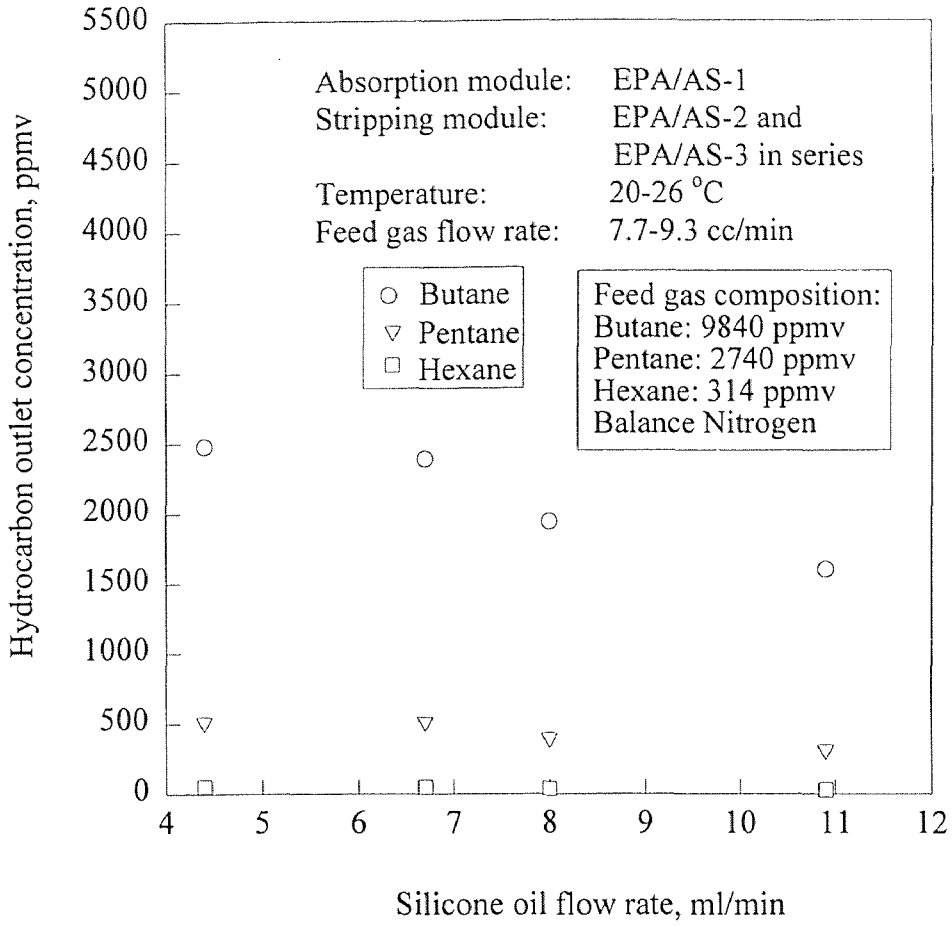

Figure 4.12 Variation of Hydrocarbon Outlet Concentration with Silicone Oil Flow Rate (Combined Absorption-Stripping)

absorbent due to the lower membrane surface area of the module and the lower operating temperature of the stripping module. Actually, at the beginning, it took 3 days to reach the steady state by using one stripping module (module EPA/AS-2). Therefore, two modules in series were later used as the stripper.

As in traditional desorption, the way to improve the stripping process was to increase the stripping temperature, increase the contact area of the two phases (in the present case, the membrane area), or decrease the pressure. Since full vacuum was pulled on the tube side of the stripping module (~29 in Hg), increasing the stripping temperature was selected.

4.4 Results of Combined Absorption-Stripping with a Heating-Cooling System

Results of combined absorption-stripping with a heating-cooling system are first compared with that of combined absorption-stripping at room temperature (Table 4.6). The feed gas was a gasoline mixture in N_2; the feed flow rate was controlled at about 8.0 cc/min for all runs. The first two runs were at room temperatures (29 ^{o}C for both absorption and stripping modules, EPA/AS-1 and 2). The next three runs were at room temperature (29 ^{o}C) for the absorption module and at a higher temperature (59 ^{o}C) for the stripping module. By comparing the data at roughly the same absorbent flow rate, it is clear that the purified gas concentration under the latter operating conditions was almost half of that under the former operating conditions. The VOC percent removal was definitely increased.

More data are provided in Figures 4.13 and 4.14 for hydrocarbon removal from nitrogen by this process. The removal of more than 92.5% of butane, 96.4% of pentane and 97.9% of hexane was achieved using the stripping module EPA/AS-2 at a flow rate of the

Table 4.6 Comparison of VOC Removal by Combined Absorption-Stripping with and without Heating-Cooling System

Feed Flow Rate, cc/min	Purified Gas Flow Rate, cc/min	T_A °C	T_S °C	Oil Flow Rate, ml/min	Purified Gas Concentration, ppmv			Percent Removal, %		
					Butane	Pentane	Hexane	Butane	Pentane	Hexane
8.1	7.5	29	29	21.4	1809	258	20	83.0	91.3	94.1
8.2	7.5	29	29	24.7	1907	333	21.6	82.3	88.9	93.7
7.8	7.4	23	59	18.6	970	143	10	90.6	95.0	97.0
7.7	7.3	21.5	59	21.6	899	137	10	91.3	95.3	97.0
7.8	7.5	24.5	59	24.7	901	138	10	91.2	95.2	96.9

Feed Concentration: Butane: 9840 ppmv
Pentane: 2740 ppmv
Hexane: 314 ppmv
Balance Nitrogen

Absorption Module: EPA/AS-1
Stripping Module: EPA/AS-2

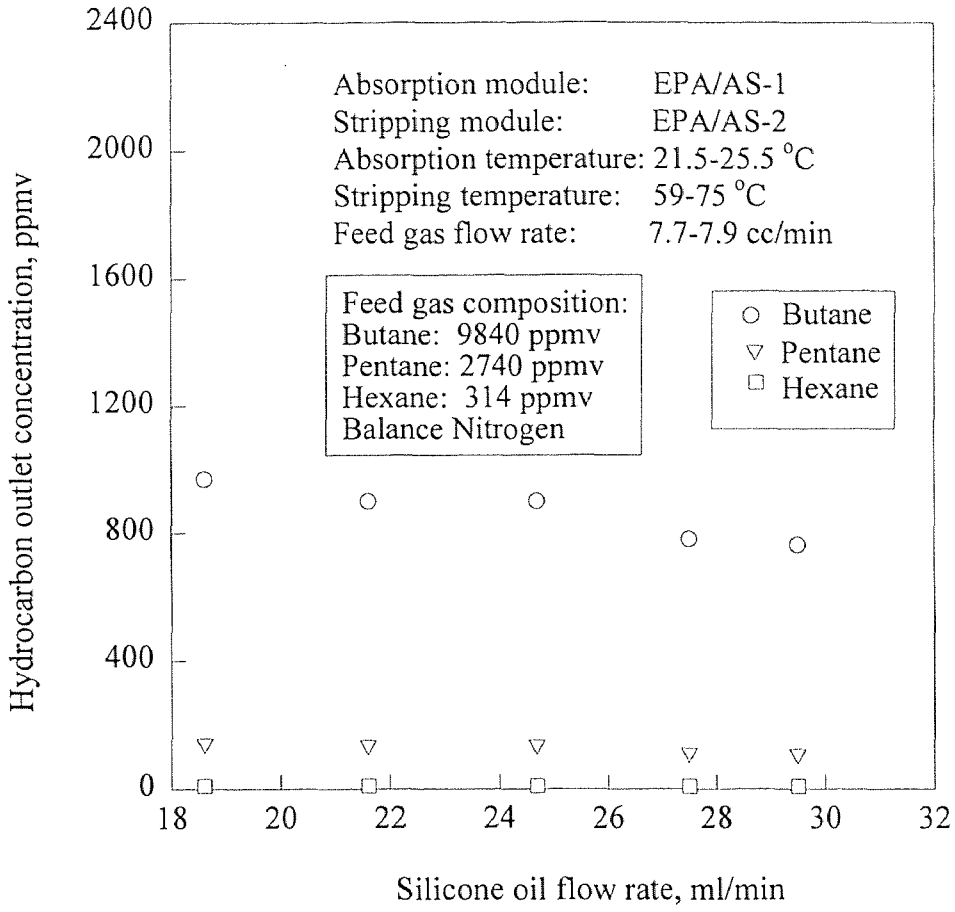

Figure 4.13 Variation of Hydrocarbon Outlet Concentration with Silicone Oil Flow Rate (Combined Absorption-Stripping with Heating-Cooling System)

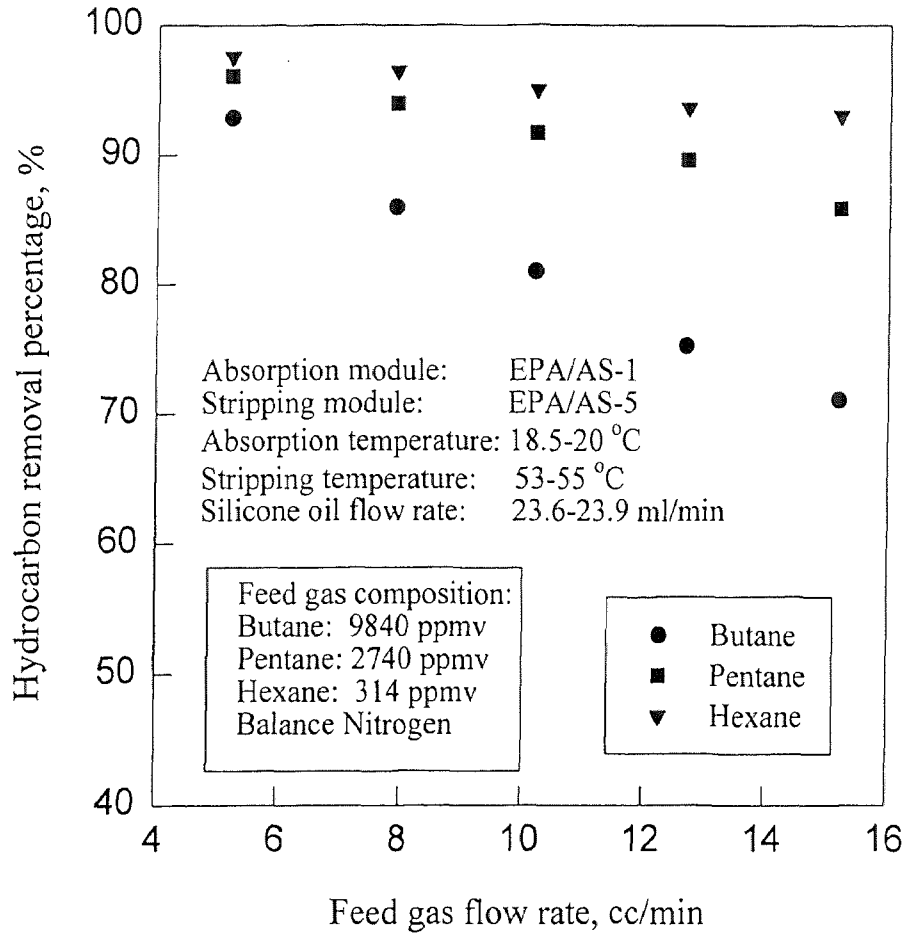

Figure 4.14 Variation of Hydrocarbon Removal Percentage with Feed Gas Flow Rate (Combined Absorption-Stripping with Heating-Cooling System

feed gas (7.7-7.9 cc/min) and high absorbent flow rate (>18.6 ml/min) (Figure 4.13). For the stripping module EPA/AS-5, the removal percentages were larger than 71.1% for butane, 85.9% for pentane, and 93.1% for hexane at an absorbent flow rate of about 23 ml/min and in a feed gas flow rate range of 5.2-15.2 cc/min (Figure 4.14).

Results for methanol-nitrogen system with stripping module EPA/AS-5 and for toluene-nitrogen system with module EPA/AS-6 are reported in Figures 4.15 to 4.18. The effects of feed gas flow rate and silicone oil flow rate on separation of these two VOCs are similar to those of gasoline removal. About 75.4%-96.0% of methanol and 96.2%-98.7% of toluene were removed in the range of variables investigated, depending upon the gas and absorbent flow rates maintained.

The effect of different stripping modules on the separation performance was also studied. Figures 4.19 and 4.20 indicate that module EPA/AS-4 (with silicone fluoropolymer coating) performs slightly better than module EPA/AS-2 and 5 (both with silicone coating) for gasoline separation under the same operating conditions.

By comparing gasoline separation results obtained by this process (Figure 4.13) with that earlier reported in simple absorption (Figure 4.9), one notices that the combined absorption-stripping with the heating-cooling system does not perform as well as absorption. To determine if the problem comes from the absorption or stripping, the performances for gasoline system with module EPA/AS-1 and EPA/AS-5 were studied in different temperature ranges: one was within a lower absorption temperature range (18.5-23 ^{o}C) and the other one within a slightly higher absorption temperature range (26-30 ^{o}C). It is apparent from Figure 4.21 that the absorption temperature does not significantly affect the performance. So, the overall performance of this process is controlled by

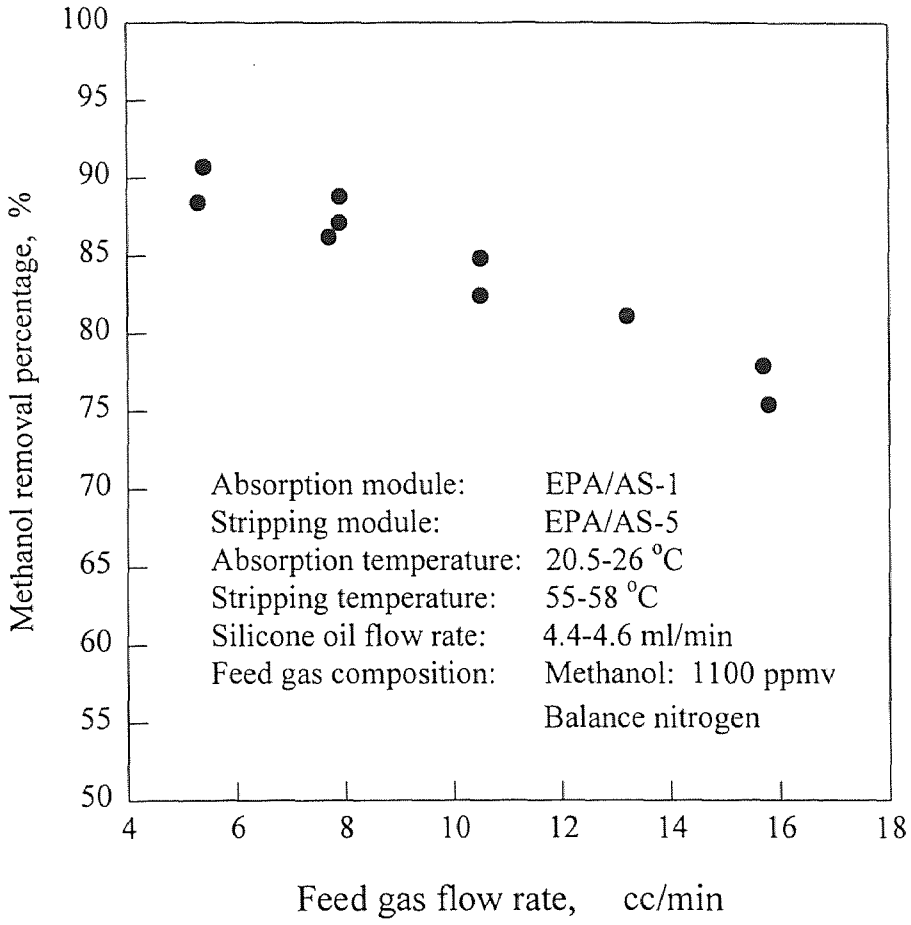

Figure 4.15 Variation of Methanol Removal Percentage with Feed Gas Flow Rate (Combined Absorption-Stripping with Heating-Cooling System)

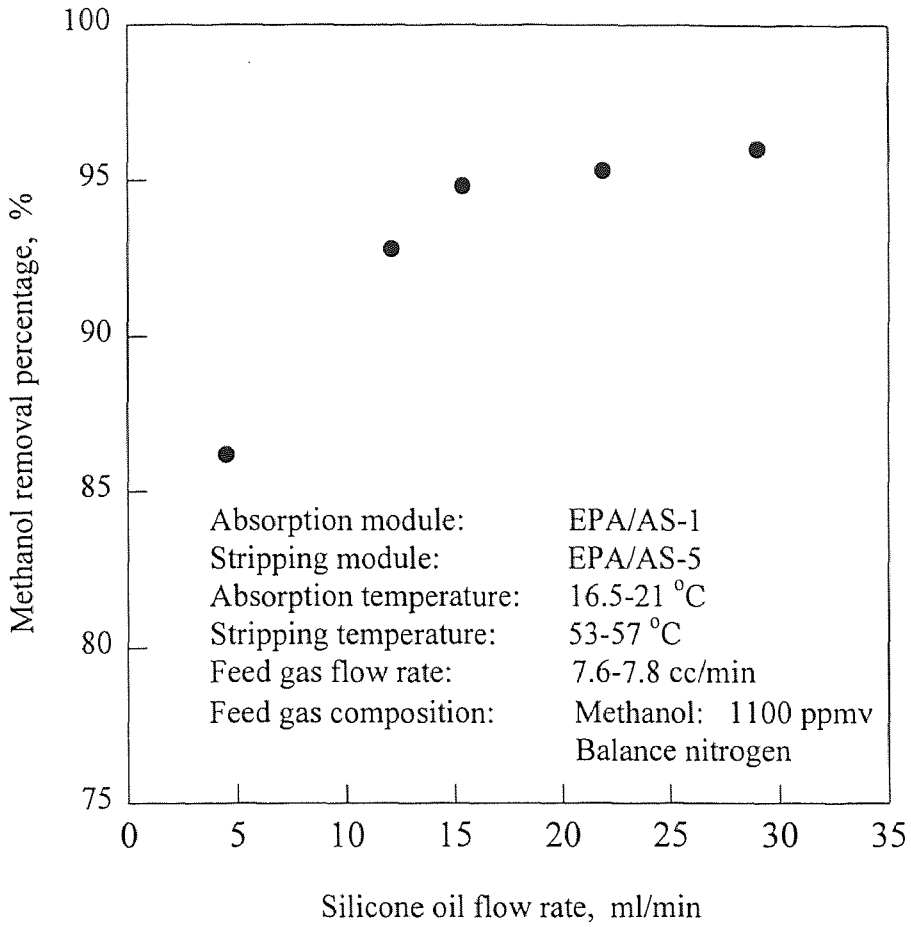

Figure 4.16 Variation of Methanol Removal Percentage with Silicone Oil Flow Rate (Combined Absorption-Stripping with Heating-Cooling System)

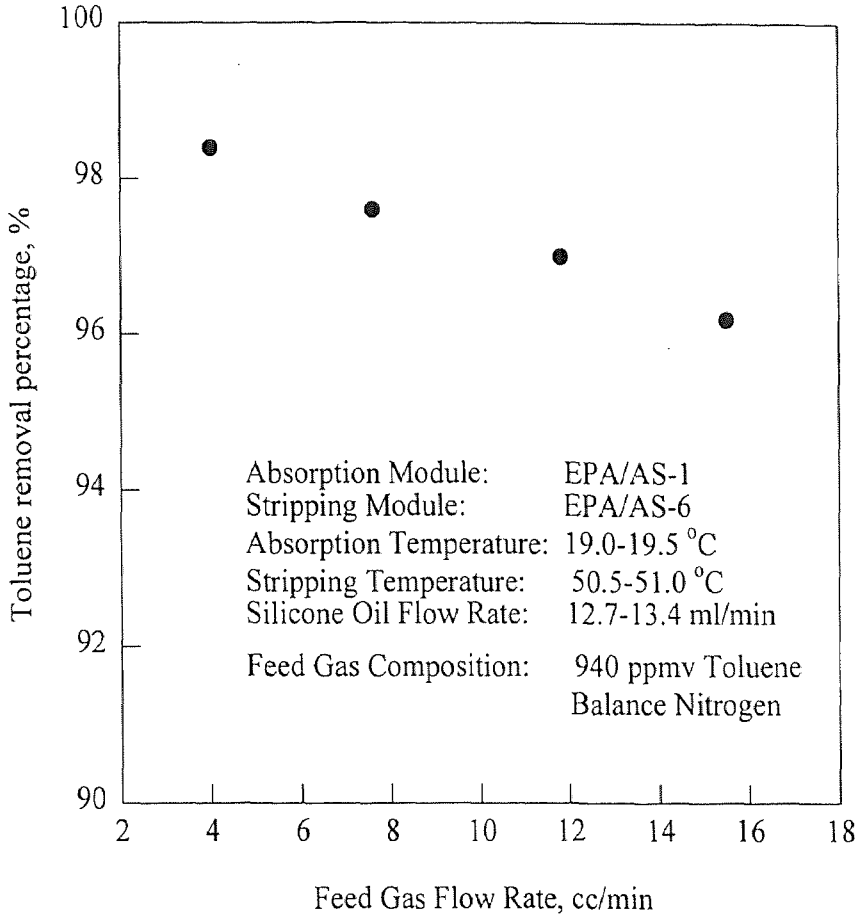

Figure 4.17 Variation of Toluene Removal Percentage with Feed Gas Flow Rate (Combined Absorption-Stripping with Heating-Cooling System)

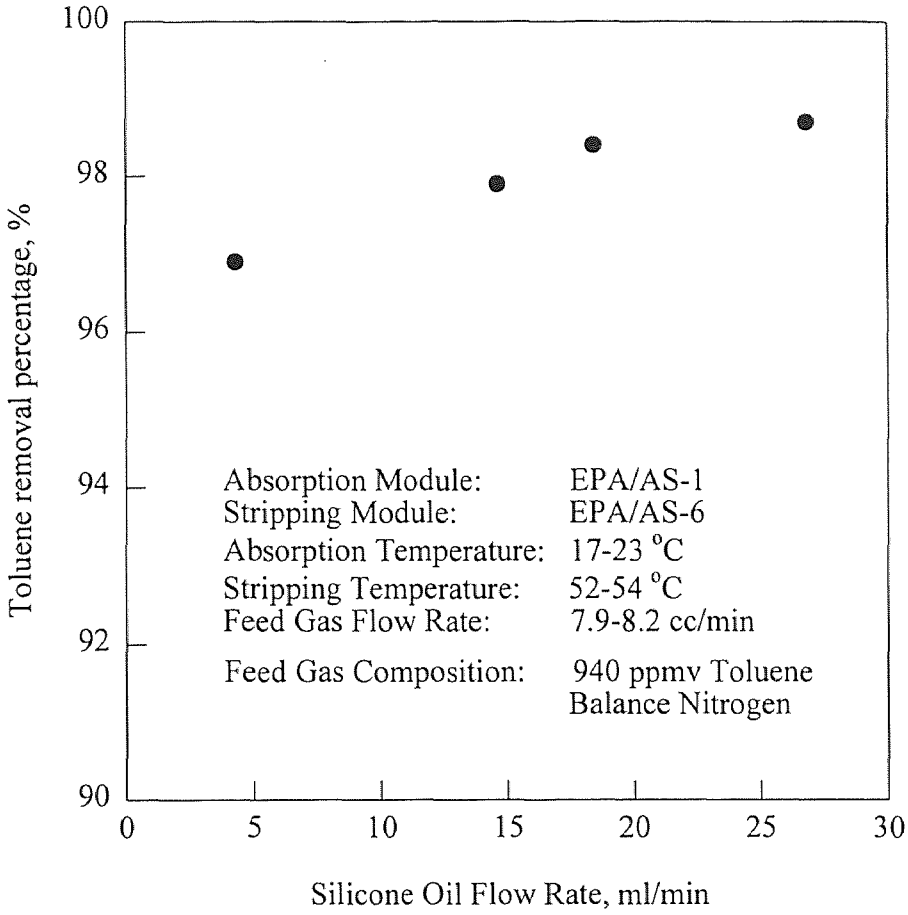

Figure 4.18 Variation of Toluene Removal Percentage with Silicone Oil Flow Rate (Combined Absorption-Stripping with Heating-Cooling System)

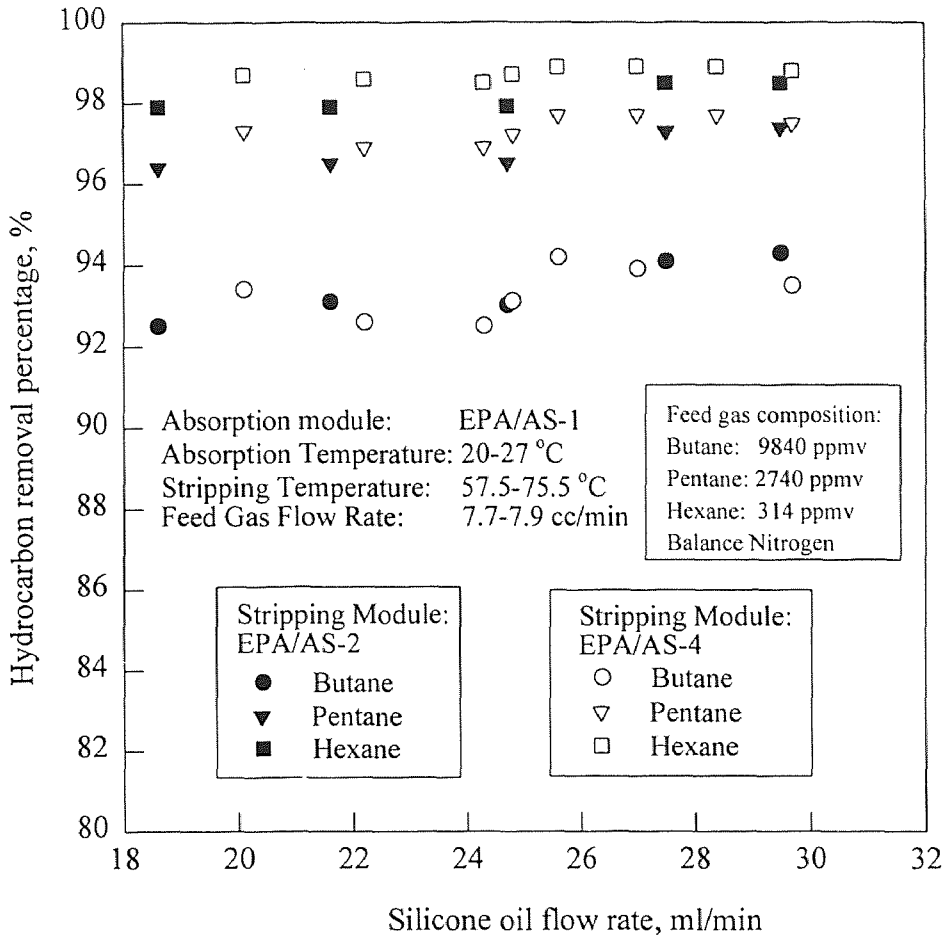

Figure 4.19 Comparison of Hydrocarbon Removal Percentages by Different Stripping Modules (EPA/AS-2, 5) (Combined Absorption-Stripping with Heating-Cooling System)

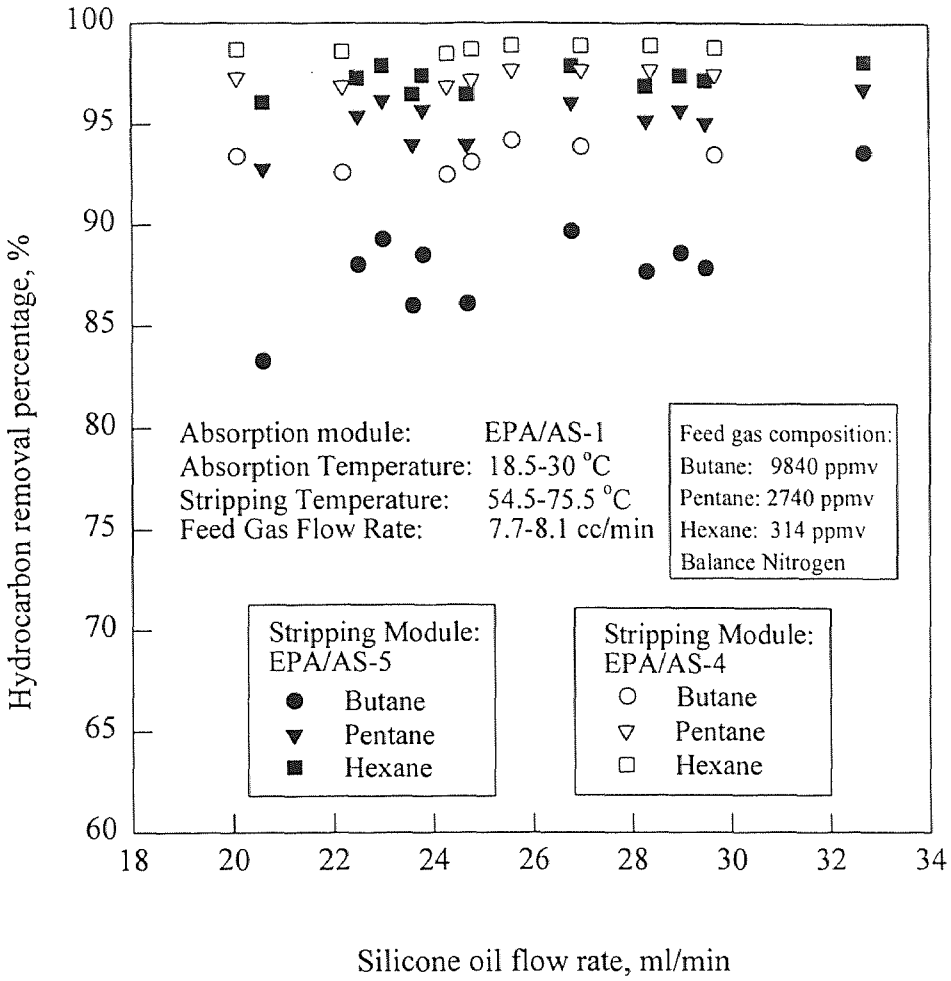

Figure 4.20 Comparison of Hydrocarbon Removal Percentages by Different Stripping Modules (EPA/AS-4, 5) (Combined Absorption-Stripping with Heating-Cooling System)

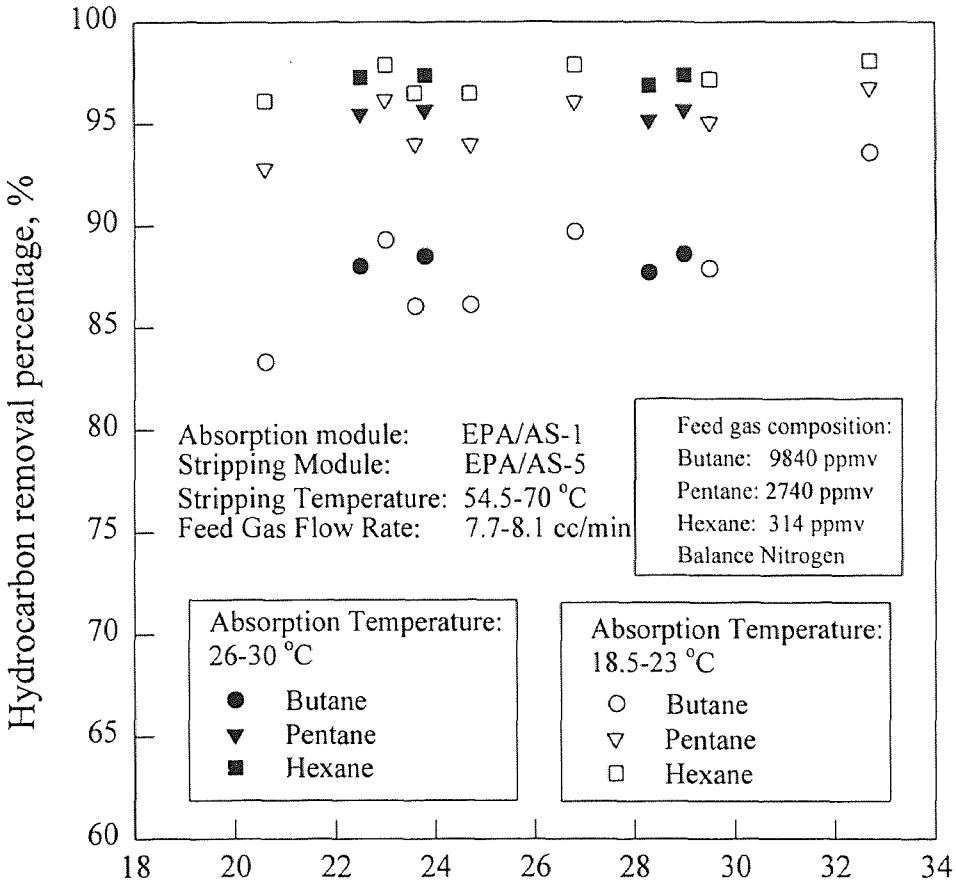

Figure 4.21 Comparison of Hydrocarbon Removal Percentages at Different Absorption Temperatures (Combined Absorption-Stripping with Heating-Cooling System)

stripping, which may result from the stripping temperature being not sufficiently high, and/or limited membrane surface area; bypassing of the absorbent flow in the shell side of the stripping module could also be responsible. Further, higher temperature for the stripping module is not possible since the coating of fibers or the potting part of the module may be damaged. For higher performance efficiency, a traditional stripper, which can be operated at a very high temperature, may be used instead of the membrane stripping module.

4.5 Comparison of Experimental Results and Model Simulation

As mentioned in Chapter 2, a mathematical model (Poddar et al., 1996a, 1996b) was modified to simulate methanol-nitrogen and pentane/hexane-nitrogen separation by the combined absorption-stripping process with a heating-cooling system. The Henry's Law constant correlations of VOCs in silicone oil used here were experimentally obtained throughout the temperature range of experiments in the separation process. The correlation of temperature dependence of VOC diffusivity in silicone oil was used in the simulation instead of a value at room temperature. Other physical parameters used in the simulations (critical pressure, temperature and volume, and Lennard-Jones potentials) were found in Reid et al. (1977) and listed in Appendix A.

Figure 4.22 shows the simulation results for pentane-nitrogen and hexane-nitrogen separations under conditions of absorption temperature of 19 ^{o}C, stripping temperature of 54 ^{o}C, and silicone oil flow rate of 23.7 ml/min, which are the average values of experimental ranges of absorption temperature, stripping temperature and silicone oil flow rate. The experimental data and operating conditions are shown in Figure 4.22. The

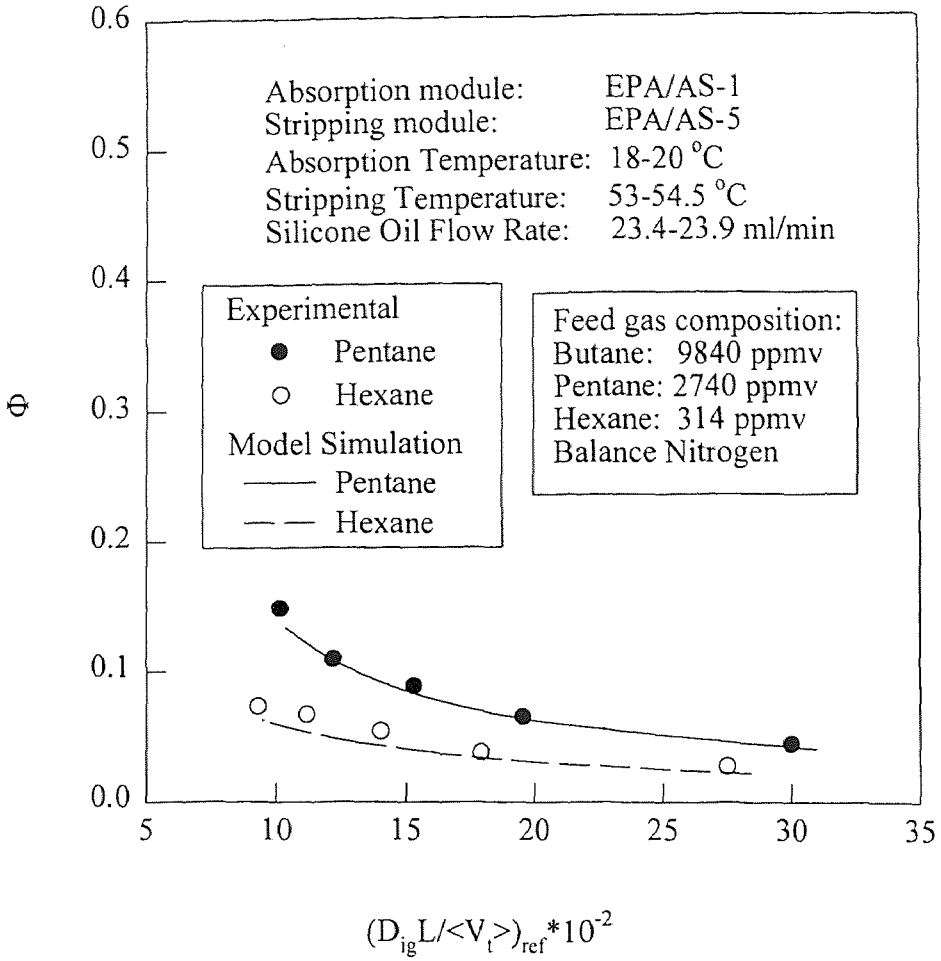

Figure 4.22 Ratio of Outlet to Inlet Gas Phase Concentration of Hydrocarbons as a Function of Inverse of Graetz Number; Modules EPA/AS-1 and 5 (Combined Absorption-Stripping with Heating-Cooling System)

horizontal axis is the inverse of a dimensionless number, namely Graetz number, which is defined as:

$$N_{GZ} = \frac{\pi r}{2L}(N_{\mathrm{Re}}N_{Sc})_{ref} = \left(\frac{< V_t >}{D_{ig}L}\right)_{ref} \tag{4.5}$$

The subscript "ref" refers to the reference condition, which is the ambient temperature and atmospheric pressure. The vertical axis (Φ) is the dimensionless gas concentration defined as a ratio of outlet to inlet gas phase concentration ($C_{i,out}/C_{i,in}$).

Comparison of experimental and predicted results for pentane-nitrogen and hexane-nitrogen separations with variation in silicone oil flow rate is illustrated in Figures 4.23 and 4.24. The horizontal axis was changed to silicone oil flow rate since there is no change in Graetz number with the liquid phase flow rate. The experimental conditions are shown in the Figures 4.23 and 4.24. Again, the absorption temperature, stripping temperature, and feed gas flow rate for model simulation were taken as the averages of their experimental ranges.

The pentane and hexane permeance data through module EPA/AS-5 used in the simulation were the data obtained via module EPA/AS-7 since they are not available at present.

Simulation results for methanol-nitrogen separation are provided in Figures 4.25 and 4.26.

One could see from Figures 4.22, 4.23 and 4.24 that the predicted values from the model are in good agreement with the experimental data for pentane-nitrogen and hexane-nitrogen separations. However, the experimental Φ values were much larger than the

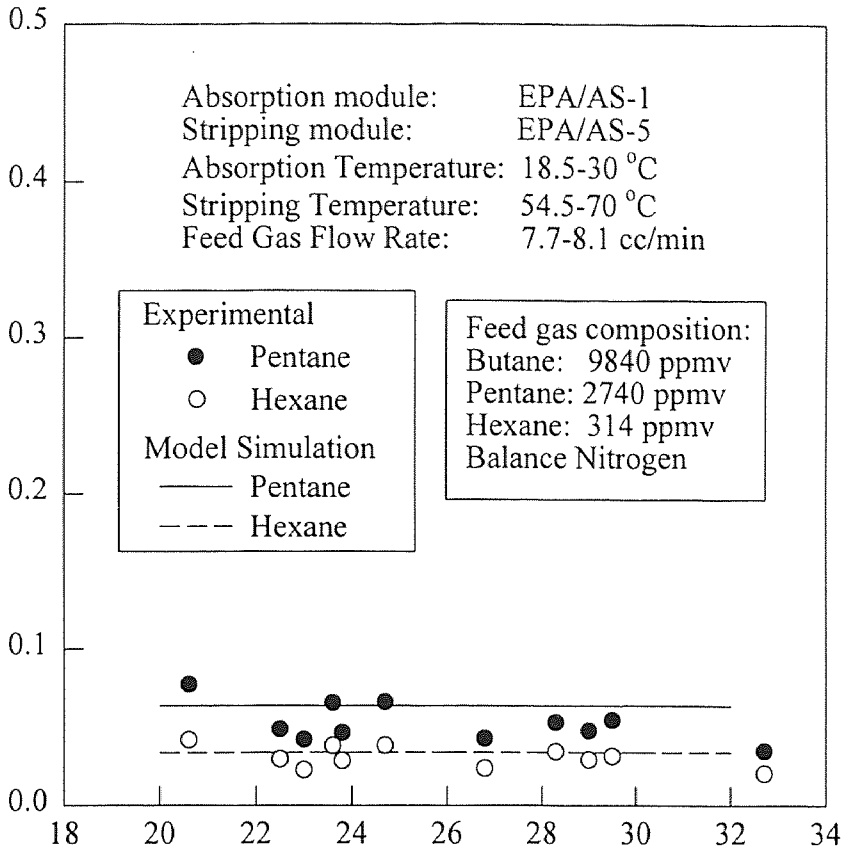

Figure 4.23 Ratio of Outlet to Inlet Gas Phase Concentration of Hydrocarbons as a Function of Silicone Oil Flow Rate; Modules EPA/AS-1 and 5 (Combined Absorption-Stripping with Heating-Cooling System)

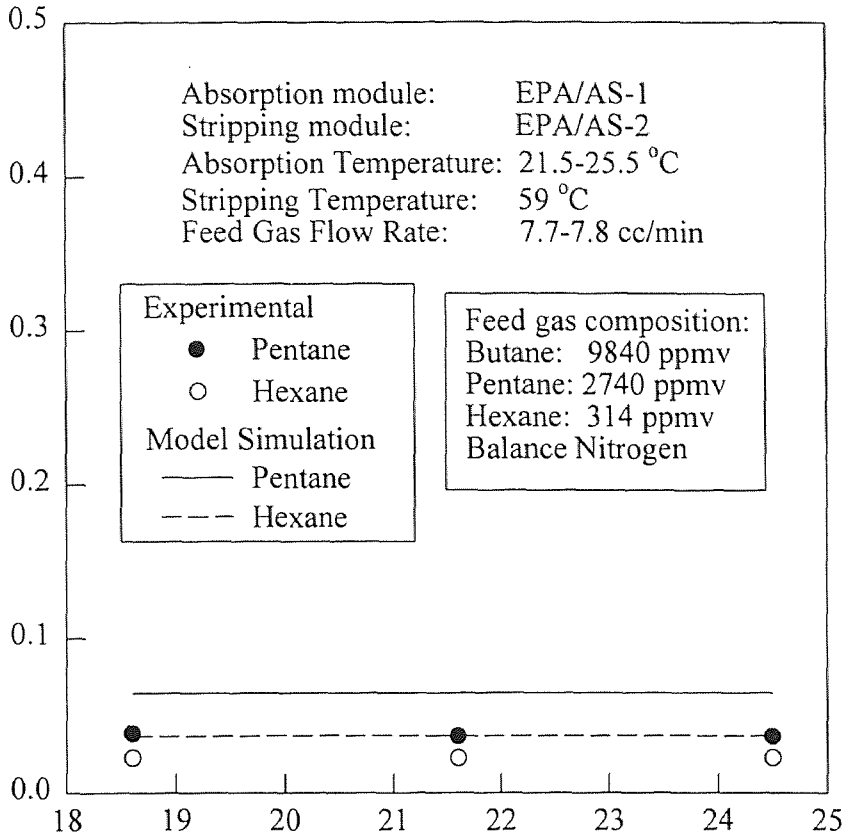

Figure 4.24 Ratio of Outlet to Inlet Gas Phase Concentration of Hydrocarbons as a Function of Silicone Oil Flow Rate; Modules EPA/AS-1 and 2 (Combined Absorption-Stripping with Heating-Cooling System)

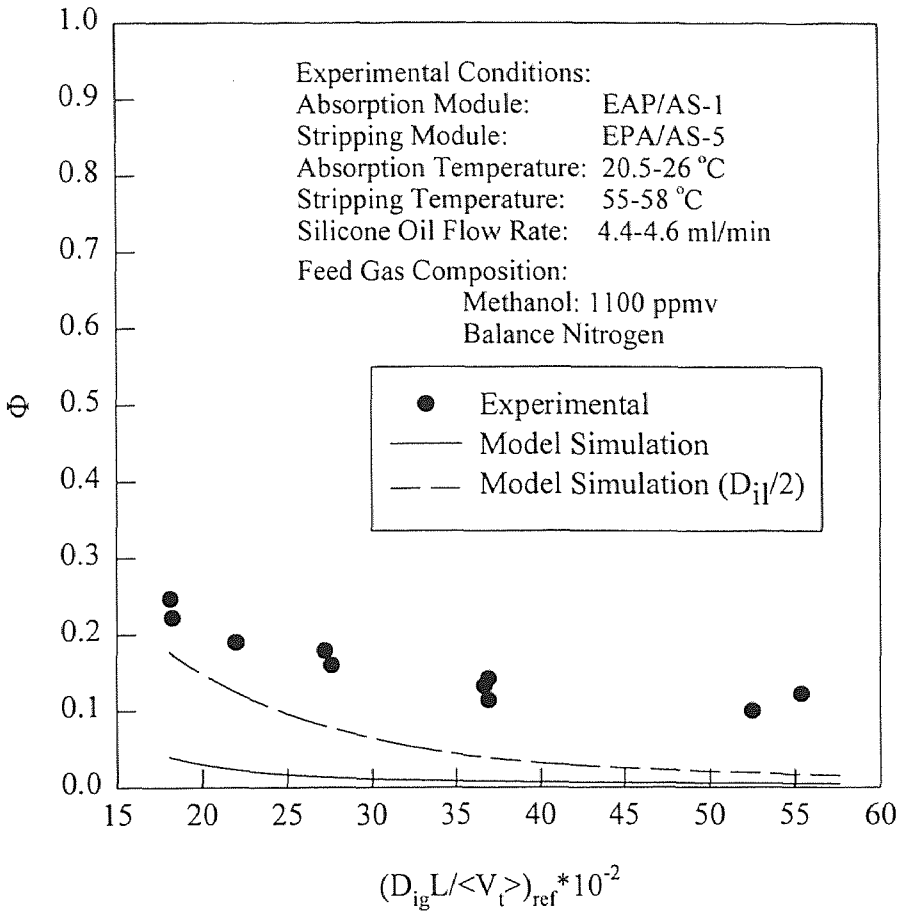

Figure 4.25 Ratio of Outlet to Inlet Gas Phase Concentration of Methanol as a Function of Inverse of Graetz Number (Combined Absorption-Stripping with Heating-Cooling System)

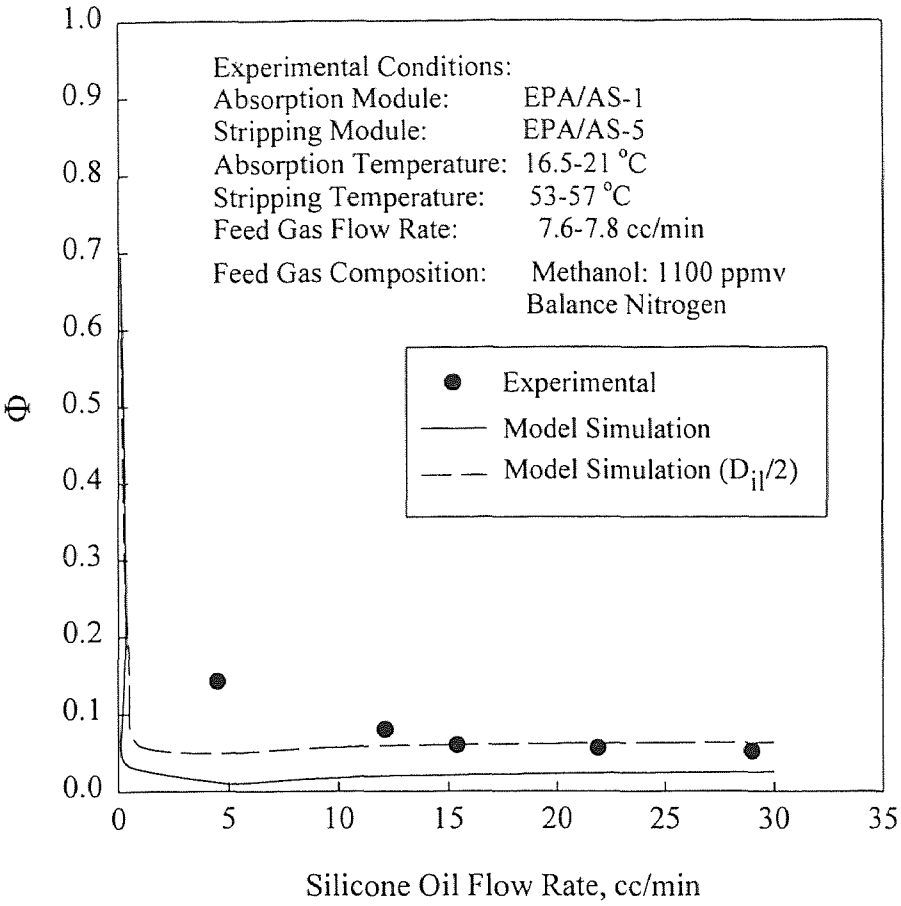

Figure 4.26 Ratio of Outlet to Inlet Gas Phase Concentration of Methanol as a Function of Silicone Oil Flow Rate (Combined Absorption-Stripping with Heating-Cooling System)

predicted values from the mathematical model for methanol-nitrogen separation (Figures 4.25 and 4.26). The deviation could be due to several reasons:

1. Fibers are not distributed evenly in the module. There may be some bypass or backmixing with the absorbent flow in the shell side to make the separation worse.
2. To reduce the resistance of mass transfer, the coating outside the fibers must be very thin. There may be some defects on the fiber surface so that the coating over some locations was easily damaged at high temperature. Small amount of silicone oil was found in the vacuum line of the stripping module during experiments. Separation will be poor if the membrane area is reduced due to some silicone oil occupying in the tube side of the stripping module.
3. Accurate physical parameter values are important in the simulation. The observed value of methanol diffusivity in this work is much larger than that published by Poddar et al. (1996a). Large diffusivity gives low outlet gas phase concentration from the model simulations.

The first and the second reasons are not important since the same problems were encountered for the pentane and hexane-nitrogen separation but the experimental data follows the prediction of the model quite well. The major reason might be the third one. The values of methanol diffusivities divided by two (with the same order of magnitude as Poddar's data (1996a) were tried in the simulation and the predicted Φ value fitted the experimental data better (dash lines in Figures 4.25 and 4.26). The diffusivity value of methanol in silicone oil needs to be further verified.

CHAPTER 5

CONCLUSIONS AND RECOMMENDATIONS

5.1 Conclusions

This research is focused on VOC removal by a membrane-based absorption-stripping process. Silicone oil was used as the absorbent. Experiments were carried out in three different ways: (1) absorption using fresh absorbent; (2) absorption and stripping both at room temperature; (3) absorption at room temperature and stripping at a high temperature. A mathematical model (Poddar et al., 1996a and 1996b) was used to predict the performance of the combined absorption-stripping process at different absorption and stripping temperatures. The Henry's law constants and diffusivities of VOCs at different temperatures were measured to assist in the model simulation. The following concluding remarks can be made from the investigation of the results:

- A high degree removal of VOCs from nitrogen stream was achieved by the membrane-based absorption-stripping process.
- Henry's law constant of VOC varies significantly with temperature. The correlations of temperature dependence of Henry's law constants of methanol, toluene, pentane and hexane in silicone oil were obtained in the temperature range of about 25-80 °C.
- Diffusivity of a VOC in silicone oil increases with increasing temperature. Empirical correlations for methanol, toluene, pentane and hexane were obtained by the regression of experimental results.

- The extent of gas purification increased with increasing absorbent flow rate or decreasing feed gas flow rate.
- The combined absorption-stripping process showed lower gas cleanup level than absorption process using fresh absorbent.
- The VOC removal efficiency of the combined absorption-stripping process increased considerably when the stripping module was operated at a high temperature.
- Model simulations were done for methanol-nitrogen, pentane-nitrogen and hexane-nitrogen separation. The experimental results follow the prediction of the model quite well for pentane-nitrogen and hexane-nitrogen system. The deviation of the model simulation from the experiments is large for methanol-nitrogen system. The reliability of the methanol diffusivity data should be verified.

5.2 Recommendations for Future Work

As discussed earlier, efficient VOC removal from nitrogen was achieved by the membrane-based absorption-stripping process with a heating-cooling system. Model simulation of this process showed some difference from the experimental results for methanol-nitrogen system. The following suggestions may provide improved simulation:

1. There was considerable difference between the diffusivity of methanol in silicone oil obtained in this study and in Poddar et al. (1996a). The accuracy of the diffusivity data should be investigated in order to get better simulation results.
2. Henry's law constant of butane in silicone oil should be measured using an appropriate method so that the model simulation could be done for butane.

A hybrid process of the vapor permeation and combined absorption-stripping needs to be examined. The removal of 99% hydrocarbons was achieved from a multicomponent gas mixture of a high concentration by vapor permeation process (Bagavandoss, 1996). The combined absorption-stripping process can bring the hydrocarbon concentrations further down to a very low level. The overall performance of these two combined processes should be investigated.

APPENDIX A

EXPERIMENTAL RESULTS

Experimental results are provided in the form of tables here.

Table A1 Experimental Data for Calculation of Henry's Law Constant

SN	WE	WES	WS	Vl	Vg	Vg/Vl	(1/PA)*108
16	18.0058	18.9512	0.9454	1.0029	20.9971	20.9364	1.4420
17	18.0019	19.2812	1.2793	1.3571	20.6429	15.2110	1.4133
18	17.9171	19.6736	1.7565	1.8633	20.1367	10.8070	1.4008
19	18.0823	20.9694	2.8871	3.0626	18.9374	6.1834	1.3646
20	17.9661	23.5370	5.5709	5.9095	16.0905	2.7228	1.3242

VOC: Toluene
Absorbent: Silicone Oil
Temperature: 44.9 ^{o}C

SN: Sample number
WE: Weight of the empty vial (gm)
WES: Weight of the vial with sample (gm)
WS: Weight of the sample (gm)
V_l: Volume of the sample (ml)
V_g: Volume of the headspace (cc)
PA: Peak area

Table A2 Henry's Law Constant as a Function of Temperature; Methanol-Silicone Oil

Experiment #	t (°C)	1/T (°K)$^{-1}$	H	ln(H)
1	45.95	0.0031338	8.8533	2.1808
2	54.80	0.0030492	8.9663	2.1935
3	64.85	0.0029586	8.3468	2.1219
4	75.00	0.0028723	5.8662	1.7692

Table A3 Henry's Law Constant as a Function of Temperature; Toluene-Silicone Oil

Experiment #	t (°C)	1/T (°K)$^{-1}$	H	ln(H)
1	44.90	0.0031442	214.5027	5.3683
2	54.80	0.0030492	146.0730	4.9841
3	59.85	0.0030030	167.2300	5.1194
4	74.95	0.0028727	126.4438	4.8398

Table A4 Henry's Law Constant as a Function of Temperature; Hexane-Silicone Oil

Experiment #	t (°C)	1/T (°K)$^{-1}$	H	ln(H)
1	24.85	0.0033557	146.6784	4.9882
2	39.85	0.0031949	103.6400	4.6409
3	59.85	0.0030030	55.5698	4.0176
4	79.95	0.0028321	45.7239	3.8226

Table A5 Henry's Law Constant as a Function of Temperature; Pentane-Silicone Oil

Experiment #	t (°C)	1/T (°K)$^{-1}$	H	ln(H)
1	25.45	0.0033490	71.6519	4.2718
2	39.95	0.0031939	54.9635	4.0067
3	59.85	0.0030030	34.5919	3.5436
4	79.95	0.0028321	30.6592	3.4229

Table A6 Experimental Results for Estimation of VOC Permeance through the Silicone Skin

Module	VOC	t, °C	F_{in} cc/min	F_{out} cc/min	$F_{ppm,in}$ ppmv	$F_{ppm,out}$ ppmv	P cc/min	$(q_o/\delta_o)*10^3$ cm/s	$(q_c/\delta_c)*10^3$ cm/s
EPA/AS-6	Toluene	22	64.6	36.3	940	469	28.5	3.2133	3.2552
	Methanol	22	50.8	22.0	1100	99	30.9	5.4420	5.5128
EPA/AS-7	Butane	22	60.3	23.2	9840	6066	36.5	2.6515	2.6810
	Pentane	22	60.3	23.2	2740	1330	36.5	3.0468	3.0838
	Hexane	22	60.3	23.2	314	116	36.5	3.5339	3.5812

F_{in} : Feed gas inlet flow rate

F_{out} : Feed gas outlet flow rate

$F_{ppm,in}$: VOC concentration in feed gas inlet

$F_{ppm,out}$: COC concentration in feed gas outlet

P : Permeate gas flow rate

q_o/δ_o : VOC permeance through the composite membrane

q_c/δ_c : VOC permeance through the silicone skin

t : Temperature

Table A7 Experimental Results for Estimation of Diffusivity of VOCs in Silicone Oil

VOC	t °C	F_{in} cc/min	F_{out} cc/min	$F_{ppm,in}$ ppmv	$F_{ppm,out}$ ppmv	S cc/min	Hi	$D_{il}*10^6$ cm^2/s
Methanol	23	35.3	35.3	1100	258	30.8	17.3975	10.6282
	48	51.1	50.8	1100	391	30.6	10.1871	21.8620
	60	50.7	50.0	1100	402	30.7	8.1074	25.4806
Toluene	20	51.3	50.6	912	152	30.8	400.8808	2.6073
	49	50.6	50.2	912	170	30.5	199.5786	3.7977
	66	50.6	50.0	912	178	30.5	14.01668	4.8767
Pentane	20	48.8	48.3	2740	1198	29.5	78.4783	1.8115
	47	49.3	49.2	2740	1365	30.4	47.6602	2.2631
	66	49.2	48.6	2740	1430	30.8	35.1901	2.7383
Hexane	20	48.8	48.3	314	93	29.5	165.5646	1.7840
	47	49.3	49.2	314	111	30.4	84.2914	2.4877
	66	49.2	48.6	314	121	30.8	55.9068	3.1474

F_{in} : Feed gas inlet flow rate

F_{out} : Feed gas outlet flow rate

$F_{ppm,in}$: VOC concentration in feed gas inlet

$F_{ppm,out}$: COC concentration in feed gas outlet

H_i : Henry's law constant

S : Sweeping gas flow rate

t : Temperature

Table A8 Hydrocarbon Separation Performance with Variation in Feed Gas Flow Rate (Absorption Only)

Feed Gas Flow Rate, cc/min	Retentate Gas Flow Rate, cc/min	Hydrocarbon Concentration in Purified Gas, ppmv			Percent Removal, %		
		Butane	Pentane	Hexane	Butane	Pentane	Hexane
3.1	3.0	3	0	0	99.97	100	100
5.0	4.7	46	0	0	99.6	100	100
8.5	7.9	256	~0.1	0	97.6	99.99	100
10.6	10.5	668	2	0	93.3	99.9	100
15.2	14.8	1395	16	0	86.2	99.4	100

Feed Gas Composition: Butane: 9840 ppmv
Pentane:2740 ppmv
Hexane: 314 ppmv
Balance Nitrogen

Silicone Oil Flow Rate: 3.8-3.9 ml/min

Module: EPA/AS-1

Temperature: 20-27^{o}C

Table A9 Hydrocarbon Separation Performance with Variation in Silicone Oil Flow Rate; High Gas Flow Rate (Absorption Only)

Silicone Oil Flow Rate, ml/min	Hydrocarbon Concentration in Purified Gas, ppmv			Percent Removal, %		
	Butane	Pentane	Hexane	Butane	Pentane	Hexane
0.7	1236	5	0	87.6	99.9	100
1.3	554	0.2	0	94.4	99.99	100
2.3	457	0.2	0	95.5	99.99	100
3.4	357	0	0	96.4	100	100
3.8	256	~0.1	0	97.6	99.99	100
4.4	274	0	0	97.2	100	100
5.2	268	0	0	97.4	100	100
7.0	260	0	0	97.4	100	100

Feed Gas Composition: Butane: 9840 ppmv
Pentane: 2740 ppmv
Hexane: 314 ppmv
Balance Nitrogen

Feed Gas Flow Rate: 7.7-8.9 cc/min

Module: EPA?AS-1

Temperature: 20-27 °C

Table A10 Hydrocarbon Separation Performance with Variation in Silicone Oil Flow Rate; Low Gas Flow Rate (Absorption Only)

Silicone Oil Flow Rate, ml/min	Hydrocarbon Concentration in Purified Gas, ppmv			Percent Removal, %		
	Butane	Pentane	Hexane	Butane	Pentane	Hexane
0.9	70	0	0	99.3	100	100
2.7	6	0	0	99.94	100	100
3.9	3	0	0	99.97	100	100
7.4	6	0	0	99.94	100	100

Feed gas concentration: Butane: 9840 ppmv
Pentane:2740 ppmv
Hexane: 314 ppmv
Balance nitrogen

Module: EPA/AS-1
Feed Gas Flow Rate: 3.1-3.7 cc/min
Temperature: 20-27°C

Table A11 Hydrocarbon Separation Performance with Variation in Feed Gas Flow Rate (Combined Absorption-Stripping)

Feed Gas Flow Rate, cc/min	Retentate Gas Flow Rate, cc/min	Hydrocarbon Concentration in Purified Gas, ppmv			Percent Removal, %		
		Butane	Pentane	Hexane	Butane	Pentane	Hexane
7.7	7.4	2478	512	52	75.7	81.9	84.0
10.8	10.5	2680	398	32	73.4	85.8	90.0
20.3	19.5	4497	646	44	56.1	77.4	86.5
41.0	40.7	6624	1216	80	33.2	55.9	74.7
60.3	60	7707	1595	122	22.1	42.1	61.3
82.2	82.2	8170	1799	148	17.0	34.3	52.9

Feed Gas Composition: Butane: 9840 ppmv Pentane:2740 ppmv
Hexane: 314 ppmv Balance Nitrogen

Absorption Module: EPA/AS-1
Stripping Module: EPA/AS-2 and 3 in Series
Silicone Oil Flow Rate: 4.4-4.8 ml/min
Temperature: 20-26°C

Table A12 Hydrocarbon Separation Performance with Variation in Silicone Oil Flow Rate (Combined Absorption-Stripping)

Silicone Oil Flow Rate, ml/min	Hydrocarbon Concentration in Purified Gas, ppmv			Percent Removal, %		
	Butane	Pentane	Hexane	Butane	Pentane	Hexane
4.4	2478	512	52	75.7	81.9	84.0
6.7	2383	511	50	76.3	81.8	84.4
8.0	1936	392	38	81.7	86.7	88.8
10.9	1596	312	28	85.5	90.0	92.2

Feed Gas Composition: Butane: 9840 ppmv Hexane: 314 ppmv
Pentane:2740 ppmv Balance Nitrogen

Absorption Module: EPA/AS-1
Stripping Module: EPA/AS-2 and 3 in Series
Feed Gas Flow Rate: 7.7-9.3 cc/min
Temperature: 20-26°C

Table A13 Hydrocarbon Separation Performance with Variation in Silicone Oil Flow Rate; Modules EPA/AS-1 and 5 (Combined Absorption-Stripping with Heating-Cooling System)

Feed Flow Rate, cc/min	Purified Gas Flow Rate, cc/min	T_A[1] °C	T_S[2] °C	Oil Flow Rate, ml/min	Purified Gas Composition, ppmv			Percent Removal, %		
					Butane	Pentane	Hexane	Butane	Pentane	Hexane
8.0	7.4	21.5	55.5	20.6	1779	212	13.1	83.3	92.8	96.1
8.0	7.5	29	62	22.5	1258	133	9.2	88.0	95.4	97.3
8.0	7.3	21	70	23.0	1157	115	7.1	89.3	96.2	97.9
7.9	7.2	18.5	54.5	23.6	1515	179	11.9	86.0	94.0	96.5
8.1	7.5	26	68	23.8	1218	127	8.9	88.5	95.7	97.4
7.9	7.2	19	55	24.7	1500	181	12.0	86.1	94.0	96.5
7.9	7.2	20	66.5	26.8	1116	117	7.4	89.7	96.1	97.9
8.1	7.4	30	57.5	28.3	1321	145	10.7	87.7	95.2	96.9
8.1	7.4	29	68	29.0	1221	130	9.1	88.6	95.7	97.4
8.1	7.3	23	65	29.5	1322	149	9.8	87.9	95.1	97.2
7.7	7.0	19	66	32.7	690	95	6.4	93.6	96.8	98.1

1: T_A : Absorption Temperature
2: T_S: Stripping Temperature
Feed Composition: Butane: 9840 ppmv, Pentane:2740 ppmv, Hexane: 314 ppmv, Balance nitrogen
Absorption Module: EPA/AS-1 Stripping Module: EPA/AS-5

Table A14 Hydrocarbon Separation Performance with Variation in Feed Gas Flow Rate; Modules EPA/AS-1 and 5 (Combined Absorption-Stripping with Heating-Cooling System)

Feed Gas Flow Rate, cc/min	Purified Gas Flow Rate, cc/min	T_A[1] °C	T_S[2] °C	Oil Flow Rate, ml/min	Purified Gas Composition, ppmv			Percent Removal, %		
					Butane	Pentane	Hexane	Butane	Pentane	Hexane
5.2	4.6	20	55	23.9	791	122	8.6	92.9	96.1	97.6
7.9	7.2	18.5	54.5	23.6	1515	179	11.9	86.0	94.0	96.5
10.2	9.5	20	54	23.7	2004	243	17	81.0	91.7	95.0
12.7	12.0	19	53	23.6	2571	300	21	75.3	89.7	93.7
15.2	14.4	18	53	23.4	3005	407	23	71.1	85.9	93.1

1: T_A: Absorption Temperature
2: T_S: Stripping Temperature

Feed Composition: Butane: 9840 ppmv
Pentane:2740 ppmv
Hexane: 314 ppmv
Balance Nitrogen

Absorption Module: EPA/AS-1
Stripping Module: EPA/AS-5

Table A15 Hydrocarbon Separation Performance with Variation in Silicone Oil Flow Rate; Modules EPA/AS-1 and 4 (Combined Absorption-Stripping with Heating-Cooling System)

Feed Flow Rate, cc/min	Purified Gas Flow Rate, cc/min	T_A[1] °C	T_S[2] °C	Oil Flow Rate, ml/min	Purified Gas Composition, ppmv			Percent Removal, %		
					Butane	Pentane	Hexane	Butane	Pentane	Hexane
7.8	7.5	20	57.5	20.1	678	76	4.3	93.4	97.3	98.7
7.8	7.5	21	59	22.2	755	88	4.5	92.6	96.9	98.6
7.8	7.4	21	59	24.3	774	90	5.0	92.5	96.9	98.5
7.8	7.4	23	59	24.8	713	80	4.4	93.1	97.2	98.7
7.8	7.4	24	71.5	25.6	604	66	3.5	94.2	97.7	98.9
7.8	7.5	24	75	27.0	627	66	3.5	93.9	97.7	98.9
7.8	7.4	23.5	72.5	28.4	610	65	3.5	94.1	97.7	98.9
7.9	7.6	27	75.5	29.7	668	71	3.9	93.5	97.5	98.8

1: T_A : Absorption Temperature
2: T_S : Stripping Temperature

Feed Composition: Butane: 9840 ppmv
Pentane:2740 ppmv
Hexane: 314 ppmv
Balance nitrogen

Absorption Module: EPA/AS-1
Stripping Module: EPA/AS-4

Table A16 Methanol Separation Performance with Variation in Silicone Oil Flow Rate; Modules EPA/AS-1 and 5 (Combined Absorption-Stripping with Heating-Cooling System)

Feed Gas Flow Rate, cc/min	Purified Gas Flow Rate, cc/min	T_A[1] °C	T_S[2] °C	Silicone Oil Flow Rate, ml/min	Methanol Concentration in Purified Gas, ppmv	Methanol Percent Removal, %
7.7	7.5	21	56	4.5	156	86.2
7.7	6.9	16.5	57	12.1	88	92.8
7.8	6.7	17	57	15.4	66	94.8
7.6	6.3	17	53	21.9	62	95.3
7.7	6.0	19	53.5	29.0	57	96.0

1: T_A: Absorption Temperature
2: T_S: Stripping Temperature
Feed Gas Composition: Methanol: 1100 ppmv; Balance Nitrogen
Absorption Module: EPA/AS-1
Stripping Module: EPA/AS-5

Table A17 Methanol Separation Performance with Variation in Feed Gas Flow Rate; Modules EPA/AS-1 and 5 (Combined Absorption-Stripping with Heating-Cooling System)

Feed Gas Flow Rate, cc/min	Purified Gas Flow Rate, cc/min	T_A[1] °C	T_S[2] °C	Silicone Oil Flow Rate, ml/min	Methanol Concentration in Purified Gas, ppmv	Methanol Percent Removal, %
5.3	5.0	26	58	4.4	135	88.4
5.4	5.0	20.5	56	4.5	110	90.7
7.7	7.5	21	56	4.5	156	86.2
7.9	7.8	25	57	4.6	125	88.8
7.9	7.7	24	58	4.5	146	87.1
10.5	10.3	21.5	56.5	4.5	197	82.4
10.5	10.0	24	55	4.4	176	84.8
13.2	13.1	24	58	4.5	209	81.1
15.7	15.6	22	57	4.5	245	77.9
15.8	15.7	22	57	4.4	272	75.4
15.8	15.7	22	57	4.4	272	75.4

1: T_A: Absorption Temperature
2: T_S: Stripping Temperature
Feed Gas Composition: Methanol: 1100 ppmv; Balance Nitrogen
Absorption Module: EPA/AS-1
Stripping Module: EPA/AS-5

Table A18 Toluene Separation Performance with Variation in Silicone Oil Flow Rate; Modules EPA/AS-1 and 6 (Combined Absorption-Stripping with Heating-Cooling System)

Feed Gas Flow Rate, cc/min	Purified Gas Flow Rate, cc/min	T_A[1] °C	T_S[2] °C	Silicone Oil Flow Rate, ml/min	Toluene Concentration in Purified Gas, ppmv	Toluene Percent Removal, %
8.0	7.7	23	54	4.3	30	96.9
7.9	7.4	18	52	14.6	21	97.9
8.2	7.4	17	52	18.4	16.7	98.4
8.2	7.2	17	53	26.8	13.6	98.7

1: T_A: Absorption Temperature
2: T_S: Stripping Temperature
Feed Gas Composition: Toluene: 940 ppmv; Balance Nitrogen
Absorption Module: EPA/AS-1
Stripping Module: EPA/AS-6

Table A19 Toluene Separation Performance with Variation in Feed Gas Flow Rate; Modules EPA/AS-1 and 6 (Combined Absorption-Stripping with Heating-Cooling System)

Feed Gas Flow Rate, cc/min	Purified Gas Flow Rate, cc/min	T_A[1] °C	T_S[2] °C	Silicone Oil Flow Rate, ml/min	Toluenel Concentration in Purified Gas, ppmv	Toluene Percent Removal, %
4.0	3.4	19	51	12.7	17.7	98.4
7.6	6.9	19	50.5	12.8	24.6	97.6
11.8	11.3	19	51	13.0	29.9	97.0
15.2	15.2	19.5	51	13.4	36.4	96.2

1: T_A: Absorption Temperature
2: T_S: Stripping Temperature
Feed Gas Composition: Toluene: 940 ppmv; Balance Nitrogen
Absorption Module: EPA/AS-1
Stripping Module: EPA/AS-6

Table A20 Hydrocarbon Separation Performance with Variation in Silicone Oil Flow Rate; Modules EPA/AS-1 and 2 (Combined Absorption-Stripping with Heating-Cooling System)

Feed Gas Flow Rate, cc/min	Purified Gas Flow Rate, cc/min	T_A[1] °C	T_S[2] °C	Silicone Oil Flow Rate, ml/min	Hydrocarbon Concentration in Purified Gas, ppmv			Percent Removal, %		
					Butane	Pentane	Hexane	Butane	Pentane	Hexane
7.8	7.4	23	59	18.6	780	105	7	92.5	96.4	97.9
7.7	7.3	21.5	59	21.6	718	100	7	93.1	96.5	97.9
7.8	7.5	24.5	59	24.7	720	100	7	93.0	96.5	97.9
7.9	7.5	25	72	27.5	614	79	5	94.1	97.3	98.5
7.9	7.4	25.5	75	29.5	598	75	5	94.3	97.4	98.5

1: T_A: Absorption Temperature
2: T_S: Stripping Temperature
Feed Gas Composition: Butane: 9840 ppmv
Pentane:2740 ppmv
Hexane: 314 ppmv
Balance Nitrogen
Absorption Module: EPA/AS-1
Stripping Module: EPA/AS-2

Table A21 Thermodynamic Properties of Nitrogen and VOCs

VOC/N_2	Mol. Wt.	T_c (^oK)	P_c (atm)	V_c (cc/mole)	ε/K (^oK)	σ (Å)
Methanol	32.042	512.6	79.9	118.0	481.8	3.626
Butane	58.124	425.2	37.5	255	531.4	4.687
Pentane	72.151	469.6	33.3	304	341.1	5.784
Hexane	86.178	507.4	29.3	370.0	399.3	5.949
Nitrogen	28.013	126.2	33.5	90.1	71.4	3.798

APPENDIX B

SAMPLE CALCULATION OF DIMENSIONLESS HENRY'S LAW CONSTANT

Data of experimental number 16 in Table A1 was taken as a sample calculation:

WE=18.0058 gm

WES=18.9512 gm

WS=WES-WE=18.9512-18.0058=0.9454 gm

t=44.9 °C

Density of silicone oil at 44.9 °C is calculated from equation 3.1:

ρ_l=0.9802-8.356*10^{-4}*44.9=0.9427 gm/ml

V_l=0.9454/0.9427=1.0029 ml

V_g=22.0-1.0029=20.9971 CC

V_g/ V_l=20.9364

From Figure 4.1, the following data were obtained:

y-intercept=$H_i R_f/C_{io}$=1.3202*10^{-7}

Slope= R_f/C_{io}=6.1547*10^{-10}

H_i=1.3202*10^{-7}/6.1547*10^{-10}=214.5027

APPENDIX C

PROGRAM FOR CALCULATION OF THE CO_2/N_2 PERMEANCE AND THE SEPARATION FACTORS

```
(*---This is a program for calculation of the CO2/N2 permeance and separation factor---*)

(*----------input data section----------*)

area=137.3                (* membrane surface area of the module, cm^2 *)
feedpres=15.0+14.69       (* feed gas pressure, psia *)
permpres=14.69            (* permeate side gas pressure, psia *)
x1=0.0504                 (* feed gas inlet conc. mole% *)
x2=0.007627               (* feed gas outlet conc. mole% *)
y1=0.070626               (* permeate gas conc.at feed end mole% *)
flowperm=158.97           (* co2+n2 permeate flow rate, cc/min *)
co2perm=1160              (* pure co2 permeate flow rate, cc/min *)
n2perm=74.2               (* pure n2 permeate flow rate, cc/min *)

(*----------calculaton section----------*)
r=permpres/feedpres
permeanceco2=co2perm/60/area/(feedpres-permpres)/76*14.69
                          (* co2 permeance, scc/cm^2.s.cmHg *)
permeancen2=n2perm/60/area/(feedpres-permpres)/76*14.69
                          (* n2 permeance, scc/cm^2.s.cmHg *)
alpha=permeanceco2/permeancen2        (* ideal separation factor *)
eqn=(y/(1-y))-alpha*(x2-r*y)/((1-x2)-r*(1-y))
solution=FindRoot[eqn==0,{y,0.01}]
y2=y/.solution            (* y2: permeate conc. at feed out end *)

(*---------- driving force for co2----------*)
deltap1co2=feedpres*x1-permpres*y1
deltap2co2=feedpres*x2-permpres*y2
deltaplmco2=(deltap1co2-deltap2co2)/Log[(deltap1co2/deltap2co2)]

(*---------- driving force for n2----------*)
deltap1n2=feedpres*(1-x1)-permpres*(1-y1)
deltap2n2=feedpres*(1-x2)-permpres*(1-y2)
deltaplmn2=(deltap1n2-deltap2n2)/Log[(deltap1n2/deltap2n2)]

(*----------overal separation factor----------*)
```

```
flowpermco2=flowperm*y1          (*co2 permeate flow rate,cc/min  *)
flowpermn2=flowperm*(1-y1)       (*n2 permeate flow rate,cc/min  *)
alphaoveral=flowpermco2*deltaplmn2/flowpermn2/deltaplmco2
TableForm[{permeanceco2,permeancen2,alphaoveral},TableHeadings->{{"co2
permeance=","n2 permeance=","alpha="},{"  "}}]
```

REFERENCES

Bagavandoss, S. October 1996. "Removal of Gasoline-Based Hydrocarbons by Vapor Permeation Membranes." *M. S. Thesis, Department of Chemical Engineering, Chemistry and Environmental Science*, New Jersey Institute of Technology, Newark, NJ.

Baker, R. W., J. Kaschemekat, and J. G. Wijmans. 1996. "Membrane Systems for Profitable VOC Recovery." *CHEMTECH*, **26** (7): 37-43.

Cha, J. S., V. Malik, D. Bhaumik, R. Li, and K. K. Sirkar. 1997. "Removal of VOCs from Waste Gas Stream by Permeation in a Hollow Fiber Permeator." *J. Membr. Sci.* **128**: 195-211.

Lee, Joo H., and Neil R. Foster. 1990. "Mass Transfer and Solubility of O_2 and CH_4 in Silicone Fluids." *Ind. Eng. Chem. Res.* **29**: 691-696.

Mackay, D., and W. Y. Shiu. 1981. "A Critical Review of Henry's Law Constants for Chemicals of Environmental Interest." *J. Phys. Chem. Ref. Data*, **10**(4): 1175-1199.

Poddar, T. K., and K. K. Sirkar. 1997. "Hybrid of Vapor Permeation and Membrane-Based Absorption-Stripping for VOC Removal and Recovery from Gaseous Emmision." *J. Membr. Sci.* **132**: 229-233.

Poddar, T. K., S. Majumdar, and K. K. Sirkar. 1996a. "Membrane-Based Absorption of VOCs from a Gas Stream." *AIChE J.* **42**: 3267-3282.

Poddar, T. K., S. Majumdar, and K. K. Sirkar. 1996b. "Removal of VOCs from Air by Membrane-Based Absorption and Stripping." *J. Membr. Sci.* **120**: 221-237.

Poddar T. K., and K. K. Sirkar. 1996. "Henry's Law Constant for Selected Volatile Organic Compounds in High-Boiling Oils." *J. Chem. Eng. Data* **41**: 1329-1332.

Poddar, T. K. May 1995. "Removal of VOCs from Air by Absorption and Stripping in Hollow Fiber Devices." *Ph. D. Dissertation, Department of Chemical Engineering, Chemistry and Environmental Science*, New Jersey Institute of Technology, Newark, NJ.

Reid, R. C., J. M. Prausnitz, and T. K. Sherwood. 1997. *The Properties of Gases and Liquids*. Third Edition. McGraw-Hill, New York, N.Y.

Robbins, G. A., S. Wang, and J. D. Stuart. 1993. "Using the Static Headspace Method to Determine Henry's Law Constants," *Anal. Chem.* **65**: 3113-3118.

REFERENCES
(Continued)

Ruddy, E. N., and L. A. Carroll. 1993. "Select the Best VOC Control Strategy." *Chem. Eng. Prog.* **89** (7): 28-35.

Sirkar, K. K. 1992. "Other New Membrane Processes." *Membrane Handbook*. Ho, W. S. Winston and K. K. Sirkar (Eds). Van Nostrand Reinhold, New York, N.Y.

U.S. Department of Health, Education, and Welfare. March 1970. *Air Quality Criteria for Hydrocarbons*. Washington, D. C.: National Air Pollution Control Administration.